Published as Chapter 5 in "*Handbook of Surface and Colloid Chemistry*"
Second Expanded and Updated Edition; K. S. Birdi, Ed.; CRC Press, New York, 2002.

CHEMICAL PHYSICS OF COLLOID SYSTEMS AND INTERFACES

Authors: Peter A. Kralchevsky, Krassimir D. Danov, and Nikolai D. Denkov

Laboratory of Chemical Physics and Engineering, Faculty of Chemistry, University of Sofia, Sofia 1164, Bulgaria

CONTENTS

5.5. HYDRODYNAMIC INTERACTIONS IN DISPERSIONS

5.5.1 BASIC EQUATIONS AND LUBRICATION APPROXIMATION

In addition to the surface forces (see Section 5.4 above), two colliding particles in a liquid medium also experience hydrodynamic interactions due to the viscous friction, which can be rather long range (operative even at distances above 100 nm). The hydrodynamic interaction among particles depends on both the type of fluid motion and the type of interfaces. The quantitative description of this interaction is based on the classical laws of mass conservation and momentum balance for the bulk phases:[410-415]

$$\frac{\partial \rho}{\partial t} + \mathrm{div}(\rho \mathbf{v}) = 0 \tag{240}$$

$$\frac{\partial}{\partial t}(\rho \mathbf{v}) + \mathrm{div}(\rho \mathbf{v}\mathbf{v} - \mathbf{P} - \mathbf{P}_\mathrm{b}) = 0 \tag{241}$$

where ρ is the mass density, $\mathbf{v}$ is the local mass average velocity, $\mathbf{P}$ is the hydrodynamic stress tensor; $\mathbf{P}_\mathrm{b}$ is the body-force tensor which accounts for the action of body forces such as gravity, electrostatic forces (the Maxwell tensor), etc. In a fluid at rest, and in the absence of body forces, the only contact force given by the hydrodynamic stress tensor is the scalar thermodynamic pressure, p, and $\mathbf{P}$ can be written as $\mathbf{P} = -p\mathbf{I}$, where $\mathbf{I}$ is the unit tensor in space. For a fluid in motion, the viscous forces become operative and:

$$\mathbf{P} = -p\mathbf{I} + \mathbf{T} \tag{242}$$

where $\mathbf{T}$ is the viscous stress tensor. From the definition of the stress tensor (Equation 242), it follows that the resultant hydrodynamic force, $\mathbf{F}$, exerted by the surrounding fluid on the particle surface, S, and the torque, $\mathbf{M}$, applied to it are given by the expressions[410,412]

$$\mathbf{F} = \int_S \mathbf{P} \cdot \mathbf{n}\, dS\,, \qquad \mathbf{M} = \int_S \mathbf{r}_0 \times \mathbf{P} \cdot \mathbf{n}\, dS \tag{243}$$

where $\mathbf{r}_0$ is the position vector of a point of S with respect to an arbitrarily chosen coordinate origin, and $\mathbf{n}$ is the vector of the running unit normal to the surface S. In the presence of body forces, the total force, $\mathbf{F}_\mathrm{tot}$, and torque, $\mathbf{M}_\mathrm{tot}$, acting on the particle surface are:

$$\mathbf{F}_\mathrm{tot} = \mathbf{F} + \int_S \mathbf{P}_\mathrm{b} \cdot \mathbf{n}\, dS\,, \qquad \mathbf{M}_\mathrm{tot} = \mathbf{M} + \int_S \mathbf{r}_0 \times \mathbf{P}_\mathrm{b} \cdot \mathbf{n}\, dS \tag{244}$$

The dependence of the viscous stress on the velocity gradient in the fluid is a constitutive law, which is usually called the bulk rheological equation. The general linear relation between the viscous stress tensor, $\mathbf{T}$, and the rate of strain tensor,

$$\mathbf{D} = \frac{1}{2}\left[\nabla\mathbf{v} + (\nabla\mathbf{v})^T\right] \tag{245}$$

(the superscript T denotes conjugation) reads

$$\mathbf{T} = \zeta(\mathrm{div}\mathbf{v})\mathbf{I} + 2\eta\left[\mathbf{D} - \frac{1}{3}(\mathrm{div}\mathbf{v})\mathbf{I}\right] \tag{246}$$

The latter equation is usually referred as the Newtonian model or Newton's law of viscosity. In Equation 246, ζ is the dilatational bulk viscosity and η is the shear bulk viscosity. The usual liquids comply well with the Newtonian model. On the other hand, some concentrated macromolecular solutions, colloidal dispersions, gels, etc. may exhibit non-Newtonian behavior; their properties are considered in detail in some recent review articles and books.[415-418] From Equations 241 and 246, one obtains the Navier-Stokes equation:[419,420]

$$\rho\frac{d\mathbf{v}}{dt} = -\nabla p + \left(\zeta + \frac{1}{3}\eta\right)\nabla(\nabla\cdot\mathbf{v}) + \eta\nabla^2\mathbf{v} + \mathbf{f}\,, \qquad (\mathbf{f} \equiv \nabla\cdot\mathbf{P}_\mathrm{b}) \tag{247}$$

for homogeneous Newtonian fluids, for which the dilatational and shear viscosities, ζ and η, do not depend on the spatial coordinates. In Equation 247, the material derivative d/dt can be presented as a sum of a local time derivative and a convective term:

$$\frac{d}{dt} = \frac{\partial}{\partial t} + (\mathbf{v}\cdot\nabla) \tag{248}$$

If the density, ρ, is constant, the equation of mass conservation (Equation 240) and the Navier-Stokes equation (247) reduce to:

$$\mathrm{div}\mathbf{v} = 0\,, \qquad \rho\frac{d\mathbf{v}}{dt} = -\nabla p + \eta\nabla^2\mathbf{v} + \mathbf{f} \tag{249}$$

For low shear stresses in the dispersions, the characteristic velocity, V_z, of the relative particle motion is small enough in order for the Reynolds number, $\mathrm{Re} = \rho V_z L/\eta$, to be a small parameter, where L is a characteristic length scale. In this case, the inertia terms in Equations 247 and 249 can be neglected. Then, the system of equations becomes linear and the different types of hydrodynamic motion become additive,[278,421,422] e.g., the motion in the liquid flow can be presented as a superposition of elementary translation and rotational motions.

The basic equations can be further simplified in the framework of the lubrication approximation, which can be applied to the case when the Reynolds number is small and when the distances between the particle surfaces are much smaller than their radii of curvature (see Figure 31).[423,424] There are two ways to take into account the molecular interactions between the two particles across the liquid film intervening between them: (i) the body force approach; (ii) the disjoining pressure approach. The former approach treats the molecular forces as components of the body force, **f** (Equation 247); consequently, they give

contributions to the normal and tangential stress boundary conditions.[425,426] In the case (ii), the molecular interactions are incorporated only in the normal stress boundary conditions at the particle surfaces. When the body force can be expressed as a gradient of potential, $\mathbf{f} = \nabla U$ (that is $\mathbf{P}_\mathrm{b} = U\,\mathbf{I}$), the two approaches are equivalent.[427]

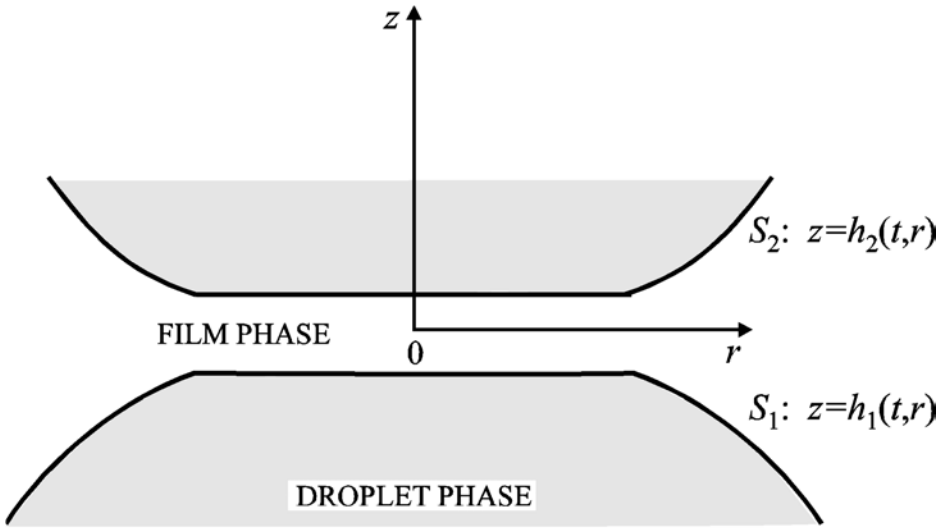

FIGURE 31. Sketch of a plane-parallel film formed between two identical fluid particles.

If two particles are interacting across an electrolyte solution, the equations of continuity and the momentum balance, Equation 249, in lubrication approximation read[428]

$$\nabla_{\mathrm{II}} \cdot \mathbf{v}_{\mathrm{II}} + \frac{\partial v_z}{\partial z} = 0\,, \qquad \eta \frac{\partial^2 \mathbf{v}_{\mathrm{II}}}{\partial z^2} = \nabla_{\mathrm{II}} \cdot p + kT \sum_{i=1}^{N} z_i c_i \nabla_{\mathrm{II}} \Phi\,, \qquad \frac{\partial p}{\partial z} + kT \sum_{i=1}^{N} z_i c_i \frac{\partial \Phi}{\partial z} = 0 \qquad (250)$$

where $\mathbf{v}_{\mathrm{II}}$ and ∇_{II} are the projection of the velocity and the gradient operator on the plane *xy*; the *z*-axis is (approximately) perpendicular to the film surfaces S_1 and S_2 (see Figure 31); $c_i = c_i(r,z,t)$ is the ion concentration (i = 1, 2, …, N); Φ is the dimensionless electric potential (see Sections 5.2.1.2 and 5.2.2). It turns out that in lubrication approximation, the dependence of the ionic concentrations on the z-coordinate comes through the electric potential $\Phi(r,z,t)$: one obtains a counterpart of the Boltzmann equation $c_i = c_{i,\mathrm{n}}(r,z,t)\exp(-z_i\Phi)$, where $c_{i,\mathrm{n}}$ refers to an imaginary situation of "switched off" electric charges ($\Phi \equiv 0$). The kinematic boundary condition for the film surfaces has the form:

$$\frac{\partial h_j}{\partial t} + \mathbf{u}_j . \nabla_{\mathrm{II}} h_j = (v_z)_j \qquad \text{at} \qquad S_j \ \ (j = 1,2) \qquad (251)$$

where: $\mathbf{u}_i$ is the velocity projection in the plane xy at the corresponding film surface, S_i, which is close to the interfacial velocity; $(v_z)_i$ is the z component of the velocity at the surface S_i. The general solution of Equations 250 to 251 could be written as:

$$p = p_{\mathrm{n}} + kT\sum_{i=1}^{N}(c_i - c_{i,\mathrm{n}}) \tag{252}$$

$$\mathbf{v}_{\mathrm{II}} = \frac{(z-h_1)(z-h_2)}{2\eta}\nabla_{\mathrm{II}}p_{\mathrm{n}} + \frac{h_2 - z}{h}\mathbf{u}_1 + \frac{z-h_1}{h}\mathbf{u}_2 +$$

$$+\frac{kTh^2}{4\eta}\sum_{i=1}^{N}[m_{2,i}(z) - \frac{h_2 - z}{h}m_{2,i}(h_1) - \frac{z-h_1}{h}m_{2,i}(h_2)]\nabla_{\mathrm{II}}c_{i,\mathrm{n}} \tag{253}$$

Here $h = h_2 - h_1$ is the local film thickness; the meaning of $p_{\mathrm{n}}(x,y,t)$ is analogous to that of and $c_{i,\mathrm{n}}(x,y,t)$; the functions, $m_{k,i}(z)$, account for the distribution of the i-th ionic species in the electric double layer:

$$m_{0,i} \equiv \exp(-z_i\Phi) - 1, \qquad m_{k,i}(z) \equiv \frac{2}{h}\int_0^z m_{k-1,i}(\hat{z})\,d\hat{z} \qquad (k = 1, 2, 3,\ i = 1, 2, \ldots, N) \tag{254}$$

The equation determining the local thickness, h, of a film with fluid surfaces (or, alternatively, determining the pressure distribution at the surfaces of the gap between two solid particles of known shape) is

$$\frac{\partial h}{\partial t} + \nabla_{\mathrm{II}}\cdot[\frac{h}{2}(\mathbf{u}_1 + \mathbf{u}_2)] = \frac{1}{12\eta}\nabla_{\mathrm{II}}\cdot(h^3\nabla_{\mathrm{II}}p) +$$

$$+\frac{kT}{8\eta}\nabla_{\mathrm{II}}\cdot\{h^3\sum_{i=1}^{N}[m_{2,i}(h_1) + m_{2,i}(h_2) - m_{3,i}(h_2) + m_{3,i}(h_1)]\nabla_{\mathrm{II}}c_{i,\mathrm{n}}\} \tag{255}$$

The problem for the interactions upon central collisions of two axisymmetric particles (bubbles, droplets or solid spheres) at small surface-to-surface distances was first solved by Reynolds[423] and Taylor[429] for solid surfaces and by Ivanov et al.[430,431] for films of uneven thickness. Equation 255 is referred to as the general equation for films with deformable surfaces[430,431] (see also the more recent reviews[164,289,432]). The asymptotic analysis[433-435] of the dependence of the drag and torque coefficient of a sphere, which is translating and rotating in the neighborhood of a solid plate, is also based on Equation 255 applied to the special case of stationary conditions.

Using Equation 244, one can obtain expressions for the components of the total force exerted on the particle surface, S, in the lubrication approximation:

$$F_{\mathrm{tot},z} = \int_S [p_{\mathrm{n}} + kT\sum_{i=1}^{N}(c_{i\mathrm{s}} - c_{i,\mathrm{n}}) + \Pi_{\mathrm{nel}} - p_\infty]\, dS \tag{256}$$

$$\mathbf{F}_{\mathrm{tot,II}} = -\int_S (\eta \frac{\partial \mathbf{v}_{\mathrm{II}}}{\partial \mathrm{z}} + \frac{2kT}{\kappa_{\mathrm{c}}^2}\frac{\partial \Phi}{\partial \mathrm{z}}\nabla_{\mathrm{II}}\Phi)\, dS \tag{257}$$

where p_∞ is the pressure at infinity in the meniscus region (Figure 31) and $\Pi_{\mathrm{nel}} \equiv \Pi - \Pi_{\mathrm{el}}$ accounts for the contribution of non-electrostatic (non-double-layer) forces to the disjoining pressure (see Section 5.4). The normal and the lateral force resultants, F_z and $\mathbf{F}_{\mathrm{II}}$, are the hydrodynamic resistance and shear force, respectively.

5.5.2 Interaction Between Particles of Tangentially Immobile Surfaces

The surfaces of fluid particles can be treated as being tangentially immobile when they are covered by dense surfactant adsorption monolayers which can resist tangential stresses.[164,289,432,436,437] In such a case, the bubbles or droplets behave as flexible balls with immobile surfaces. When the fluid particles are rather small (say, microemulsion droplets), they can behave like hard spheres; therefore, some relations considered below, which are originally derived for solid particles, can be also applied to fluid particles.

5.5.2.1 Taylor and Reynolds Equations, and Influence of the Particle Shape

In the case of two axisymmetric particles moving along the z-axis towards each other with velocity $V_z = -dh/dt$ Equation 255 can be integrated, and from Equation 256 the resistance force can be calculated. The latter turns out to be proportional to the velocity and bulk viscosity and depends on the shape in a complex way. For particles with tangentially immobile surfaces and without surface electric charge ($\mathbf{u}_1 = \mathbf{u}_2 = 0$, $\Phi = 0$) Charles and Mason[438] have derived

$$F_z = 6\pi\eta V_z \int_0^\infty \frac{r^3}{h^3}\, dr \tag{258}$$

where r is the radial coordinate in a cylindrical coordinate system. In the case of two particles of different radii, R_1 and R_2, film radius R, and uniform film thickness h (see Figure 32), from Equation 258 the following expression can be derived:[439,440]

$$F_z = \frac{3}{2}\pi\eta V_z \frac{R_*^2}{h}(1 + \frac{R^2}{hR_*} + \frac{R^4}{h^2 R_*^2}) \ , \qquad R_* \equiv 2R_1R_2/(R_1{+}R_2) \tag{259}$$

This geometrical configuration has proven to be very close to the real one in the presence of electrostatic disjoining pressure.[180] The Charles-Mason formula (Equation 258) and Equation

256 have been used to calculate the velocity of film thinning for a large number of cases, summarized by Hartland[441] in tables for more than 50 cases (two- and three-dimensional small drops, fully deformed large drops subjected to large forces, two-dimensional hexagonal drops, etc.).

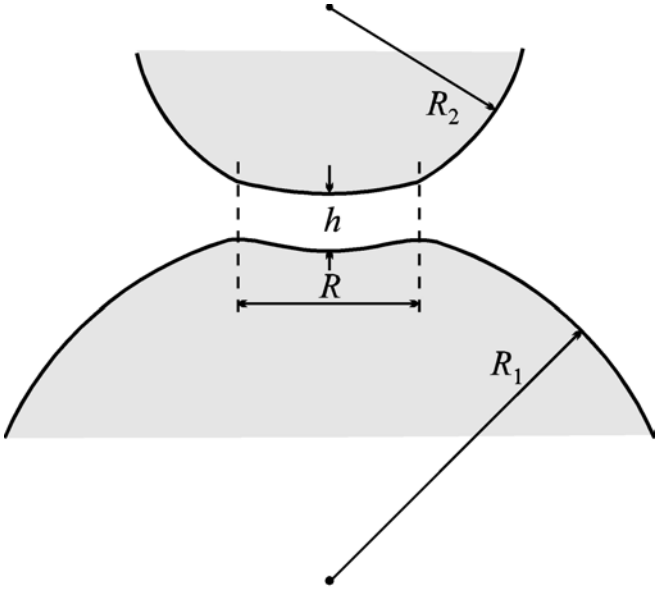

FIGURE 32. Sketch of a film between two nonidentical fluid particles of radii R_1 and R_2. The film thickness and radius are denoted by h and R.

Setting $R = 0$ in Equation 259, one can derive a generalized version of the Taylor formula[429] for the velocity of approach of two nondeformable spheres under the action of an external (non-viscous) force, F_z:[440]

$$V_{\mathrm{Ta}} = \frac{2hF_z}{3\pi\eta R_*^2} \tag{260}$$

When a solid sphere of radius R_c approaches a flat solid surface, one may use the Taylor formula with $R_* = 2R_c$ when the gap between the two surfaces is small compared to R_c.

In the case when two plane-parallel ellipsoidal discs of tangentially immobile surfaces are moving against each other under the action of an external force, $F_{\mathrm{tot},z}$, from Equations 255 and 256, one can derive the Reynolds equation[423] for the velocity of film thinning:

$$V_{\mathrm{Re}} = \frac{F_z h^3 (a^2 + b^2)}{3\pi\eta a^3 b^3} \tag{261}$$

where a and b are the principal radii of curvature. If there is a contribution of the disjoining pressure, Π, the Reynolds equation for a flat axisymmetrical film ($a = b = R$) between two fluid particles of capillary pressure P_c can be written in the form:[143]

$$V_{\mathrm{Re}} = \frac{2F_z h^3}{3\pi\eta R^4} = \frac{2(P_c - \Pi)h^3}{3\eta R^2} \tag{262}$$

From Equations 259 and 262 the ratio between the Reynolds velocity and the velocity of film thinning for a given force is obtained. In Figure 33, this ratio is plotted as a function of the film thickness, h, divided by inversion thickness, $h_i = R^2 / R_*$.[432] One sees that the influence of the viscous friction in the zone encircling the film (this influence is not accounted for in Equation 262) decreases the velocity of thinning about three times for the larger distances, whereas for the small distances this influence vanishes. From Equations 259 and 260, the ratio between the Taylor velocity (corresponding to nondeformable spheres) and the approaching velocity of two deformable particles can be calculated. The dependence of this ratio on the distance between the particles for different film radii is illustrated in Figure 34. One sees that an increase of the film radius, R, and a decrease of the distance, h, lead to a decrease in the velocity. The existence of a film between the particles can decrease the velocity of particle approach, V_z, by several orders of magnitude.

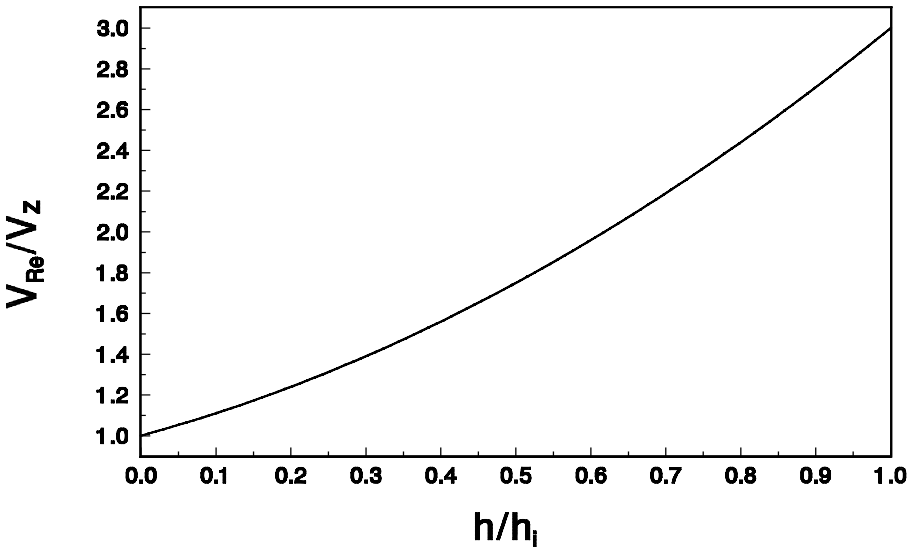

FIG. 33 Plot of V_{Re}/V_z vs. h/h_i for two fluid particles (Equation 259) which are deformed because of the viscous friction in the transition zone between the film and the bulk phase (see Figure 32).

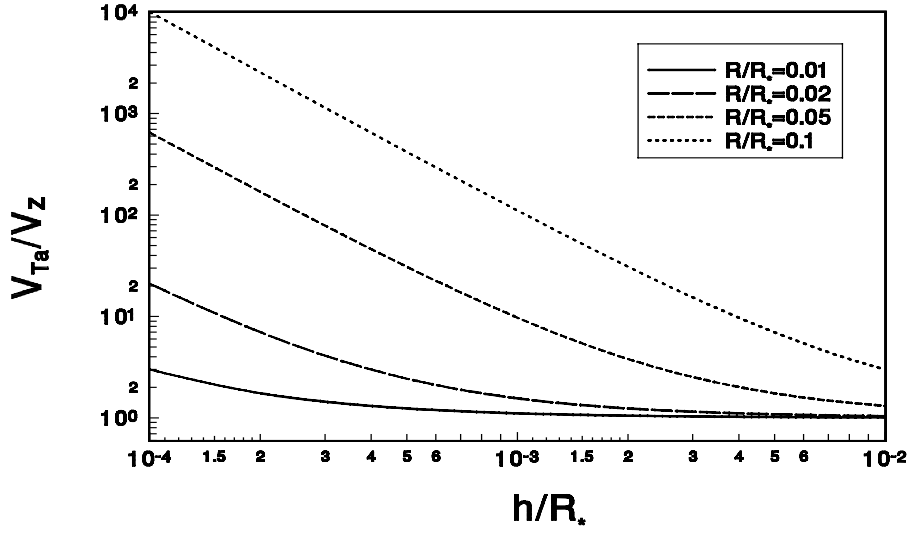

FIG. 34. Plot of V_{Ta}/V_z vs. h/R_* for various values of the dimensionless film radius, R/R_*. V_{Ta} corres-ponds to two nondeformed (spherical) particles (Equation 260), whereas V_z is the velocity of approach of two deformed particles (Eq. 259).

5.5.2.2 Interactions Among Nondeformable Particles at Large Distances

The hydrodynamic interaction between members of a group of small particles suspended in a viscous fluid has fundamental importance for the development of adequate models for calculating the particle collective diffusion coefficient and the effective viscosity of suspension.[278,421,437,442,443] The Stokesian resistance is determined for a number of specific particle shapes under the condition that the particles are located so far apart that the hydrodynamic interactions can be ignored.[421] A general theory applicable to a single particle of arbitrary shape has been developed by Brenner.[444,445] This method gives the first-order correction (with respect to the particle volume fraction) of the viscosity and diffusivity. Matrix relations between resistance and velocity for the pure translational and rotational motions of the members of a general multiparticle system involved in a linear shear flow are given by Brenner and O'Neill.[446] In principle, from these relations one can further obtain the higher order terms in the series expansion of the viscosity and diffusivity with respect to the powers of the particle volume fraction.

At present, the only multiparticle system for which exact values of the resistance tensors can be determined is that of two spheres. It turns out that all types of hydrodynamic flows related to the motion of two spherical particles (of radii R_1 and R_2) can be expressed as superpositions of the elementary processes depicted in Figure 35.[278,412,421,422,447-456]

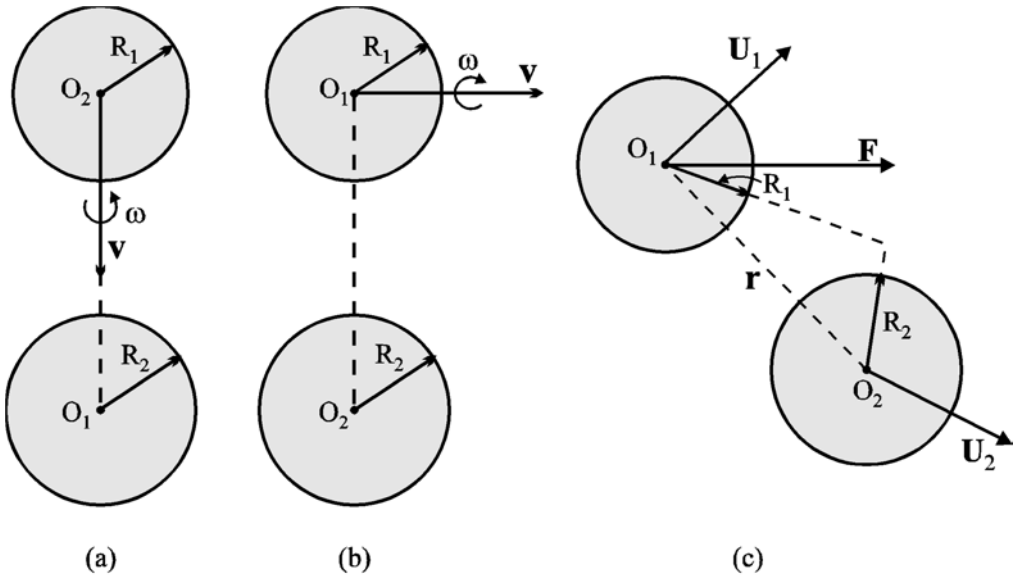

FIGURE 35. Types of hydrodynamic interactions between two spherical particles: (a) motion along and rotation around the line of centers; (b) motion along and rotation around an axis perpendicular to the line of centers; (c) the first particle moves under the action of an applied external force, **F**, whereas the second particle is subjected to the hydrodynamic disturbance created by the motion of the first particle.

The first particle moves toward the second immobile particle and rotates around the line of centers (see Figure 35(a)). This is an axisymmetric rotation problem (a two-dimensional hydrodynamic problem) which was solved by Jeffery[448] and Stimson and Jeffery[449] for two identical spheres moving with equal velocities along their line of centers. Cooley and O'Neill[450,451] calculated the forces for two nonidentical spheres moving with the same speed in the same direction, or alternatively, moving toward each other. A combination of these results permits evaluation of the total forces and torques acting on the particles.

The first particle then moves along an axis perpendicular to the center line and rotates around this axis, whereas the second particle is immobile; see Figure 35(b) (this is a typical three-dimensional hydrodynamic problem). The contribution of this asymmetric motion of the spheres to the resistance tensors was determined by Davis[452] and O'Neill and Majumdar.[453]

The first particle moves with linear velocity, $\mathbf{U}_1$, under the action of an applied external force, $\mathbf{F}$, whereas the second particle is subjected to the hydrodynamic disturbances (created by the motion of the first particle) and moves with a linear velocity, $\mathbf{U}_2$ (see Figure 35(c)). As a rule, this is a three-dimensional hydrodynamic problem. For this case, Batchelor[457] and Batchelor and Wen[458] have derived the following expressions for the instantaneous translational velocities of the two particles in an otherwise quiescent and unbounded fluid:

$$\mathbf{U}_1 = \frac{\mathbf{F}}{6\pi\eta R_1}\cdot\left[A_{11}(r)\frac{\mathbf{rr}}{r^2} + B_{11}(r)\left(\mathbf{I} - \frac{\mathbf{rr}}{r^2}\right)\right] \tag{263}$$

$$\mathbf{U}_2 = \frac{\mathbf{F}}{6\pi\eta (R_1 + R_2)}\cdot\left[A_{12}(r)\frac{\mathbf{rr}}{r^2} + B_{12}(r)\left(\mathbf{I} - \frac{\mathbf{rr}}{r^2}\right)\right] \tag{264}$$

where $\mathbf{r}$ is the vector connecting the particle centers and $r = |\mathbf{r}|$. Expressions for the mobility functions A_{ij} and B_{ij} (i,j = 1,2) at large values of the dimensionless distance $s = 2r/(R_1+R_2)$ and comparable particle radii $\lambda = R_2/R_1 = O(1)$ have been derived by Jeffrey and Onishi[459] and Davis and Hill.[456] The derived far-field expansions are

$$1 - B_{11} = \frac{68\lambda^5}{(1+\lambda)^6 s^6} + \frac{32\lambda^3(10 - 9\lambda^2 + 9\lambda^4)}{(1+\lambda)^8 s^8} + \frac{192\lambda^5(35 - 18\lambda^2 + 6\lambda^4)}{(1+\lambda)^{10} s^{10}} + O(s^{-12})$$

$$B_{11} - A_{11} = \frac{60\lambda^3}{(1+\lambda)^4 s^4} - \frac{60\lambda^3(8 - \lambda^2)}{(1+\lambda)^6 s^6} + \frac{32\lambda^3(20 - 123\lambda^2 + 9\lambda^4)}{(1+\lambda)^8 s^8}$$

$$+ \frac{64\lambda^2(175 + 1500\lambda - 426\lambda^2 + 18\lambda^4)}{(1+\lambda)^{10} s^{10}} + O(s^{-12})$$

$$A_{11} - \frac{2A_{12}}{1+\lambda} = 1 - \frac{3}{(1+\lambda)s} + \frac{4(1+\lambda^2)}{(1+\lambda)^3 s^3} - \frac{60\lambda^3}{(1+\lambda)^4 s^4} + \frac{32\lambda^3(15 - 4\lambda^2)}{(1+\lambda)^6 s^6} - \frac{2400\lambda^3}{(1+\lambda)^7 s^7}$$

$$-\frac{192\lambda^3(5-22\lambda^2+3\lambda^4)}{(1+\lambda)^8 s^8}+\frac{1920\lambda^3(1+\lambda^2)}{(1+\lambda)^9 s^9}-\frac{256\lambda^5(70-375\lambda-120\lambda^2+9\lambda^3)}{(1+\lambda)^{10} s^{10}}$$

$$-\frac{1536\lambda^3(10-151\lambda^2+10\lambda^4)}{(1+\lambda)^{11} s^{11}}+O(s^{-12}) \qquad (265)$$

$$B_{11}-\frac{2B_{12}}{1+\lambda}=1-\frac{3}{2(1+\lambda)s}-\frac{2(1+\lambda^2)}{(1+\lambda)^3 s^3}-\frac{68\lambda^5}{(1+\lambda)^6 s^6}-\frac{32\lambda^3(10-9\lambda^2+9\lambda^4)}{(1+\lambda)^8 s^8}$$

$$-\frac{192\lambda^5(35-18\lambda^2+6\lambda^4)}{(1+\lambda)^{10} s^{10}}-\frac{16\lambda^3(560-553\lambda^2+560\lambda^4)}{(1+\lambda)^{11} s^{11}}+O(s^{-12})$$

In the case of a small heavy sphere falling through a suspension of large particles (fixed in space), one has $\lambda >> 1$; the respective expansions, corresponding to Equation 265, were obtained by Fuentes et al.[460] In the opposite case, when $\lambda << 1$, the suspension of small background spheres will reduce the mean velocity of a large heavy particle (as compared with its Stokes velocity[461]) because the suspension behaves as an effective fluid of larger viscosity as predicted by the Einstein viscosity formula.[457,460]

5.5.2.3 Stages of Thinning of a Liquid Film

Experimental and theoretical investigations[162,170,289,432,437,462,463] show that during the approach of two fluid colloidal particles, a flat liquid film can appear between their closest regions (see Figure 23). The hydrodynamic interactions as well as the buoyancy, the Brownian, electrostatic, van der Waals, and steric forces and other interactions can be involved in film formation.[134,180,439,464,465] The formation and the evolution of a foam or emulsion film usually follows the stages shown in Figure 36.

Under the action of an outer driving force, the fluid particles approach each other. The hydrodynamic interaction is stronger at the front zones and leads to a weak deformation of the interfaces in this front region. In this case, the usual hydrodynamic capillary number, $Ca = \eta V_z/\sigma$, which is a small parameter for nondeformable surfaces, should be modified to read $Ca = \eta V_z R_*/\sigma h$, where the distance, h, between the interfaces is taken into account. The shape of the gap between two drops for different characteristic times was calculated numerically by many authors.[465-485] Experimental investigation of these effects for symmetric and asymmetric drainage of foam films were carried out by Joye et al.[474,475] In some special cases, the deformation of the fluid particle can be very fast: for example, the bursting of a small air bubble at an air-water interface is accompanied by a complex motion resulting in the production of a high-speed liquid jet (see Boulton-Stone and Blake[485]).

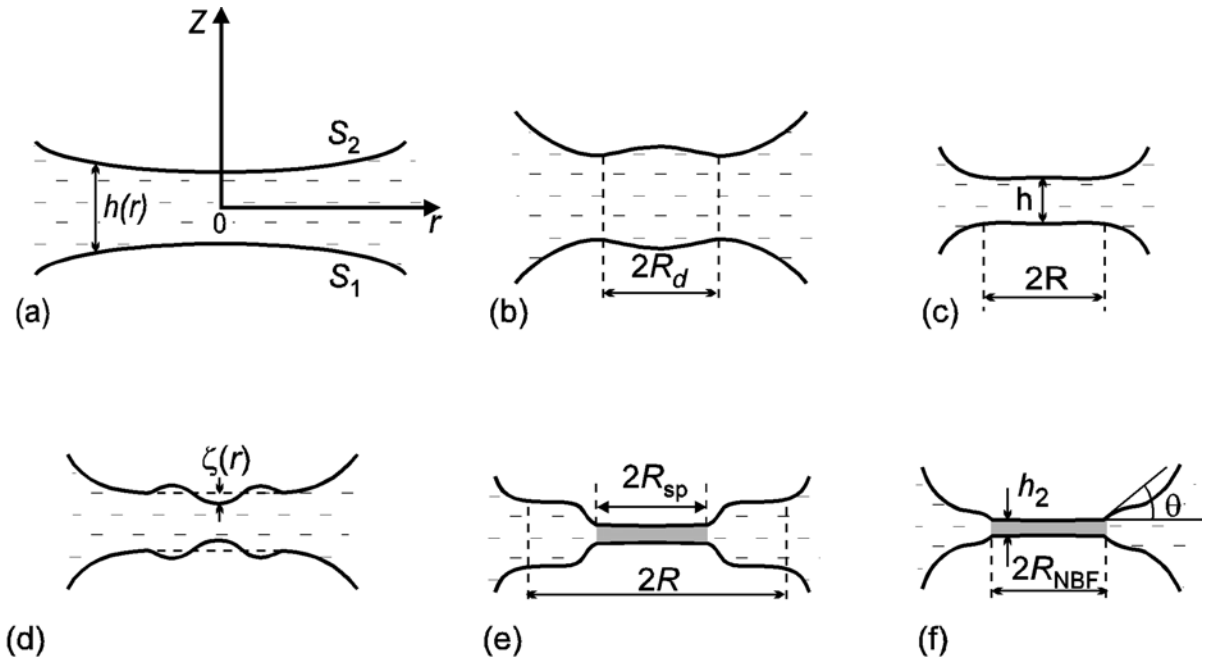

FIGURE 36 Main stages of formation and evolution of a thin liquid film between two bubbles or drops: (a) mutual approach of slightly deformed surfaces; (b) at a given separation, the curvature at the center inverts its sign and a dimple arises; (c) the dimple disappears, and eventually an almost plane-parallel film forms; (d) due to thermal fluctuations or other disturbances the film either ruptures or transforms into a thinner Newton black film (e) which expands until reaching the final equilibrium state (f).

When a certain small separation, h_i, the inversion thickness, is reached, the sign of the curvature in the of contact of the fluid particles (drops, bubbles) changes. A concave lens-shaped formation called a *dimple* is formed (see Frankel and Mysels[486]). This stage is also observed for asymmetric films.[475] A number of theoretical studies described the development of a dimple at the initial stage of film thinning.[465-485] The inversion thickness can be calculated from a simple equation in which the van der Waals interaction is explicitly taken into account (see Section 5.4.2)[164,431,465]

$$h_i = \frac{F_z(\sigma_1 + \sigma_2)}{4\pi\sigma_1\sigma_2}\left(1 - \frac{A_H R_*}{12 F_z h_i}\right) \tag{266}$$

where σ_1 and σ_2 are the interfacial tensions of the phase boundaries S_1 and S_2; in this case F_z is the external force (of non-viscous and non-van-der-Waals origin) experienced by the approaching particles; A_H is the Hamaker constant. In the case, when the van der Waals force is negligible, Equation 266 reduces to $h_i = F_z(\sigma_1 + \sigma_2)/(4\pi\sigma_1\sigma_2)$.[164,431] Danov et al.[439] have shown that in the case of Brownian flocculation of identical small droplets, h_i obeys the following transcendental equation:

$$h_i = \frac{kT}{2\pi\sigma z_i}\{\int_0^{z_i}(\frac{z_i}{z})^2 \frac{\gamma(z)}{\gamma(z_i)}\exp[\frac{U(z)-U(z_i)}{kT}]\frac{dz}{z_i}\}^{-1} \tag{267}$$

where kT is the thermal energy; $\gamma(z) = F_z/V_z$ is the hydrodynamic resistance given by Equation 259; U is the potential energy due to the surface forces (see Equation 164); and z is the distance between the droplet mass centers. These authors pointed out that with an increase of droplet size the role of the Brownian force in the film formation decreases, but for micrometer-sized liquid droplets the Brownian force is still by several orders of magnitude greater than the buoyancy force due to gravity. If the driving force is large enough, so that it is able to overcome the energy barrier created by the electrostatic repulsion and/or the increase of the surface area during the droplet deformation, then film with a dimple will be formed. On the contrary, at low electrolyte concentration (i.e. strong electrostatic repulsion) such a dimple might not appear. Parallel experiments[487] on the formation and thinning of emulsion films of macroscopic and microscopic areas, prepared in the Scheludko cell[143] and in a miniaturized cell, show that the patterns and the time scales of the film evolution in these two cases are significantly different. There is no dimple formation in the case of thin liquid films of small diameters.[487]

In the case of predominant van der Waals attraction, instead of a dimple, a reverse bell-shape deformation, called *pimple*, appears and the film quickly ruptures. [465,472,481,484] The thickness, h_p, at which pimple appears can be calculated from the relationship:[465]

$$h_p = \left(\frac{A_H R_*}{12F_z}\right)^{1/2} \tag{268}$$

The pimple formation thickness depends significantly on the radius, R_*. If a drop of tangentially immobile surfaces and radius R_d is driven by the buoyancy force, then we have:

$$F_z = \frac{4}{3}\pi R_d^3 \Delta\rho g \tag{269}$$

where $\Delta\rho$ is the density difference, and g is the gravity acceleration. For the collision of this drop with another immobile one we have $h_p^2 = A_{\mathrm{H}}/(16\pi\Delta\rho g R_d^2)$. One sees that h_p is inversely proportional to the drop radius. For typical values of the Hamaker constant $A_{\mathrm{H}} = 4\times10^{-20}$ J, density difference $\Delta\rho = 0.12\times10^3$ g/cm^3, and R_d = 10 μm, the thickness of pimple formation is h_p = 82.3 nm. Note that this thickness is quite large. The pimple formation can be interpreted as the onset of instability without fluctuations (stability analysis of the film intervening between the drops has been carried out elsewhere[52]).

As already mentioned, if the van der Waals force (or other attractive force) is not predominant, first a dimple forms in the thinning liquid films. Usually the dimple exists for a short period of time; initially it grows, but as a result of the swift outflow of liquid it decreases

and eventually disappears. The resulting plane-parallel film thins at almost constant radius R. When the electrostatic repulsion is strong, a thicker primary film forms (see point 1 in Figure 13). From the viewpoint of conventional DLVO theory, this film must be metastable. Indeed, the experiments with microscopic foam films, stabilized with sodium octyl sulfate or sodium dodecyl sulfate in the presence of different amount of electrolyte,[488] show that a black spot may suddenly form and a transition to secondary (Newton black) film may occur (see point 2 in Figure 13). The rate of thinning depends not only on the capillary pressure (the driving force) but also very strongly on the surfactant concentration (for details, see Section 5.5.3.2 below).

The appearance of a secondary film (or film rupture, if the secondary film is not stable) is preceded by corrugation of the film surfaces due to thermally excited fluctuations or outer disturbances. When the derivative of the disjoining pressure, $\partial\Pi/\partial h$, is positive, the amplitude of the fluctuations (ζ in Figure 36(d)) spontaneously grows. As already mentioned, the instability leads to rupture of the film or to formation of black spots. The theory of film stability was developed by de Vries,[489] Vrij,[490] Felderhof,[425] Sche and Fijnaut,[426] Ivanov et al.,[491] Gumerman and Homsy,[492] Malhotra and Wasan,[493] Maldarelli and Jain,[427] and Valkovska et al.[494] On the basis of the lubrication approximation for tangentially immobile surfaces, Ivanov et al.[491] and Valkovska et al.[494] derived a general expression for the critical film thickness, h_{cr}, by using long-waves stability analysis:

$$h_{cr} = h_{tr}\left(\frac{\sigma h_{tr}^2}{kT}\right)^{1/4} \exp\left(-\frac{k_{cr}^2 R^2}{32 h_{cr}^3}\int_{h_{cr}}^{h_{tr}} \frac{h^3\Pi'}{P_c-\Pi}dh\right) \tag{270}$$

where k_{cr} is the wave number of the critical wave defined as:

$$k_{cr}^2 = \frac{1}{\sigma}\int_{h_{cr}}^{h_{tr}} \frac{h^3\Pi'}{P_c-\Pi}dh \Big/ \int_{h_{cr}}^{h_{tr}} \frac{h^6}{P_c-\Pi}dh \tag{271}$$

In Equation 271, h_{tr} is the so-called transitional thickness[490,491,494] at which the increase of free energy due to the increased film area and the decrease of free energy due to the van der Waals interaction in the thinner part (Figure 36(d)) compensate each other. At h_{tr} the most rapidly growing fluctuation (the critical wave) becomes unstable. The transitional thickness obeys the following equation:[491,494]

$$\frac{24 h_{cr}^3[P_c-\Pi(h_{tr})]}{R^2 k_{cr}^2 h_{tr}^4} + \frac{\sigma k_{cr}^2 h_{tr}^3}{2 h_{cr}^3} = \Pi'(h_{tr}) \tag{272}$$

Figures 37 and 38 show the critical thicknesses of rupture, h_{cr}, for foam and emulsion films, respectively, plotted vs. the film radius.[495] In both cases the film phase is the aqueous phase, which contains 4.3×10^{-4} M SDS + added NaCl.

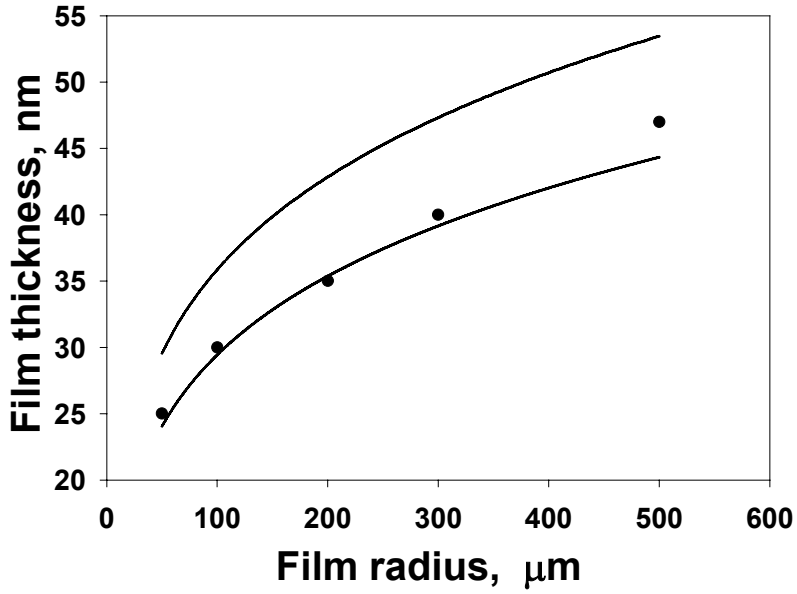

FIGURE 37. Dependence of the critical thickness, h_{cr}, on the radius, R, of foam films. The experimental points are data from Reference 495; the films are formed from a solution of 4.3×10^{-4} M SDS + 0.25 M NaCl. Curve 1 is the prediction of the simplified theory,[493] whereas Curve 3 is calculated using Equations 270 to 272; no adjustable parameters.

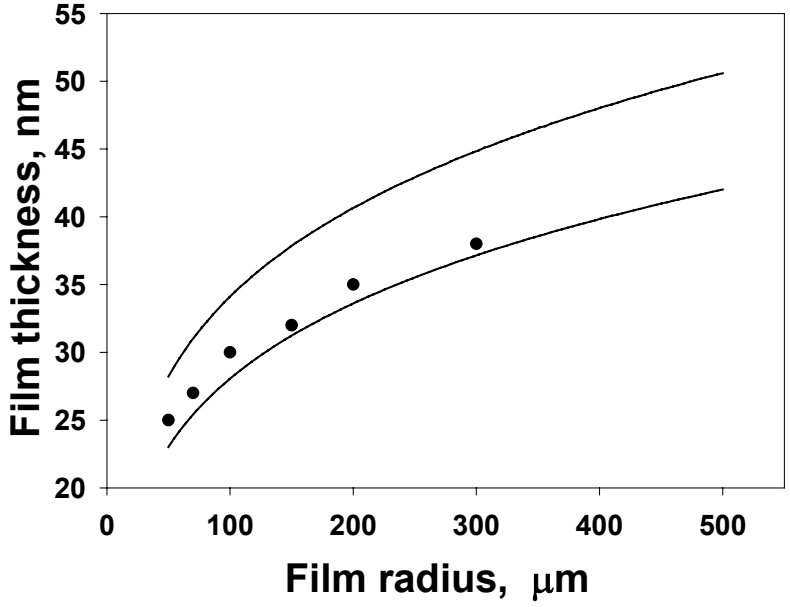

FIGURE 38. Critical thickness, h_{cr}, vs. radius, R, of emulsion films, toluene/water/toluene. The experimental points are data from Reference 495; the films are formed from a solution of 4.3×10^{-4} M SDS + 0.1 M NaCl. Curve 1 is the prediction of the simplified theory,[493] whereas Curve 3 is calculated using Equations 270 to 272; no adjustable parameters.

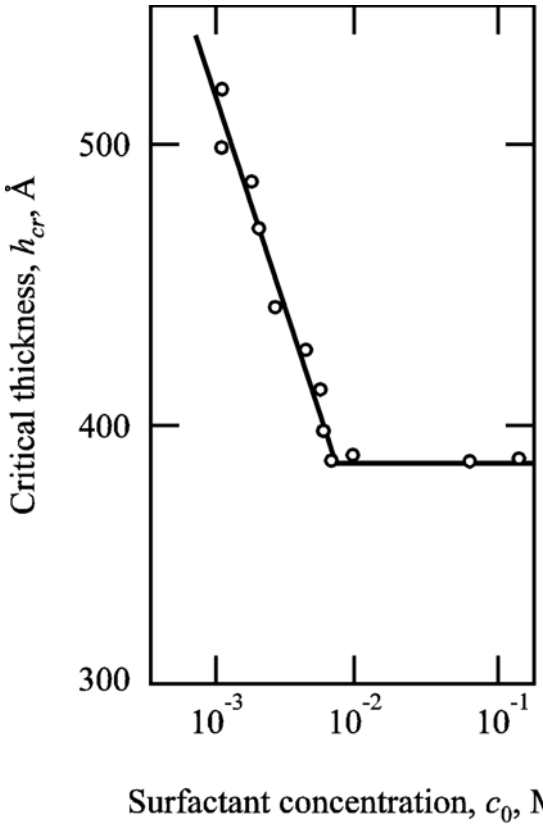

FIGURE 39. Dependence of the critical thickness, h_{cr}, of aniline films on the concentration of dodecanol, c_0. (Modified from Ivanov, I.B., *Pure Appl. Chem.*, 52, 1241, 1980.)

The emulsion film is formed between two toluene drops. Curve 1 is the prediction of a simpler theory, which identifies the critical thickness with the transitional one. [493] Curve 2 is the theoretical prediction of Equations 270 to 272 (no adjustable parameters); in Equation 171 for the Hamaker constant the electromagnetic retardation effect has also been taken into account.[278] In addition, Figure 39 shows the experimental dependence of the critical thickness vs. the concentration of surfactant (dodecanol) for aniline films. Figures 37 to 39 demonstrate that when the film area increases and/or the electrolyte concentration decreases the critical film thickness becomes larger.

The surface corrugations do not necessarily lead to film rupture. Instead, black spots (secondary films of very low thickness; h_2 in Figure 13) can be formed. The typical thickness of plane-parallel films at stage (c) (Figure 36(c)) is about 200 nm, while the characteristic thickness h_2 of the Newton black film (Figures 36(e) and (f)) is about 5 to 10 nm. The black spots either coalesce or grow in diameter, forming an equilibrium secondary (Newton black) film with a thickness h_2 and radius R_{sp}. These spots grow until they cover the whole film area.

After the entire film area is occupied by the Newton black film, the film radius increases until it reaches its equilibrium value, $R = R_{NBF}$ (Figure 36(f)). Finally, the equilibrium contact angle is established. For more details about this last stage of film thinning, see part IV.C of Reference 164.

5.5.2.4 Dependence of Emulsion Stability on the Droplet Size

Experimental data[497,498] shows that the emulsion stability correlates well with the lifetime of separate thin emulsion films or of drops coalescing with their homophase. To simplify the treatment we will consider here the lifetime of a single drop pressed against its homophase under the action of gravity. To define the *lifetime* (or drainage time) τ, we assume that in the initial and final moments the film has some known thicknesses h_{in} and h_f:

$$\tau = \int_{h_f}^{h_{in}} \frac{dh}{V_z} = \frac{3\pi\eta R_*^2}{2F_z}\left[\ln\left(\frac{h_{in}}{h_f}\right) + \frac{R^2}{h_f R_*}\left(1 - \frac{h_f}{h_{in}}\right) + \frac{R^4}{2h_f^2 R_*^2}\left(1 - \frac{h_f^2}{h_{in}^2}\right)\right] \tag{273}$$

The final thickness, h_f, may coincide with the critical thickness of film rupture. Equation 273 is derived for tangentially immobile interfaces from Equation 259 at a fixed driving force (no disjoining pressure).

In the case of gravity-driven coalescence of a droplet with its homophase, the driving force is given by Equation (269) and the mean drop radius is $R_* = 2R_d$. Then from Equations 269 and 273 one can deduce the droplet lifetime in the so-called Taylor regime, corresponding to nondeformed droplets ($R = 0$):

$$\tau_{\mathrm{Ta}} = \frac{6\pi\eta R_d^2}{F_z}\ln\left(\frac{h_{in}}{h_f}\right) = \frac{9\eta}{2gR_d\Delta\rho}\ln\left(\frac{h_{in}}{h_f}\right) \tag{274}$$

One sees that τ_{Ta} depends logarithmically on the ratio of the initial and final thickness. Moreover, in the Taylor regime the lifetime, τ, decreases with the increase of the driving force, F_z, and the drop radius, R_d. The latter fact is confirmed by the experimental data of Dickinson et al.[499] (see Figure 40).

In the case of deformed drops ($R \neq 0$), the drainage time, τ, is determined by Equation 273, and in such a case the fluid particles approach each other in the Reynolds regime.[432,496] The dependence of τ on R_d in Equation 273 is very complex, because the driving force, F_z, and the film radius, R, depend on R_d. The film radius can be estimated from the balance of the driving and capillary force:[432,496]

$$R^2 = \frac{F_z R_d}{2\pi\sigma} \tag{275}$$

In this regime, the lifetime, τ, increases with an increase of the driving force, F_z. This is exactly the opposite trend compared to results for the Taylor regime (see Equation 274). The result can be rationalized in view of Reynolds equation (Equation 262). In the numerator of this equation, $F_z \propto R_d^3$, whereas in the denominator $R^4 \propto R_d^8$ (see Equation 275); as a result, the drainage rate becomes proportional to R_d^{-5}, i.e., V_z decreases as the droplet radius increases.

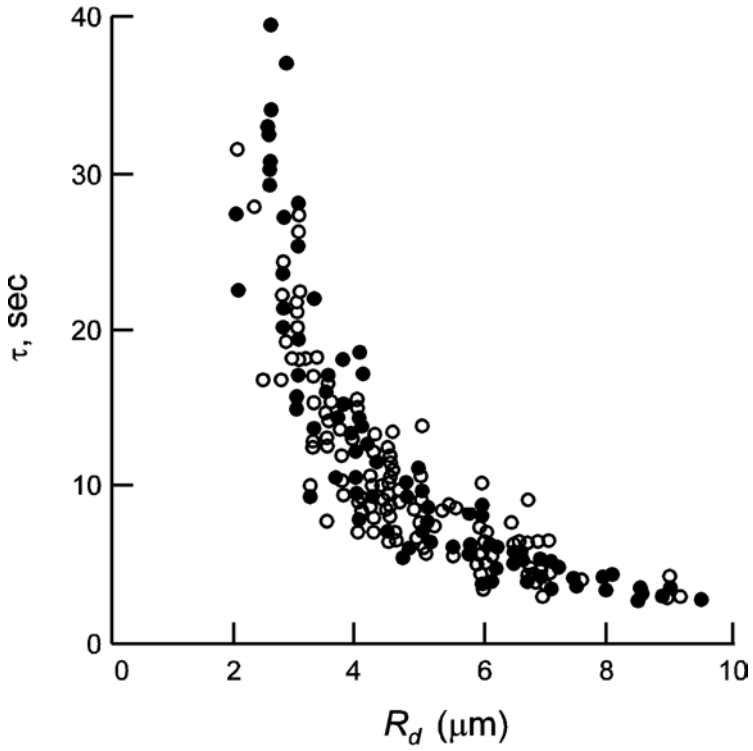

FIGURE 40. Experimental data of Dickinson et al.[499] for the lifetime, τ, of drops vs. their radius, R_d. The oil drops are pressed against their homophase by the buoyancy force. (From Dickinson, E., et al., *J. Chem. Soc. Faraday Trans.*, 84, 871, 1988. With permission.)

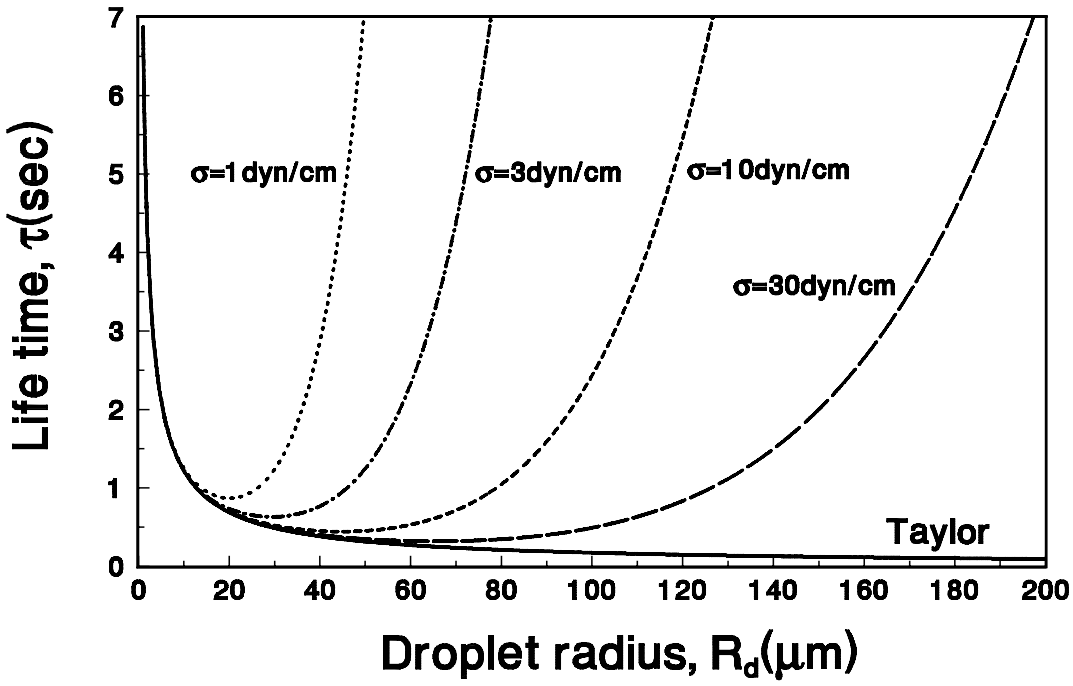

FIGURE 41. Calculated lifetime, τ, of drops approaching a fluid interface in Taylor regime (the solid line) and in Reynolds regime (the other lines) as a function of the droplet radius, R_d.

The numerical results from Equations 273 to 275 for the lifetime or drainage time, τ, vs. the droplet radius, R_d, are plotted in Figure 41 for parameter values typical for emulsion systems: $\Delta\rho = 0.2$ g/cm^3, $\eta = 1$ cP, $h_f = 5$ nm, and $h_{in} = R_d/10$. The various curves in Figure 41 correspond to different values of the surface tension, σ, shown in the figure. The left branches of the curves correspond to the Taylor regime (nondeformed droplets), whereas the right branches correspond to the Reynolds regime (formation of film between the droplets). In particular, the data shown in Figure 40 correspond to the left branch (Figure 41); in addition, data also complies with the right branch.[432] The presence of a deep minimum on the τ vs. R_d curve was first pointed out by I.B. Ivanov.[500,501] The theoretical dependencies in Figure 41 agree well with experimental data[502] for the lifetime of oil droplets pressed by the buoyancy force against a large oil/water interface in a system containing protein: bovine serum albumin.

5.5.3 Effect of Surface Mobility

The hydrodynamic interactions between fluid particles (drops, bubbles) suspended in a liquid medium depend on the interfacial mobility. In the presence of surfactants, the bulk fluid motion near an interface disturbs the homogeneity of the surfactant adsorption monolayer. The ensuing surface tension gradients act to restore the homogeneous equilibrium state of the monolayer. The resulting transfer of adsorbed surfactant molecules from the regions of lower surface tension toward the regions of higher surface tension constitutes the Marangoni effect. The analogous effect, for which the surface tension gradient is caused by a temperature gradient, is known as the Marangoni effect of thermocapillarity. In addition, the interfaces possess specific surface rheological properties (surface elasticity and dilatational and shear surface viscosities) which give rise to the so-called Boussinesq effect, (see below).[503]

5.5.3.1 Diffusive and Convective Fluxes at an Interface - Marangoni Effect

To take into account the influence of surfactant adsorption, Equations 240 and 241 are to be complemented with transport equations for each of the species (k = 1,2,...,N) in the bulk phases[410,413,436,437]

$$\frac{\partial c_k}{\partial t} + \mathrm{div}\left(c_k \mathbf{v} + \mathbf{j}_k\right) = r_k \qquad (k = 1,2, \ldots ,N) \tag{276}$$

where c_k and $\mathbf{j}_k$ are bulk concentration and flux, respectively, of the k-th species – note that $\mathbf{j}_k$ includes the molecular diffusive flux, the flux driven by external forces (e.g. electro-diffusion[428,436,437]) and the thermodiffusion flux;[436] and r_k is the rate of production due to chemical reactions, including surfactant micellization or micelle decay. The surface mass-balance equation for the adsorption, Γ_k, has the form[428,436,437]

$$\frac{\partial \Gamma_k}{\partial t} + \nabla_s \cdot \left(\Gamma_k \mathbf{v}_s + \mathbf{j}_k^s \right) = r_k^s + \mathbf{n} \cdot \langle \mathbf{j}_k \rangle \tag{277}$$

where **n** is the unit normal to the interface directed from phase 1 to phase 2; $\langle\ \rangle$ denotes the difference between the values of a given physical quantity at the two sides of the interface; ∇_s is the surface gradient operator;[504] $\mathbf{v}_s$ is the local material surface velocity; $\mathbf{j}_k^s$ is the two-dimensional flux of the *k*-th component along the interface; and r_k^s accounts for the rate of production of the *k*-th component due to interfacial chemical reactions and could include conformational changes of adsorbed proteins. Equation 277 provides a boundary condition for the normally resolved flux, $\mathbf{j}_k$. From another viewpoint, Equation 277 represents a two-dimensional analogue of Equation 276. The interfacial flux, $\mathbf{j}_k^s$, can also contain contributions from the interfacial molecular, electro-, and thermodiffusion. A simple derivation of the time-dependent convective-diffusion equation for surfactant transport along a deforming interface is given by Brenner et al.,[505-508] Davis et al.,[443] and Stone.[509] If the molecules are charged, the bulk and surfaces electro-diffusion fluxes can be expressed in the form[428,510,511]

$$\mathbf{j}_k = -D_k (\nabla c_k + z_k c_k \nabla \Phi), \qquad \mathbf{j}_k^s = -D_k^s (\nabla_s \Gamma_k + z_k \Gamma_k \nabla_s \Phi) \tag{278}$$

for the bulk and interfacial phase. Here, D_k and D_k^s are the bulk and surface collective diffusion coefficients, respectively, which are connected with the diffusion coefficients of individual molecules, $D_{k,0}$ and $D_{k,0}^s$, through the relationship:[511]

$$D_k = \frac{D_{k,0}}{kT} \frac{K_b(\phi_k)}{(1-\phi_k)} \frac{\partial \mu_k}{\partial \ln \phi_k}, \qquad D_k^s = \frac{D_{k,0}^s}{kT} K_s(\Gamma_k) \frac{\partial \mu_k^s}{\partial \ln \Gamma_k} \tag{279}$$

where μ_k and μ_k^s are the bulk and surface chemical potentials, respectively. The dimensionless bulk friction coefficient, K_b, accounts for the change in the hydrodynamic friction between the fluid and the particles (created by the hydrodynamic interactions between the particles). The dimensionless surface mobility coefficient, K_s, accounts for the variation of the friction of a molecule in the adsorption layer. Feng[512] has determined the surface diffusion coefficient, the dilatational elasticity, and the viscosity of a surfactant adsorption layer by theoretical analysis of experimental data. Stebe and Maldarelli[513,514] studied theoretically the surface diffusion driven by large adsorption gradients. The determination of bulk and surface diffusion coefficients from experimental data for the drainage of nitrobenzene films stabilized by different concentrations of dodecanol was reported.[510].

Note that the adsorption isotherms, relating the surface concentration, Γ_k, with the subsurface value of the bulk concentration, c_k (see Section 5.2.2.1 above), or the respective

kinetic equation 86 for adsorption under barrier control (see Section 5.2.2.5), should also be employed in the computations based on Equations 276 to 279 in order for a complete set of equations to be obtained.

Another boundary condition is the equation of the interfacial momentum balance:[414,432,437]

$$\nabla_s \cdot \boldsymbol{\sigma} = \mathbf{n} \cdot \left\langle \mathbf{P} + \mathbf{P}_b \right\rangle \tag{280}$$

where $\boldsymbol{\sigma}$ is the interfacial stress tensor, which is a two-dimensional counterpart of the bulk stress tensor, **P**. Moreover, a two-dimensional analogue of Equations 242, 245 and 246, called the Boussinesq-Scriven constitutive law, can be postulated for a fluid interface:[164,437,503,515-519]

$$\boldsymbol{\sigma} = \sigma_a \mathbf{I}_s + (\eta_{dl} - \eta_{sh})(\nabla_s \cdot \mathbf{v}_s)\mathbf{I}_s + \eta_{sh}[(\nabla_s \mathbf{v}_s) \cdot \mathbf{I}_s + \mathbf{I}_s \cdot (\nabla_s \mathbf{v}_s)^T] \tag{281}$$

where η_{dl} and η_{sh} are the interfacial dilatational and shear viscosities, respectively; $\mathbf{I}_s$ is the unit surface idemfactor;[504] and, as usual, σ_a is the scalar adsorption part of the surface tension (see Section 5.2.1.2.2). In view of the term $\sigma_a \mathbf{I}_s$ in Equation 281, the Marangoni effects are hidden in the left-hand side of the boundary condition (Equation 280) through the surface gradient of σ_a:

$$\nabla_s \sigma_a = -\sum_{k=1}^{N} \frac{E_k}{\Gamma_k} \nabla_s \Gamma_k - \frac{E_T}{T} \nabla_s T, \qquad E_k = -\left(\frac{\partial \sigma_a}{\partial \ln \Gamma_k} \right)_{T, \Gamma_{j \neq k}}, \qquad E_T = -\left(\frac{\partial \sigma_a}{\partial \ln T} \right)_{\Gamma_k} \tag{282}$$

where E_k is the Gibbs elasticity for the k-th surfactant species (see Equation 6) and E_T represents the thermal analogue of the Gibbs elasticity. The thermocapillary migration of liquid drops or bubbles and the influence of E_T on their motion are investigated in a number of works.[520-522]

In fact, Equation 281 describes an interface as a two-dimensional Newtonian fluid. On the other hand, a number of non-Newtonian interfacial rheological models have been described in the literature.[523-526] Tambe and Sharma[527] modeled the hydrodynamics of thin liquid films bounded by viscoelastic interfaces, which obey a generalized Maxwell model for the interfacial stress tensor. These authors[528,529] also presented a constitutive equation to describe the rheological properties of fluid interfaces containing colloidal particles. A new constitutive equation for the total stress was proposed by Horozov et al.[530] and Danov et al.[531] who applied a local approach to the interfacial dilatation of adsorption layers.

When the temperature is not constant, the bulk heat transfer equation complements the system and involves Equations 240, 241, and 276. The heat transfer equation is a special case of the energy balance equation. It should be noted that more than 20 various forms of the overall differential energy balance for multicomponent systems are available in the literature.[410,413] The corresponding boundary condition can be obtained as an interfacial

energy balance.[437,519] Based on the derivation of the bulk[532] and interfacial[531,533] entropy inequalities (using the Onsager theory), various constitutive equations for the thermodynamic mass, heat, and stress fluxes have been obtained.

5.5.3.2 Fluid Particles and Films of Tangentially Mobile Surfaces

When the surface of an emulsion droplet is mobile, it can transmit the motion of the outer fluid to the fluid within the droplet. This leads to a special pattern of the fluid flow and affects the dissipation of energy in the system. The problem concerning the approach of two nondeformed (spherical) drops or bubbles of pure phases has been investigated by many authors.[432,459,460,466,467,534-539] A number of solutions, generalizing the Taylor equation (Equation 260), have been obtained. For example, the velocity of central approach, V_z, of two spherical drops in pure liquid is related to the hydrodynamic resistance force, F_z, by means of a Padé-type expression derived by Davis et al.[466]

$$V_z = \frac{2hF_z}{3\pi\eta R_*^2}\frac{1+1.711\xi+0.461\xi^2}{1+0.402\,\xi}, \qquad \xi = \frac{\eta}{\eta_d}\sqrt{\frac{R_*}{2h}} \tag{283}$$

where h is the closest surface-to-surface distance between the two drops, and η_d is the viscosity of the disperse phase (the liquid in the droplets). In the limiting case of solid particles, one has $\eta_d \to \infty$, and Equation 283 reduces to the Taylor equation (Equation 260). Note that in the case of close approach of two drops ($\xi >> 1$), the velocity V_z is proportional to $\sqrt{h}$. This implies that the two drops can come into contact ($h = 0$) in a finite period of time ($\tau < \infty$) under the action of a given force, F_z, because the integral in Equation 273 is convergent for $h_f = 0$. This is in contrast with the case of immobile interfaces ($\xi << 1$), when $V_z \propto h$ and $\tau \to \infty$ for $h_f \to 0$.

In the other limiting case, that of two nondeformed gas bubbles ($\eta_d \to 0$) in pure liquid, Equation 283 cannot be used; instead, V_z can be calculated from the expression due to Beshkov et al.[539]

$$V_z = \frac{F_z}{2\pi\eta R_d \ln(R_d/h)} \tag{284}$$

Note that in this case $V_z \propto (\ln h)^{-1}$, and the integral in Equation 273 is convergent for $h_f \to 0$. In other words, the theory predicts that the lifetime, τ, of a doublet of two colliding spherical bubbles in pure liquid is finite. Of course, the real lifetime of a doublet of bubbles or drops is affected by the surface forces for $h < 100$ nm, which should be accounted for in F_z and which may lead to the formation of thin film in the zone of contact.[134,266]

Let us proceed with the case of deformed fluid particles (Figure 23). A number of theoretical studies[540-543] have been devoted to the thinning of plane-parallel liquid films of

pure liquid phases (no surfactant additives). Ivanov and Traykov[542] derived the following exact expressions for the velocity of thinning of an emulsion film:

$$V_z = \left(\frac{32\Delta P^2}{\rho_d \eta_d R^4} \right)^{1/3} h^{5/3}, \qquad \frac{V_z}{V_{\mathrm{Re}}} = \frac{1}{\varepsilon_e}, \qquad \varepsilon_e \equiv \left(\frac{\rho_d \eta_d h^4 F_z}{108\pi\eta^3 R^4} \right)^{1/3} \tag{285}$$

where ρ_d is the density of the disperse phase, V_{Re} is the Reynolds velocity defined by Equation 262, and ε_e is the so-called emulsion parameter. Substituting typical parameter values in Equations 283 and 285 one can check that at a given constant force the velocity of thinning of an emulsion film is smaller than the velocity of approach of two nondeformed droplets and much larger than V_{Re}. It is interesting to note that the velocity of thinning as predicted by Equation 285 does not depend on the viscosity of the continuous phase, η, and its dependence on the drop viscosity, η_d, is rather weak. There are experimental observations confirming this prediction (see Reference 32, p. 381).

The presence of surfactant adsorption monolayers decreases the mobility of the droplet (bubble) surfaces. This is due to the Marangoni effect (see Equation 282). From a general viewpoint, one may expect that the interfacial mobility will decrease with the increase of surfactant concentration until eventually the interfaces become immobile at high surfactant concentrations (see Section 5.5.2, above); therefore, a pronounced effect of surfactant concentration on the velocity of film drainage should be expected. This effect really exists (see Equation 286, below), but in the case of emulsions it is present only when the surfactant is predominantly soluble in the continuous phase.

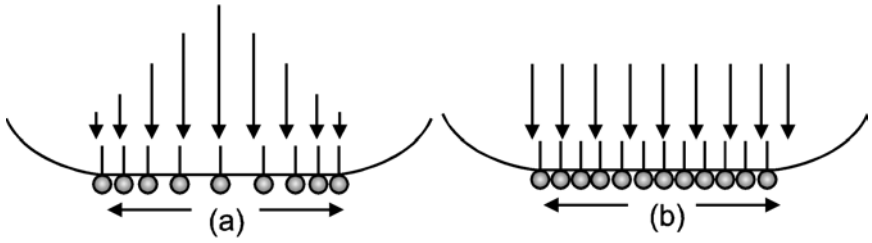

FIGURE 42. Damping of convection driven surface tension gradients by influx of surfactant from the drop interior. (a) Since the mass transport is proportional to the perturbation, the larger the perturbation the stronger the flux tending to eliminate it. (b) Uniform surfactant distribution is finally reached.

Traykov and Ivanov[543] established (both theoretically and experimentally) the interesting effect that when the surfactant is dissolved in the disperse phase (that is, in the emulsion droplets), the droplets approach each other just as in the case of pure liquid phases, i.e. Equation 285 holds. Qualitatively, this effect can be attributed to the fact that the convection-driven surface tension gradients are rapidly damped by the influx of surfactant from the drop interior; in this way, the Marangoni effect is suppressed. Indeed, during the film

drainage the surfactant is carried away toward the film border, and a nonequilibrium distribution, depicted in Figure 42(a), appears. Since, however, the mass transport is proportional to the perturbation, the larger the deviation from equilibrium the stronger the flux tending to eliminate the perturbation (the surfactant flux is denoted by thick arrows in Figure 42(b)). In this way, any surface concentration gradient (and the related Marangoni effect) disappears. The emulsion films in this case behave as if surfactant is absent.

In the opposite case, when the surfactant is soluble in the continuous phase, the Marangoni effect becomes operative and the rate of film thinning becomes dependent on the surface (Gibbs) elasticity (see Equation 282). Moreover, the convection-driven local depletion of the surfactant monolayers in the central area of the film surfaces gives rise to fluxes of bulk and surface diffusion of surfactant molecules. The exact solution of the problem[428,430,462,510,511,543] gives the following expression for the rate of thinning of symmetrical planar films (of both foam and emulsion type):

$$\frac{V_z}{V_{\mathrm{Re}}} = 1 + \frac{1}{\varepsilon_e + \varepsilon_f}, \qquad \frac{1}{\varepsilon_f} = \frac{6\eta D_s}{hE_G} + \frac{3\eta D}{\Gamma(\partial\sigma/\partial c)} \tag{286}$$

where, as usual, D and D_s are the bulk and interfacial collective diffusion coefficients (see Equation 279); E_G is the Gibbs elasticity; and ε_f is the so-called foam parameter.[496] In the special case of foam film, one substitutes $\varepsilon_e = 0$ in Equation 286. Note that the diffusive surfactant transport, which tends to restore the uniform adsorption monolayers, damps the surface tension gradients (which oppose the film drainage) and thus accelerates the film thinning. However, at large surfactant concentrations, the surface elasticity, E_G, prevails, ε_f increases, and consequently, the thinning rate decreases down to the Reynolds velocity, $V_z \to V_{\mathrm{Re}}$ (see Equation 286). Similar expressions for the rate of film thinning, which are appropriate for various ranges of values of the interfacial parameters, can be found in the literature.[164,431,432,477,544,545] A table describing the typical ranges of variation of the interfacial properties (Γ, E_G, D, D_s, $\partial\sigma/\partial c$, etc.) for emulsion and foam systems can be found in Reference 164, Table 2 therein. For $h < 100$ nm, the influence of the disjoining pressure should be taken into account (see Equation 262). In some studies,[164,440,527,546-549] the effect of the interfacial viscosity on the rate of thinning and the lifetime of plane-parallel films is investigated; this effect is found to decrease when the film thickness, h, becomes smaller and/or the film radius, R, becomes larger.

Note that Equation 286 does not hold in the limiting case of foam films ($\varepsilon_e = 0$) at low surfactant concentration, $\varepsilon_f \to 0$. The following expression is available for this special case:[496]

$$V_z / V_{\mathrm{Re}} = \left(1 + 1/\varepsilon_f\right) / \left[1 + 4h^2 / \left(3R^2\varepsilon_f\right)\right] \tag{287}$$

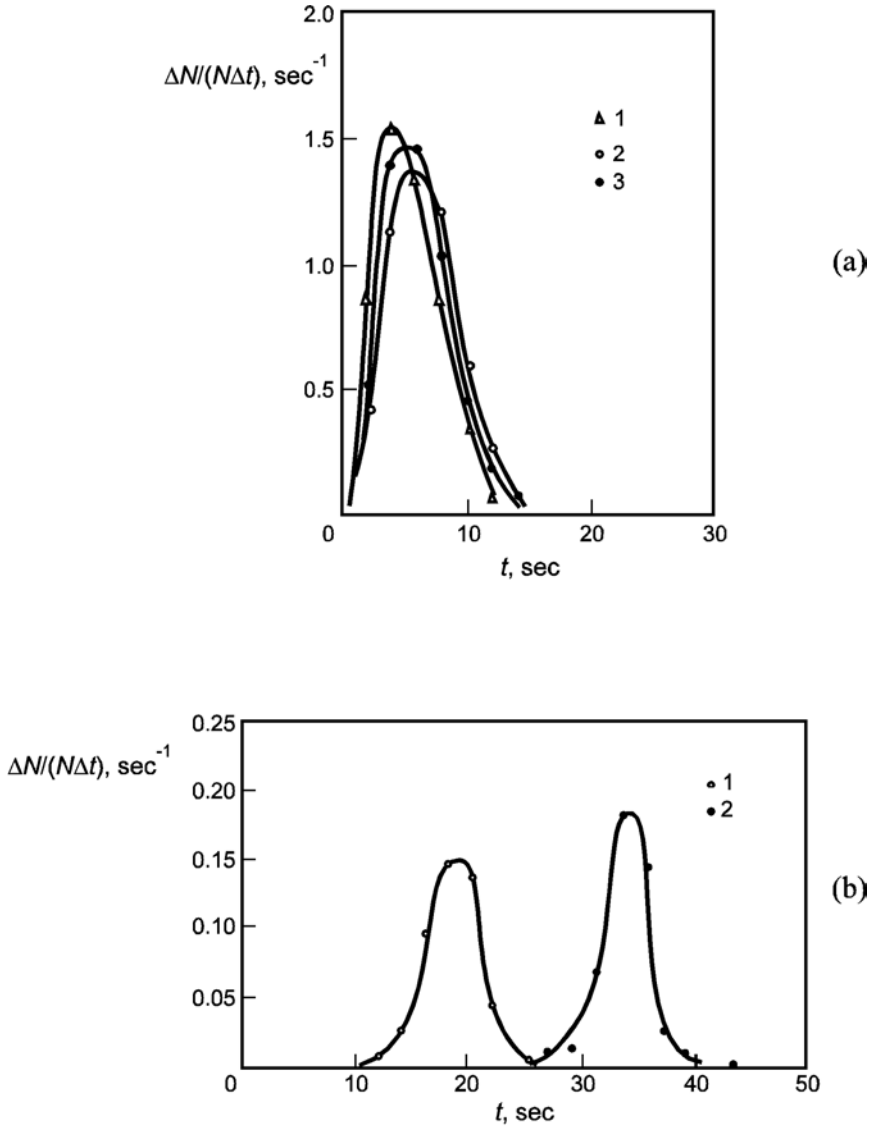

FIGURE 43. Histograms for the lifetimes of emulsion films: $\Delta N/N$ is the relative number of films which have ruptured during a time interval Δt = 0.4 sec. (a) Surfactant in the drops: benzene films between water drops containing surfactant sodium octylsulfonate of concentration (1) 0 *M*, (2) 10^{-4} *M*, and (3) 2×10^{-3} *M*; (b) Surfactant in the film: (1) benzene film with 0.1 *M* of lauryl alcohol dissolved in the film, (2) water film with 2×10^{-3} *M* of sodium octylsulfonate inside. (From Traykov, T.T. and Ivanov, I.B., *Int. J. Multiphase Flow*, 3, 471, 1977. With permission.)

The merit of this equation is that it gives as limiting cases both V_z/V_{Re} for foam films without surfactant, $\varepsilon_f \to 0$, and Equation 286 with $\varepsilon_e = 0$ (note that in the framework of the lubrication approximation, used to derive Equation 286, the terms $\propto h^2/R^2$ are being neglected). Equation 287 has also some shortcomings, which are discussed in Reference 496.

Another case, which is not described by the above equations, is the approach of two nondeformed (spherical) bubbles in the presence of surfactant. The velocity of approach in this case can be described by means of the expression:[431,440,501,511]

$$\frac{V_z}{V_{\mathrm{Ta}}} = \frac{h_{\mathrm{s}}}{2h}\{[\frac{h(1+b)}{h_s}+1]\ln[\frac{h_s}{h(1+b)}+1]-1\}^{-1} \tag{288}$$

where the parameters b and h_s account for the influence of bulk and surface diffusivity of surfactants, respectively. From Equation 279 these parameters are calculated to be:[511]

$$b \equiv \frac{3\eta c D_0 K_b(\phi)}{kT\Gamma^2(1-\phi)}, \qquad h_s \equiv \frac{6\eta D_0^s K_s(\Gamma)}{kT\Gamma} \tag{289}$$

A generalization of Equation 288 to the more complicated case of two nondeformed (spherical) emulsion droplets with account for the influence of surface viscosity has been published in Reference 440.

Returning back to the parameter values, we note that usually $\varepsilon_e << \varepsilon_f$ and $\varepsilon_e << 1$. Then, comparing the expressions for V_z/V_{Re} as given by Equations 285 and 286, one concludes that the rate of thinning is much greater when the surfactant is dissolved in the droplets (the disperse phase) in comparison with the case when the surfactant is dissolved in the continuous phase. This prediction of the theory was verified experimentally by measuring the number of films that rupture during a given period of time,[550] as well as the rate of thinning. When the surfactant was dissolved in the drop phase, the average lifetime was the same for all surfactant concentrations (Figure 43(a)), in agreement with Equation 285. For the emulsion film with the same, but inverted liquid phases (the former continuous phase becomes disperse phase and vice versa), i.e., the surfactant is in the film phase, the average lifetime is about 70 times longer – compare curve 3 in Figure 43(a) with curve 2 in Figure 43(b). The theoretical conclusions have been also checked and proved in experimental measurements with nitroethane droplets dispersed in aqueous solution of the cationic surfactant hexadecyl trimethyl ammonium chloride (HTAC).[498]

5.5.3.3 Bancroft Rule for Emulsions

There have been numerous attempts to formulate simple rules connecting the emulsion stability with the surfactant properties. Historically, the first one was the Bancroft rule[551] which states that "in order to have a stable emulsion the surfactant must be soluble in the continuous phase". A more sophisticated criterion was proposed by Griffin[552] who introduced the concept of hydrophilic-lipophilic balance (HLB). As far as emulsification is concerned, surfactants with an HLB number in the range 3 to 6 must form water-in-oil (W/O) emulsions, whereas those with HLB numbers from 8 to 18 are expected to form oil-in-water (O/W) emulsions. Different formulae for calculating the HLB numbers are available; for example, the Davies' expression[553] reads:

$$\mathrm{HLB} = 7 + (\text{hydrophilic group number}) - 0.475 n_c \tag{290}$$

where n_c is the number of -CH_2- groups in the lipophilic part of the molecule. Schinoda and Friberg[554] proved that the HLB number is not a property of the surfactant molecules only, but it also depends strongly on the temperature (for nonionic surfactants), on the type and concentration of added electrolytes, on the type of oil phase, etc. They proposed using the phase inversion temperature (PIT) instead of HLB for characterization of the emulsion stability.

Davis[555] summarized the concepts about HLB, PIT and Windsor's ternary phase diagrams for the case of microemulsions and reported topological ordered models connected with the Helfrich membrane bending energy. Since the curvature of surfactant lamellas plays a major role in determining the patterns of phase behavior in microemulsions, it is important to reveal how the optimal microemulsion state is affected by the surface forces determining the curvature energy.[163,556,557] It is hoped that lattice models[558,559] and membrane curvature models[560,561] will lead to predictive formulae for the microemulsion design.

Ivanov et al.[496,500,501,562] have proposed a semiquantitative theoretical approach that provides a straightforward explanation of the Bancroft rule for emulsions. This approach is based on the idea of Davies and Rideal[32] that both types of emulsions are formed during the homogenization process, but only the one with lower coalescence rate survives. If the initial drop concentration for both emulsions is the same, the coalescence rates for the two emulsions – $(\text{Rate})_1$ for emulsion 1 and $(\text{Rate})_2$ for emulsion 2 (see Figure 44) – will be proportional to the respective coalescence rate constants, $k_{c,1}$ and $k_{c,2}$ (see Section 5.6, below), and inversely proportional to the film lifetimes, τ_1 and τ_2:

$$\frac{(\text{Rate})_1}{(\text{Rate})_2} \approx \frac{k_{c,1}}{k_{c,2}} \approx \frac{\tau_2}{\tau_1} \approx \frac{V_1}{V_2} \tag{291}$$

Here V_1 and V_2 denote the respective velocities of film thinning. After some estimates based on Equations 262, 273, 285, and 286, one can express the ratio in Equation 291 in the form

$$\frac{(\text{Rate})_1}{(\text{Rate})_2} \approx (486\rho_d D_s^3)^{1/3}\left(\frac{h_{cr,1}^3}{h_{cr,2}^2}\right)^{1/3}\left(\frac{\eta_d}{R^2}\right)^{1/3}\frac{P_c-\Pi_1}{E_G\left(P_c-\Pi_2\right)^{2/3}} \tag{292}$$

where $h_{cr,1}$ and $h_{cr,2}$ denote the critical thickness of film rupture for the two emulsions in Figure 44. Many conclusions can be drawn, regarding the type of emulsion to be formed:

1. If the disjoining pressures, Π_1 and Π_2, are zero, the ratio in Equation 292 will be very small. Hence, emulsion 1 (surfactant soluble in the continuous phase) will coalesce much more slowly and it will survive. This underlines the crucial importance of the surfactant location (which is connected with its solubility), thus providing a theoretical foundation for Bancroft's rule. The emulsion behavior in this case will be controlled almost entirely by the hydrodynamic factors (kinetic stability).

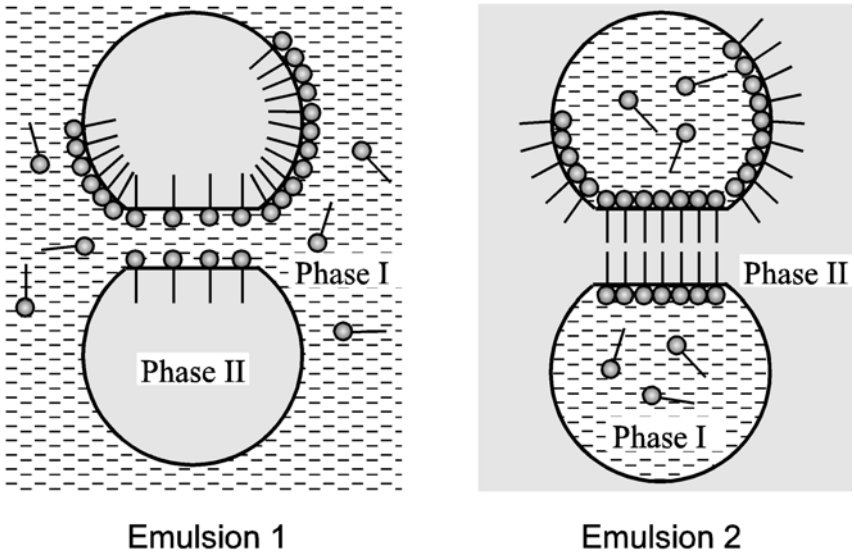

FIGURE 44. The two possible types of emulsions obtained just after the homogenization; the surfactant is soluble into Phase I.

2. The disjoining pressure, Π, plays an important role. It can substantially change and even reverse the behavior of the system if it is comparable by magnitude with the capillary pressure, P_c. For example, if $(P_c - \Pi_2) \rightarrow 0$ at a finite value of $P_c - \Pi_1$ (which may happen, for example, for an O/W emulsion with oil soluble surfactant), the ratio in Equation 292 may become much larger than unity, which means that emulsion 2 will become thermodynamically stable. In some cases the stabilizing disjoining pressure is large enough for emulsions with a very high volume fraction of the disperse phase (above 95% in some cases) to be formed.[563]

3. The Gibbs elasticity, E_G, favors the formation of emulsion 1, because it slows down the film thinning. On the other hand, increased surface diffusivity, D_s, decreases this effect, because it helps the interfacial tension gradients to relax, thus facilitating the formation of emulsion 2.

4. The film radius, R, increases and the capillary pressure, P_c, decreases with the drop radius, R_d. Therefore, larger drops will tend to form emulsion 1, although the effect is not very pronounced.

5. The difference in critical thicknesses of the two emulsions only slightly affects the rate ratio in Equation 292, although the value of h_{cr} itself is important.

6. The viscosity of the continuous phase, η, has no effect on the rate ratio, which depends only slightly on the viscosity of the drop phase, η_d. This is in agreement with the experimental observations (see Reference 32, p. 381).

7. The interfacial tension, σ, affects the rate ratio directly only through the capillary pressure, $P_c = 2\sigma/R_d$. The electrolyte primarily affects the electrostatic disjoining pressure, Π, which decreases as the salt content increases, thus destabilizing the O/W emulsion. It can also influence the stability by changing the surfactant adsorption (including the case of nonionic surfactants).

8. The temperature strongly affects the solubility and surface activity of nonionic surfactants.[3] It is well known that at higher temperature nonionic surfactants become more oil soluble, which favors the W/O emulsion. Thus solubility may change the type of emulsion formed at the PIT. The surface activity has numerous implications, the most important being the change of the Gibbs elasticity, E_G, and the interfacial tension, σ.

9. Surface active additives (cosurfactants, demulsifiers, etc.), such as fatty alcohols in the case of ionic surfactants, may affect the emulsifier partitioning between the phases and its adsorption, thereby changing the Gibbs elasticity and the interfacial tension. The surface-active additive may also change the surface charge (mainly by increasing the spacing among the emulsifier ionic headgroups), thus decreasing the repulsive electrostatic disjoining pressure and favoring the W/O emulsion. Polymeric surfactants and adsorbed proteins increase the steric repulsion between the film surfaces. They may favor either O/W or W/O emulsions, depending on their conformation at the interface and their surface activity.

10. The interfacial bending moment, B_0, can also affect the type of the emulsion, although this is not directly visible from Equation 292. (Note that $B_0 = -4k_cH_0$, where H_0 is the so-called spontaneous curvature and k_c is the interfacial curvature elastic modulus;[129] typically, B_0 is of the order of 5×10^{-11}N.) Usually, for O/W emulsions, B_0 opposes the flattening of the droplet surfaces in the zone of collision (Figure 23), but for W/O emulsions favors the flattening.[134] This effect might be quantified by the expression for the curvature contribution in the energy of droplet-droplet interaction:[134]

$$W_c = -2\pi R^2 B_0 / R_d, \qquad (R/R_d)^2 << 1 \tag{293}$$

It turns out that $W_c > 0$ for the droplet collisions in an O/W emulsion, while $W_c < 0$ for a W/O emulsion;[134] consequently, the interfacial bending moment stabilizes the O/W emulsions but destabilizes the W/O ones. There is supporting experimental evidence[564] for microemulsions, i.e., for droplets of rather small size. Moreover, the effect of the bending moment can be important even for micrometer-sized droplets.[134] This is due to the fact that the bent area increases faster ($R^2 \propto R_d^2$) than the bending energy per unit area decreases ($W_c/R^2 \propto 1/R_d$) when the droplet radius, R_d, increases (see Equation 293).

For micron-sized emulsion droplets the capillary pressure can be so high that a film may not appear between the drops. In such case, instead of Equation 292, one can use analogous expression for nondeformed (spherical) drops.[565].

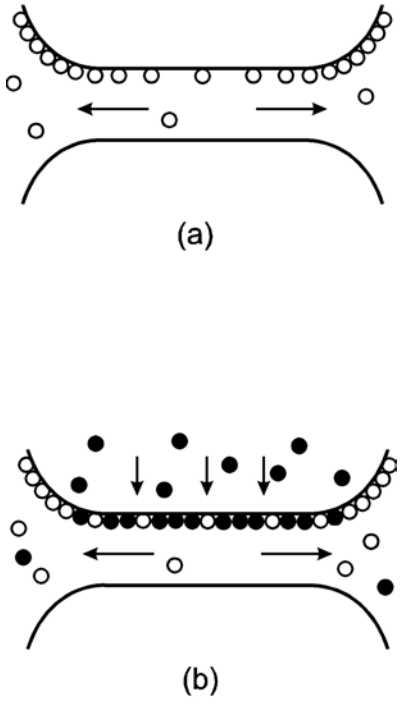

FIGURE 45. (a) Nonuniform surface distribution of an emulsifier due to drag from the draining film. (b) Suppression of the surface tension gradients by a demulsifier added in the drop phase.

5.5.3.4 Demulsification

It has been known for a long time[32] that one way to destroy an emulsion is to add a surfactant, which is soluble in the drop phase – this method is termed "chemical demulsification". To understand the underlying process, let us consider two colliding emulsion droplets with film formed in the zone of collision (see Figures 23 and 45). As discussed above, when the liquid is flowing out of the film, the viscous drag exerted on the film surfaces (from the side of the film interior) carries away the adsorbed emulsifier toward the film periphery. Thus, a nonuniform surface distribution of the emulsifier (shown in Figure 45(a) by empty circles) is established. If demulsifier (the closed circles in Figure 45(b)) is present in the drop phase, it will occupy the interfacial area freed by the emulsifier. The result will be a saturation of the adsorption layer, as shown in Figure 45(b). If the demulsifier is sufficiently surface active, its molecules will be able to decrease substantially, and even to eliminate completely, the interfacial tension gradients, thus changing the emulsion to type 2 (see Figure 44 and Section 5.5.3.2, above). This leads to a strong increase in the rate of film thinning, rapid drop coalescence, and emulsion destruction.[500,501] The above mechanism suggests that the demulsifier has to possess the following properties:

1. It must be soluble in the drop phase or in both phases, but in the latter case its solubility in the drop phase must be much higher.
2. Its diffusivity and concentration must be large enough to provide a sufficiently large demulsifier flux toward the surfaces and thus eliminate the gradients of the interfacial tension.
3. Its surface activity must be comparable and even higher than that of the emulsifier; otherwise, even though it may adsorb, it will not be able to suppress the interfacial tension gradients.

In regard to defoaming, various mechanisms are possible, which are discussed in Section 5.7, below.

5.5.4. INTERACTIONS IN NONPREEQUILIBRATED EMULSIONS

The common nonionic surfactants are often soluble in both water and oil phases. In the practice of emulsion preparation, the surfactant (the emulsifier) is initially dissolved in one of the liquid phases and then the emulsion is prepared by homogenization. In such a case, the initial distribution of the surfactant between the two phases of the emulsion is not in equilibrium; therefore, surfactant diffusion fluxes appear across the surfaces of the emulsion droplets. The process of surfactant redistribution usually lasts from many hours to several days, until finally equilibrium distribution is established. The diffusion fluxes across the interfaces, directed either from the continuous phase toward the droplets or the reverse, are found to stabilize both thin films and emulsions. In particular, even films, which are thermodynamically unstable, may exist several days because of the diffusion surfactant transfer; however, they rupture immediately after the diffusive equilibrium has been established. Experimentally, this effect manifests itself in phenomena called *cyclic dimpling*[566] and *osmotic swelling*.[567] These two phenomena, as well as the equilibration of two phases across a film,[568,569] are described and interpreted below.

5.5.4.1 Surfactant Transfer from Continuous to Disperse Phase (Cyclic Dimpling)

The phenomenon of cyclic dimpling was first oserved[501,566] with xylene films intervening between two water droplets in the presence of the nonionic emulsifier Tween 20 or Tween 80 (initially dissolved in water but also soluble in oil). The same phenomenon also has been observed with other emulsion systems.

After the formation of such an emulsion film, it thins down to an equilibrium thickness (approximately 100 nm), determined by the electrostatic repulsion between the interfaces.

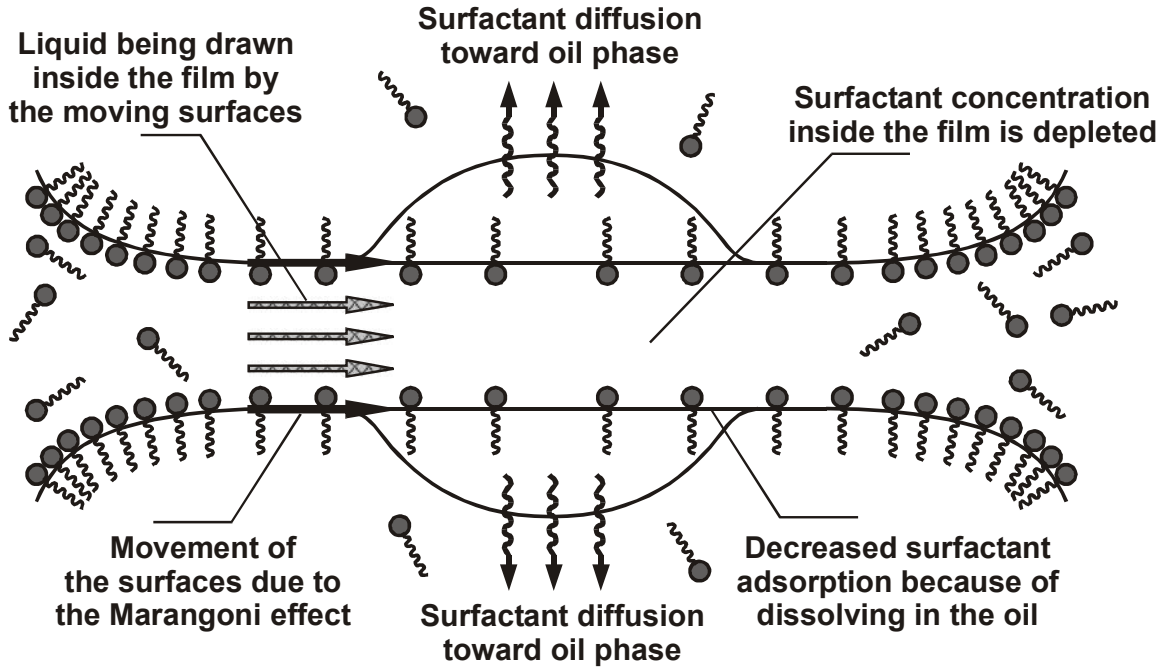

(a)

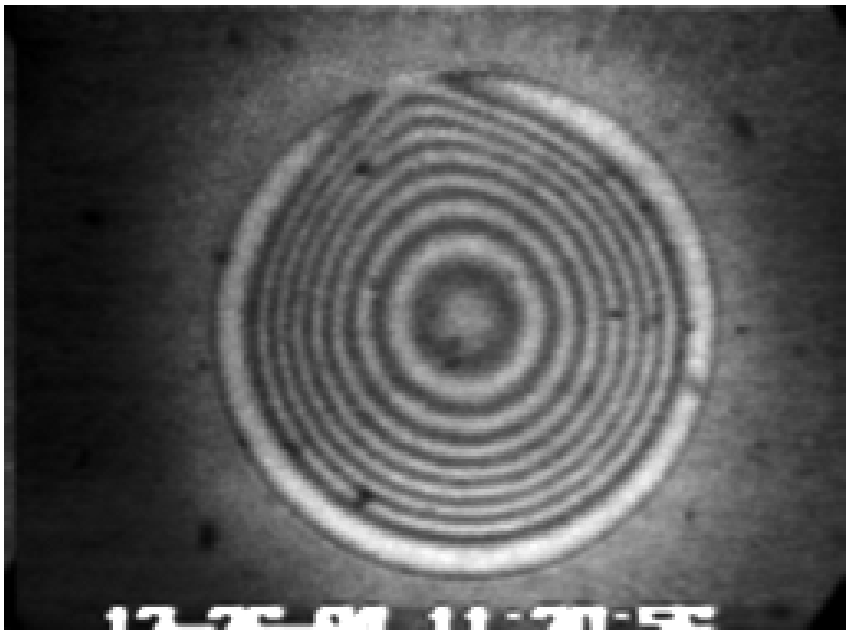

(b)

FIGURE 46. Spontaneous cyclic dimpling caused by surfactant diffusion from the aqueous film toward the two adjacent oil phases. (a) Schematic presentation of the process. (b) Photograph of a large dimple just before flowing out; the interference fringes in reflected light allow determination of the dimple shape.

As soon as the film reaches this thickness, a dimple spontaneously forms in the film center and starts growing (Figure 46(a)). When the dimple becomes bigger and approaches the film periphery, a channel forms connecting the dimple with the aqueous phase outside the film (Figure 46(b)). Then, the water contained in the dimple flows out leaving an almost plane-parallel film behind. Just afterwards, a new dimple starts to grow and the process repeats again. The period of this cyclic dimpling remains approximately constant for many cycles and could be from a couple of minutes up to more than 10 minutes. It was established that this process is driven by the depletion of the surfactant concentration on the film surfaces due to the dissolving of surfactant in the adjacent drop phases. The depletion triggers a surface convection flux along the two film surfaces and a bulk diffusion flux in the film interior. Both fluxes are directed toward the center of the film. The surface convection causes a tangential movement of the film surfaces; the latter drag along a convective influx of solution in the film, which feeds the dimple. Thus, the cyclic dimpling appears to be a process leading to stabilization of the emulsion films and emulsions due to the influx of additional liquid in the region between the droplets which prevents them from a closer approach, and eventually, from coalescence.

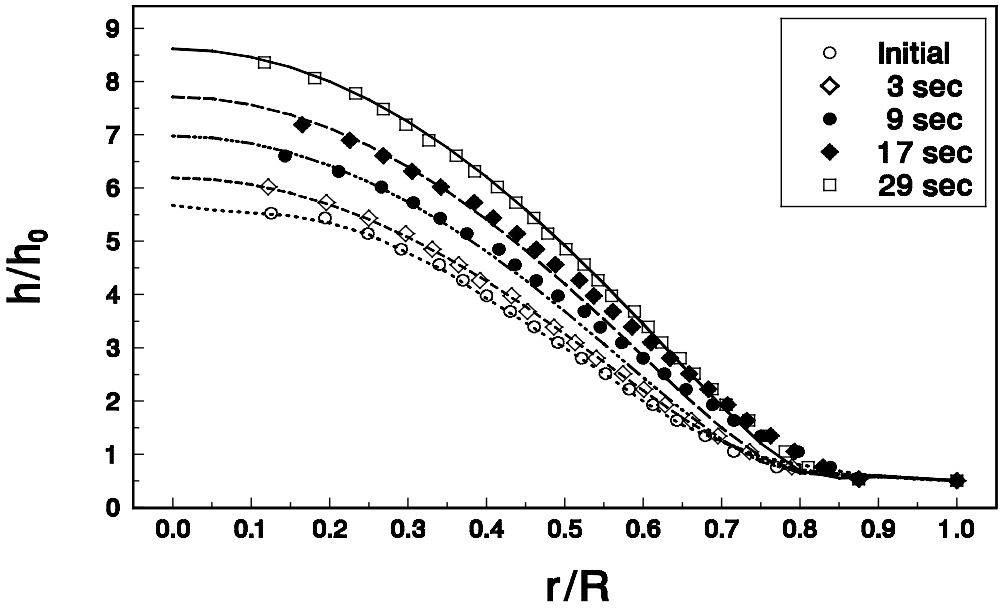

FIGURE 47. Comparison between the theory of cyclic dimpling (the lines) and the experimental data (the points) for the dimple shape, $h(r)$, determined from the interference fringes (see Figure 46(b)); emulsifier is anionic surfactant sodium nonylphenol polyoxyethylene-25 sulfate and the oil phase is styrene.

Combining the general equation of films with deformable interfaces (Equation 255), the mass balance (Equations 276 and 277), and the boundary condition for the interfacial stresses (Equation 281), one can derive:[570]

$$\frac{\partial h}{\partial t}+\frac{1}{3\eta r}\frac{\partial}{\partial r}\left\{rh^3\frac{\partial}{\partial r}\left[\frac{\sigma}{r}\frac{\partial}{\partial r}\left(r\frac{\partial h}{\partial r}\right)+\Pi(h)\right]\right\}=\frac{1}{2r}\frac{\partial}{\partial r}\left(\frac{jhr^2}{\Gamma}\right) \tag{294}$$

where j is the diffusion flux in the drop phase, and, as usual, r is radial coordinate, $h(r,t)$ is the film thickness, σ is surface tension, Γ is adsorption, and Π is disjoining pressure. The comparison between the numerical calculations based on Equation 294 and the experimental data for the cyclic dimpling with the anionic surfactant sodium nonylphenol polyoxyethylene-25 sulfate show a very good agreement (see Figure 47). The experimental points are obtained from the interference fringes (see Figure 46). The shape in the initial moment, $t = 0$, serve as an initial condition for determining $h(r,t)$ by solving Equation 294. The curves for $t = 3$, 9, 17, and 29 sec represent theoretical predictions. The scaling parameters along the h and r axes in Figure 47 are $h_0 = 350$ nm and $R = 320$ μm, the latter being the film radius; the only adjustable parameter is the diffusion flux, j.

5.5.4.2 Surfactant Transfer from Disperse to Continuous Phase (Osmotic Swelling)

Velev et al.[498] reported that emulsion films, formed from pre-equilibrated phases containing the nonionic surfactant Tween and 0.1-M NaCl, spontaneously thin down to Newton black films (thickness ≈ 10 nm) and then rupture. However, when the nonionic surfactant Tween 20 or Tween 60 is initially dissolved in the xylene drops and the film is formed from the nonpre-equilibrated phases, no black film formation and rupture is observed.[501,567] Instead, the films have a thickness above 100 nm, and one observes formation of channels of larger thickness connecting the film periphery with the film center (Figure 48). One may observe that the liquid is circulating along the channels for a period from several hours to several days. The phenomenon continues until the redistribution of the surfactant between the phases is accomplished. This phenomenon occurs only when the background surfactant concentration in the continuous (the aqueous) phase is not lower than the CMC. These observations can be interpreted in the following way.

Since the surfactant concentration in the oil phase (the disperse phase) is higher than the equilibrium concentration, surfactant molecules cross the oil-water interface toward the aqueous phase. Thus, surfactant accumulates within the film, because the bilk diffusion throughout the film is not fast enough to transport promptly the excess surfactant into the Plateau border. As the background surfactant concentration in the aqueous phase is not less than CMC, the excess surfactant present in the film is packed in the form of micelles (denoted by black dots in Figure 48(a)). This decreases the chemical potential of the surfactant inside the film. Nevertheless, the film is subjected to osmotic swelling because of the increased concentration of micelles within. The excess osmotic pressure

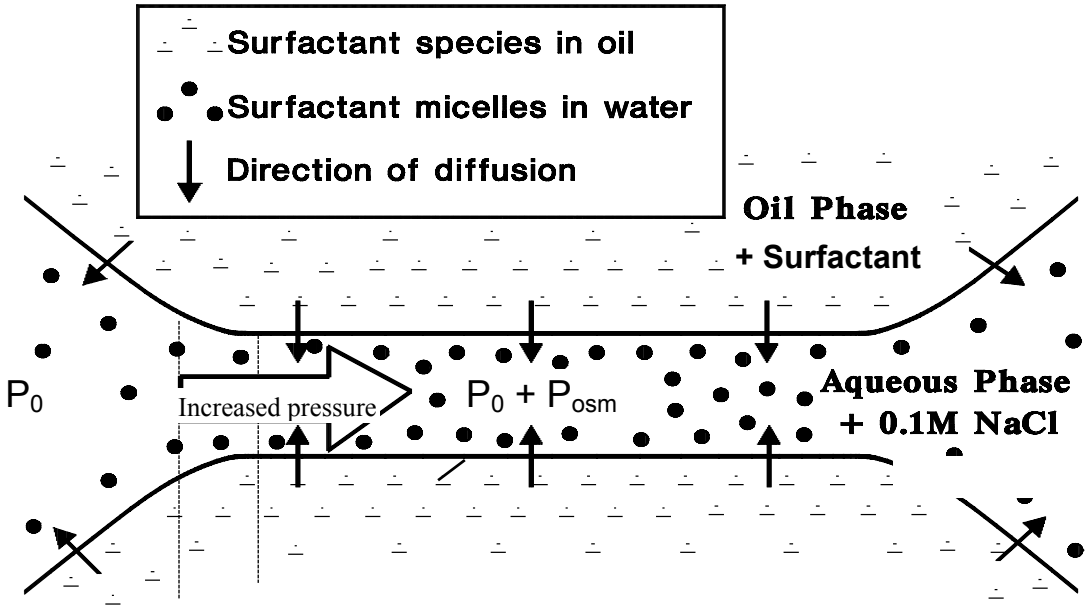

a

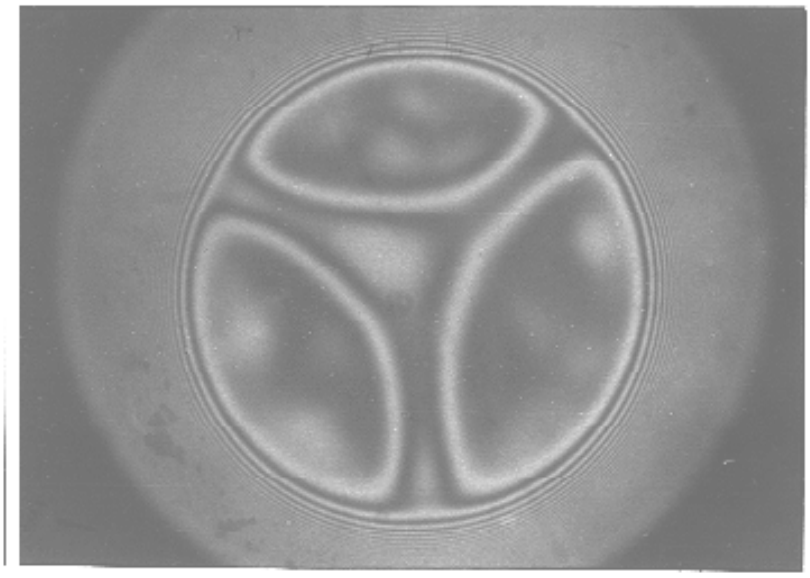

b

FIGURE 48. Osmotic swelling of an aqueous film formed between two oil droplets. (a) The surfactant dissolved in the oil is transferred by diffusion toward the film, where it forms micelles, the osmotic effects of which increase the local pressure. (b) Photograph of a typical pattern from a circular film with channels.

$$P_{\text{osm}} = kTC_{\text{mic}} \geq P_c \tag{295}$$

counterbalances the outer capillary pressure and arrests further thinning of the film. Moreover, the excess osmotic pressure in the film gives rise to a convective outflow of solution: this is the physical origin of the observed channels (Figure 48(b)).

Experimental data[501,567] show that the occurrence of the above phenomenon is the same for initial surfactant concentration in the water varying from 1 up to 500 times the CMC, if only some amount of surfactant is also initially dissolved also in the oil. This fact implies that the value of the surfactant chemical potential inside the oil phase is much greater than that in the aqueous phase, the latter being closer to its value at the CMC in the investigated range of concentrations.

5.5.4.3 Equilibration of Two Droplets across a Thin Film

In the last two sections, we considered mass transfer from the film toward the droplets and the reverse, from droplets toward the film. In both cases, the diffusion fluxes lead to stabilization of the film. Here we consider the third possible case corresponding to mass transfer from the first droplet toward the second one across the film between them. In contrast with the former two cases, in the last case the mass transfer is found to destabilize the films. Experimentally, the diffusion transfer of alcohols, acetic acid, and acetone was studied.[571,572] The observed destabilization of the films can be attributed to the appearance of Marangoni instability,[568] which manifests itself through the growth of capillary waves at the interfaces, which eventually can lead to film rupture.

The Marangoni instabilities can appear not only in thin films, but also in the simpler case of a single interface. In this case, the Marangoni instability may bring about spontaneous emulsification. This effect has been theoretically investigated by Sterling and Scriven,[573] whose work stimulated numerous theoretical and experimental studies on spontaneous emulsification. Lin and Brenner[574] examined the role of the heat and mass transfer in an attempt to check the hypothesis of Holly[575] that the Marangoni instability can cause the rupture of tear films. Their analysis was extended by Castillo and Velarde,[576] who accounted for the tight coupling of the heat and mass transfer and showed that it drastically reduces the threshold for Marangoni convection. Instability driven by diffusion flux of dissolved oil molecules across an asymmetric liquid film (oil-water-air film) has been theoretically investigated.[569] It was found that even small decrements of the water-air surface tension, caused by the adsorbed oil, are sufficient to trigger the instability.

5.5.5 HYDRODYNAMIC INTERACTION OF A PARTICLE WITH AN INTERFACE

There are various cases of particle-interface interactions, which require separate theoretical treatment. The simpler case is the hydrodynamic interaction of a solid particle with a solid interface. Other cases are the interactions of fluid particles (of tangentially mobile or immobile interfaces) with a solid surface; in these cases, the hydrodynamic interaction is accompanied by deformation of the particle. On the other hand, the colloidal particles (both solid and fluid) may hydrodynamically interact with a fluid interface, which thereby undergoes a deformation. In the case of fluid interfaces, the effects of surfactant adsorption, surface diffusivity, and viscosity affect the hydrodynamic interactions. A special class of problems concerns particles attached to an interface which are moving throughout the interface. Another class of problems is related to the case when colloidal particles are confined in a restricted space within a narrow cylindrical channel or between two parallel interfaces (solid and/or fluid); in the latter case, the particles interact simultaneously with both film surfaces.

The theoretical contributions are limited to the case of low Reynolds number[421,422,498,577-579] (mostly for creeping flows, see part 5.5.1), avoiding the difficulties arising from the nonlinearity of the equations governing the fluid motion at higher velocities. Indeed, for low Reynolds numbers, the term $\mathbf{v}\cdot\nabla\mathbf{v}$ in the Navier-Stokes equation (see Equations 247 to 249) is negligible, and one may apply the method of superposition to solve the resulting linear set of equations. This means that one may first solve the simpler problems about the particle elementary motions: (1) particle translation (without rotation) in an otherwise immobile liquid, (2) particle rotation (without translation) in an otherwise immobile liquid, and (3) streamlining of an immobile particle by a Couette or Poiseuille flow. Once the problems about the elementary motions have been solved, one may obtain the linear and angular velocity of the real particle motion combining the elementary flows. The principle of combination is based on the fact that for low Reynolds numbers the particle acceleration is negligible, and the net force and torque exerted on the particle must be zero. In other words, the hydrodynamic drag forces and torques originating from the particle translation and rotation are counterbalanced by those originating from the streamlining:

$$\mathbf{F}_{\text{translation}} + \mathbf{F}_{\text{rotation}} + \mathbf{F}_{\text{streamlining}} = \mathbf{0}, \qquad \mathbf{M}_{\text{translation}} + \mathbf{M}_{\text{rotation}} + \mathbf{M}_{\text{streamlining}} = \mathbf{0} \qquad (296)$$

That is the reason why we will now consider expressions for **F** and **M** for various types of elementary motions.

5.5.5.1. Particle of Immobile Surface Interacting with a Solid Wall

The force and torque exerted on a solid particle were obtained in the form of a power series with respect to R_d/l, where R_d is the particle radius and l is the distance from the center of the particle to the wall. Lorentz[580] derived an asymptotic expression for the motion of a sphere

along the normal to a planar wall with an accuracy of up to R_d/l. Faxen[581] developed the method of reflection for a sphere moving between two parallel planes in a viscous fluid. Using this method, Wakiya[582] considered the cases of motion in flow of Couette and Poiseuille; however, the method employed by him cannot be applied to small distances to the wall.[442] The next important step was taken by Dean and O'Neil[583] and O'Neil,[584] who found an exact solution for the force and the torque acting on a spherical particle moving tangentially to a planar wall at an arbitrary distance from the wall. The limiting case of small distances between the particle and the wall was examined by several authors.[433-435,585] Instead of an exact solution of the problem, the authors derived asymptotic formulae for the force and torque. Keh and Tseng[586] presented a combined analytical-numerical study for the slow motion of an arbitrary axisymmetric body along its axis of revolution, the latter being normal to a planar surface. The inertial migration of a small solid sphere in a Poiseuille flow was calculated by Schonberg and Hinch[587] for the case when the Reynolds number for the channel is of the order of unity.

Below we present expressions for the forces and torques for some of the elementary motions. In all cases we assume that the Reynolds number is small, the coordinate plane xy, is parallel to the planar wall and h is the shortest surface-to-surface distance from the particle to the wall.

First, we consider the case of a pure translational motion: a solid spherical particle of radius R_d which translates along the y-axis with a linear velocity U and angular velocity $\omega \equiv 0$ in an otherwise quiescent fluid. In spite of the fact that the particle does not rotate, it experiences a torque, **M,** directed along the x-axis, due to friction with the viscous fluid. The respective asymptotic expressions[433-435] for the components of the drag force, **F**, and torque, **M**, read:

$$F_x = 0 \ , \qquad F_y = -6\pi\eta U R_d f_y \ , \qquad M_x = -8\pi\eta U R_d^2 m_x \ , \qquad M_y = 0 \tag{297}$$

$$f_y = \left(\frac{8}{15} + \frac{16}{375}\frac{h}{R_d}\right)\ln\left(\frac{2R_d}{h}\right) + 0.58461 + O\left(\frac{h}{R_d}\right) \tag{298}$$

$$m_x = \left(\frac{1}{10} + \frac{43}{250}\frac{h}{R_d}\right)\ln\left(\frac{2R_d}{h}\right) - 0.26227 + O\left(\frac{h}{R_d}\right) \tag{299}$$

where f_y, and m_x, are dimensionless drag force and torque coefficients, respectively.

Second, we consider the case of pure rotation: a solid spherical particle of radius R_d is situated at a surface-to-surface distance, h, from a planar wall and rotates with angular velocity, ω, around the x-axis in an otherwise quiescent fluid. The corresponding force and torque resultants are[433-435]

$$F_x = 0 \ , \qquad F_y = -6\pi\eta\omega R_d^2 f_y \, , \qquad M_x = -8\pi\eta\omega R_d^3 m_x \ , \qquad M_y = 0 \tag{300}$$

$$f_y = \frac{2}{15}\ln\left(\frac{R_d}{h}\right) - 0.2526 + O\left(\frac{h}{R_d}\right), \qquad m_x = \frac{2}{5}\ln\left(\frac{R_d}{h}\right) + 0.3817 + O\left(\frac{h}{R_d}\right) \tag{301}$$

From Equations 297 to 301, it follows that the force and the torque depend weakly (logarithmically) on the distance, h, as compared to the Taylor or Reynolds laws (Equations 260 and 261).

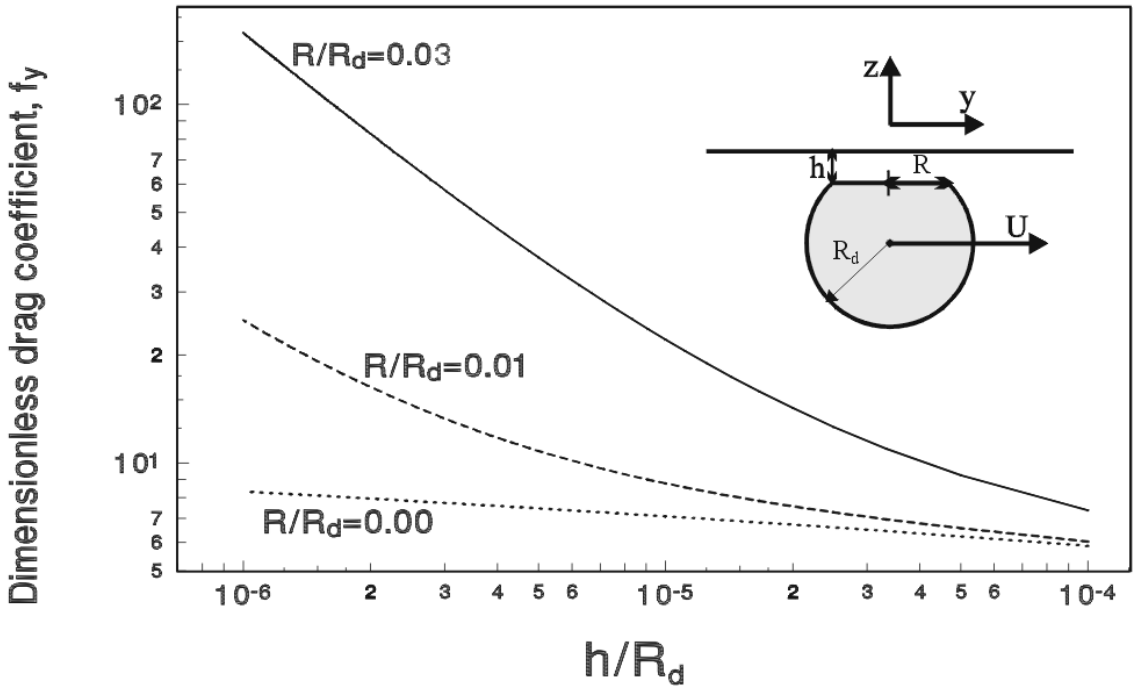

FIGURE 49. Deformed fluid particle (the inset) moving tangentially to an immobile solid surface: plot of the dimensionless drag coefficient, f_y, vs. the dimensionless film thickness, h/R_d, for three values of the dimensionless film radius, R/R_d (see Equation 303).

As discussed in Sections 5.5.2.1 and 5.5.3.2, a fluid particle in the presence of high surfactant concentration can be treated as a deformable particle of tangentially immobile surfaces. Such a particle deforms when pressed against a solid wall (see the inset in Figure 49). To describe the drag due to the film intervening between the deformed particle and the wall, one may use the expression derived by Reynolds[423] for the drag force exerted on a planar solid ellipsoidal disc, which is parallel to a solid wall and is moving along the y-axis at a distance h from the wall:

$$F_x = 0\,, \qquad F_y = -\pi\eta U\frac{h}{ab} \tag{302}$$

Here, a and b are the semi-axes of the ellipse; for a circular disc (or film), one has $a = b = R$. By combining Equations 297 and 298 with Equation 302, one can derive an expression for the net drag force experienced by the deformed particle (the inset in Figure 49) when it moves along the y-axis with a linear velocity U:

$$F_y = -6\pi\eta U R_d f_y, \qquad f_y = \frac{R^2}{6hR_d} + \left(\frac{8}{15} + \frac{16}{375}\frac{h}{R_d}\right)\ln\left(\frac{2R_d}{h}\right) + 0.58461 + O\left(\frac{h}{R_d}\right) \tag{303}$$

Here, as usual, h and R denote the film thickness and radius, and R_d is the curvature radius of the spherical part of the particle surface. The dependence of the dimensionless drag coefficient, f_y, on the distance h for different values of the ratio R/R_d is illustrated in Figure 49. The increase of R/R_d and the decrease of h/R_d may lead to an increase of the drag force, f_y, by an order of magnitude. That is the reason why the film between a deformed particle and a wall can be responsible for the major part of the energy dissipation. Moreover, the formation of doublets and flocks of droplets separated by liquid films seems to be of major importance for the rheological behavior of emulsions.

5.5.5.2 Fluid Particles of Mobile Surfaces

Let us start with the case of pure phases, when surfactant is missing and the fluid-liquid interfaces are mobile. Under these conditions, the interaction of an emulsion droplet with a planar solid wall was investigated by Ryskin and Leal,[588] and numerical solutions were obtained. A new formulation of the same problem was proposed by Liron and Barta.[589] The case of a small droplet moving in the restricted space between two parallel solid surfaces was solved by Shapira and Haber.[590,591] These authors used the Lorentz reflection method to obtain analytical solutions for the drag force and the shape of a small droplet moving in Couette flow or with constant translational velocity.

The more complicated case, corresponding to a viscous fluid particle approaching the boundary between two pure fluid phases (all interfaces deformable), was investigated by Yang and Leal,[592,593] who succeeded in obtaining analytical results.

Next, we proceed with the case when surfactant is present and the Marangoni effect becomes operative. Classical experiments carried out by Lebedev[594] and Silvey[595] show that the measured velocity of sedimentation, U, of small fluid droplets in a viscous liquid (pure liquid phases assumed) does not obey the Hadamar[596] and Rybczynski[597] equation:

$$F = 2\pi\eta U R_d \frac{3\eta_d + 2\eta}{\eta_d + \eta} \tag{304}$$

where F is the drag force. The limiting case $\eta_d \to 0$ corresponds to bubbles, whereas in the other limit, $\eta_d \to \infty$, Equation 304 describes solid particles. Note that Equation 304 is derived for the motion of a spherical fluid particle (drop or bubble) of viscosity η_d in a liquid of viscosity η in the absence of any surfactant. The explanation of the contradiction between theory and experiment[594,595] turned out to be very simple: even liquids which are pure from the viewpoint of the spectral analysis may contain some surface-active impurities, whose bulk

concentration might be vanishingly low, but which can provide a dense adsorption layer at the restricted area of the fluid particle surface. Then, the effects of Gibbs elasticity and interfacial viscosity substantially affect the drag coefficient of the fluid particle. The role of the latter two effects was investigated by Levich[436], Edwards et al.[437] and He et al.[598] for the motion of an emulsion droplet covered with a monolayer of nonsoluble surfactant (adsorption and/or desorption not present). These authors used the Boussinesq-Scriven constitutive law of a viscous fluid interface (Equation 281), and established that only the dilatational interfacial viscosity, η_{dl}, but not the shear interfacial viscosity, η_{sh}, influences the drag force. If the surfactant is soluble in both phases and the process of adsorption is diffusion-controlled (see Section 5.2.2.1) the generalization of Equation 304 is

$$F = 2\pi\eta U R_d [3 - (1 + \frac{\eta_d}{\eta} + \frac{2\eta_{dl}}{\eta R_d} + \frac{R_d E_G}{3\eta D_s} \frac{2}{2 + 2\frac{R_d D}{h_a D_s} + \frac{R_d D_d}{h_{d,a} D_s}})^{-1}] \tag{305}$$

where D_d is the surfactant diffusion coefficient in the drop phase; c and c_d are the concentrations of surfactant in the continuous and drop phases, respectively; $h_a = \partial\Gamma/\partial c$ and $h_{d,a} = \partial\Gamma/\partial c_d$ are the slopes of adsorption isotherms with respect to the surfactant concentration. In the limiting case without surfactant Equation 305 is reduced to the Hadamar[596] and Rybczynski[597] equation (Equation 304).

Danov et al.[251,599-602] investigated theoretically the hydrodynamic interaction of a fluid particle with a fluid interface in the presence of surfactant. The numerical results of these authors reveal that there is a strong influence of both shear and dilatational interfacial viscosities on the motion of the fluid particle when the particle-interface distance, h, is approximately equal to or smaller than the particle radius, R_d. For example, in the presence of an external force acting parallel to the interface (along the y-axis), the stationary motion of the spherical particle close to the viscous interface is a superposition of a translation along the y-axis with velocity V_y and a rotation (around the x-axis) with an angular velocity, ω_x (see the inset in Figure 50(a)). The numerical results of Danov et al.[601,602] for V_y and ω_x normalized by the Stokes velocity, $V_{\text{Stokes}} = F/(6\pi\eta R_d)$, are plotted in Figures 50(a) and (b) vs. h/R_d for four different types of interfaces: (1) solid particle and solid wall (see Equations 297 to 299); (2) fluid particle and fluid interface for $K = E = 100$; (3) the same system as (2) but for $K = E = 10$; (4) the same system as (2) but for $K = E = 1$, where

$$K \equiv \eta_{dl}/(\eta R_d), \qquad E \equiv \eta_{sh}/(\eta R_d) \tag{306}$$

(For the definition of the interfacial viscosities, η_{dl} and η_{sh}, see Equation 281). As seen in Figure 50(a), the velocity of the sphere, V_y, is less than V_{Stokes} for the solid (1) and the highly viscous (2) interfaces, and V_y noticeably decreases when the distance h decreases. However, in case (4), corresponding to low surface viscosities, the effect is quite different: V_y/V_{Stokes} is greater than unity (the sphere moves faster near the interface than in the bulk), and its

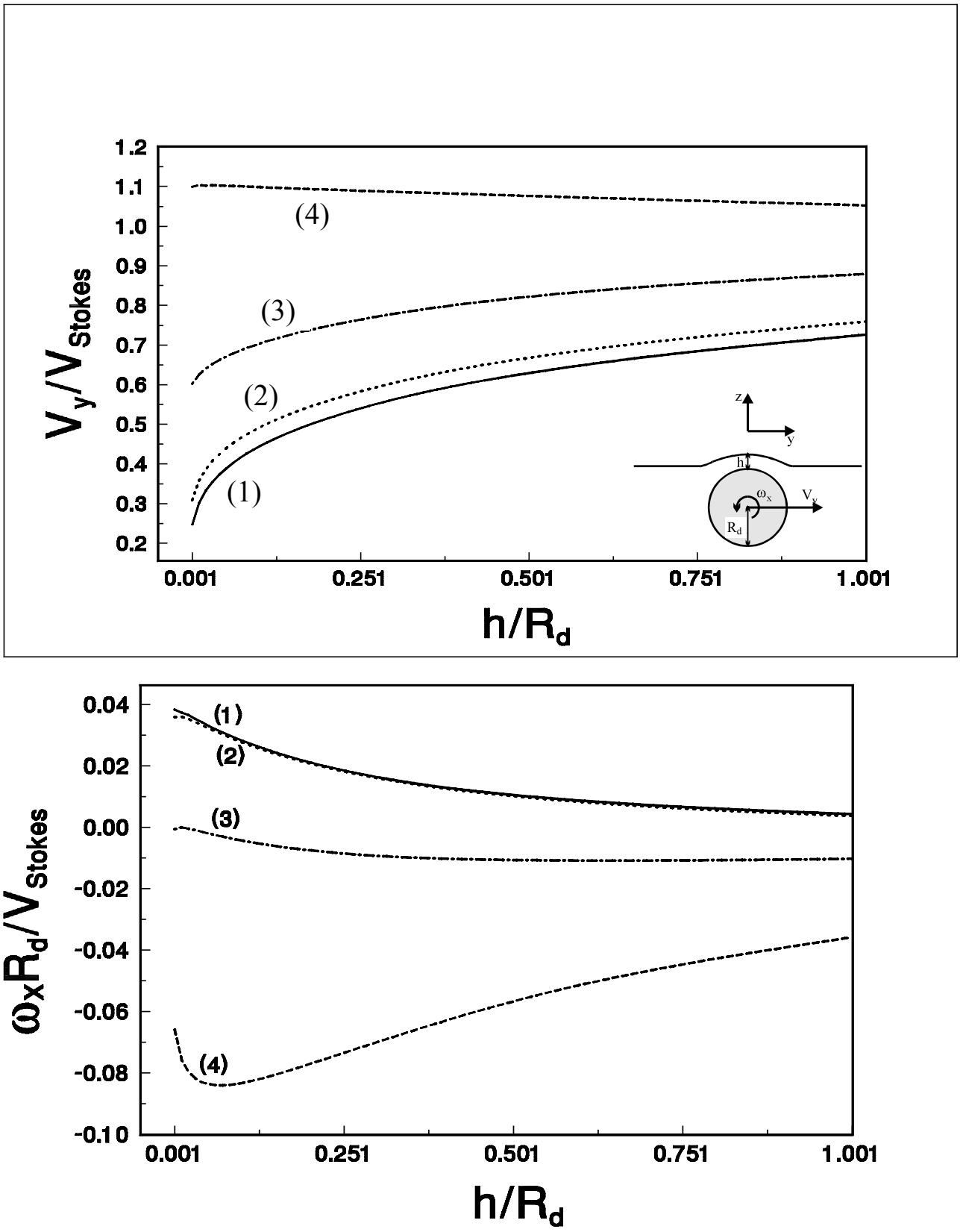

FIGURE 50. Spherical particle moving tangentially to a viscous interface: plots of the stationary dimensionless linear (V_y/V_{Stokes}) (a) and angular ($\omega_x R_d/V_{\text{Stokes}}$) velocities vs. the dimensionless thickness, h/R_d. The curves corresponds to various surface viscosities: (1) $K = E = \infty$ (solid surfaces); (2) $K = E = 100$; (3) $K = E = 10$, and (4) $K = E = 1$ (see Equation 306).

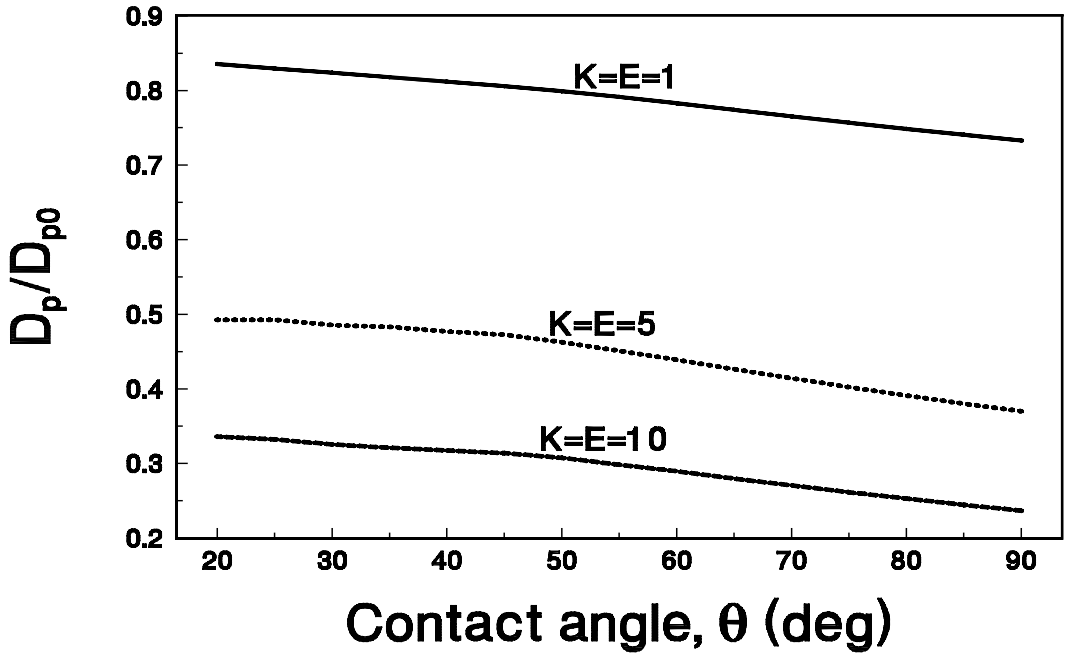

(a)

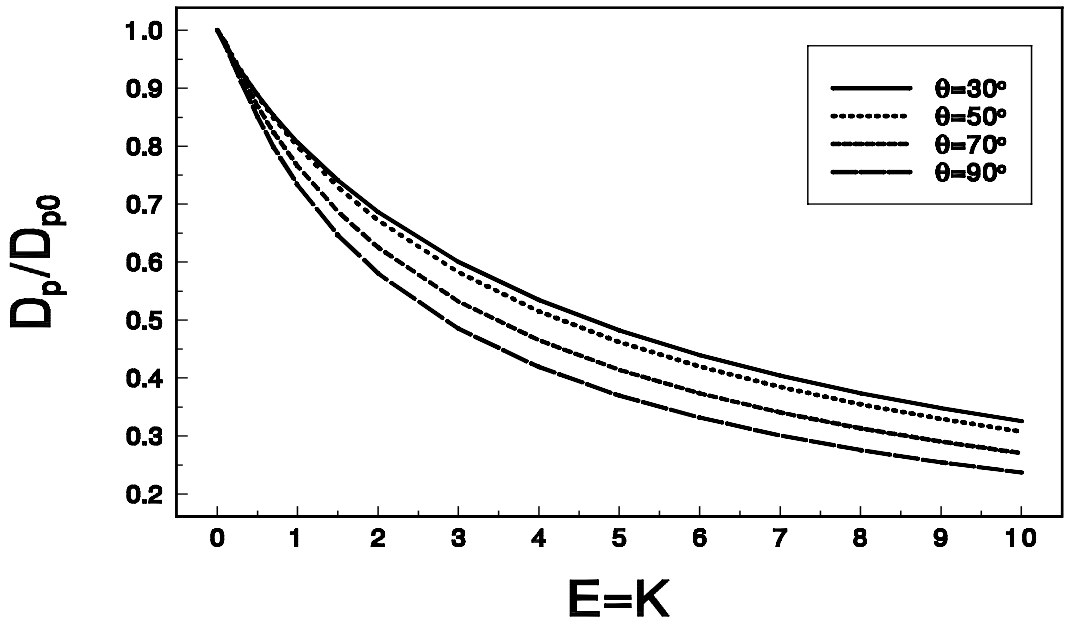

(b)

FIGURE 51. Effect of adsorbed surfactant on the surface diffusivity, D_p, of a Brownian particle attached to a fluid interface: (a) plot of D_p/D_{p0} vs. particle contact angle, θ, for various surface viscosities, (see Equation 306); (b) plot of D_p/D_{p0} vs. the dimensionless surface viscosity, $K = E$, for various θ.

dependence on h is rather weak. The result about the angular velocity, ω_x, is also intriguing (Figure 50(b)). The stationary rotation of a sphere close to a solid (1) or highly viscous (2) interface is in positive direction, i.e., $\omega_x > 0$. For the intermediate interfacial viscosity (3), the sphere practically does not rotate; whereas, for the interfaces of low viscosity (4), the drop rotates in the opposite direction, i.e., $\omega_x < 0$. The inversion of the sign of ω_x is due to the fact that the friction of the particle with the bulk fluid below it (see the inset in Figure 50(a)) becomes stronger than the friction with the interface above the particle.

Finally we consider the case of a solid particle attached to a liquid-fluid interface. This configuration is depicted in Figure 17(e); note that the position of the particle along the normal to the interface is determined by the value of the three-phase contact angle. Stoos and Leal[603] investigated the case when such an attached particle is subjected to a flow directed normally to the interface. These authors determined the critical capillary number, beyond which the captured particle is removed from the interface by the flow.

Danov et al.[251] examined the case of an attached particle moving along a liquid-gas interface under the action of an applied force directed tangentially to the interface. The effect of the contact angle (the depth of immersion), as well as the effect of adsorbed surfactant on the drag force, were investigated. These authors also calculated the surface diffusion coefficient of a Brownian particle attached to the liquid surface. Let D_p and D_{p0} be the particle surface diffusion coefficient in the presence and in the absence of surfactant, respectively. In Figure 51(a), we plot the results for D_p/D_{p0} vs. the solid-liquid-gas contact angle, θ, for three different values of the parameters K and E characterizing the surface viscosities (see Equation 306): (1) $K = E = 1$; (2) $K = E = 5$, and (3) $K = E = 10$. The relatively small slope of the curves in Figure 51(a) indicates that D_p/D_{p0} depends less significantly on the contact angle, θ, than on the surface viscosity characterized by K and E. Note, however, that D_{p0} itself depends markedly on θ: the absolute value of D_{p0} is smaller for the smaller values of θ (for deeper immersion of the particle in the liquid phase). Figure 51(b) presents the calculated dependence of D_p/D_{p0} on the surface viscosity characterized by K and E ($K = E$ is used in the calculations) for various fixed values of the contact angle, θ. Apparently, the particle mobility decreases faster for the smaller values of K and then tends to zero insofar as the fluid surface "solidifies" for the higher values of the surface viscosities. The experimental data from measurements of the drag coefficient of spherical particles attached to fluid interfaces[250] showed very good agreement with the predictions of the theory.[251]

The role of surface viscosity and elasticity on the motion of a solid particle trapped in a thin film, at an interface, or at a membrane of a spherical vesicle has been recently investigated in References 604 and 605. The theoretical results[604,605] have been applied to process the experimental data for the drag coefficient of polystyrene latex particles moving

throughout the membrane of a giant lipid vesicle;[606-612] thus the interfacial viscosity of membranes has been determined.

5.5.6 BULK RHEOLOGY OF DISPERSIONS

The description of the general rheological behavior of colloidal dispersions requires information regarding the drag forces and torques experienced by the individual particles.[278,613,614] In dilute systems, the hydrodynamic interactions between the particles can be neglected and their motion can be treated independently. In contrast, when the particle concentration is higher, the effect of hydrodynamic interactions between a spherical particle and an interface on the drag force and torque acquires considerable importance. The viscosity and the collective diffusion coefficient of colloidal dispersions can be strongly affected also by long-range surface forces, like the electrostatic double layer force, see Section 5.9.2.4 below.

Long ago Einstein[615] obtained a formula for the diffusion coefficient for solid spheres in the dilute limit:

$$D = kT/(6\pi\eta_m R_p) \tag{307}$$

where R_p is the particle radius and η_m is the viscosity of the liquid medium. This relation was later generalized by Kubo[616] for cases when the hydrodynamic resistance becomes important. The further development in this field is reviewed by Davis.[577]

The particle-particle interactions lead to a dependence of the viscosity, η, of a colloidal dispersion on the particle volume fraction, ϕ. Einstein[617] showed that for a suspension of spherical particles in the dilute limit:

$$\eta = \eta_m [1 + 2.5\phi + O(\phi^2)] \tag{308}$$

Later Taylor[618] generalized Equation 308 for emulsion systems taking into account the viscous dissipation of energy due to the flow inside the droplets. Oldroyd[619] took into account the effect of surface viscosity and generalized the theory of Taylor[618] to diluted monodisperse emulsions whose droplets have viscous interfaces. Taylor,[620] Fröhlich and Sack,[621] and Oldroyd[622] applied asymptotic analysis to derive the next term in Equation 308 with respect to the capillary number. Thus the effect of droplet interfacial tension was included. This generalization may be important at high shear rates. Another important generalization is the derivation of appropriate expressions for the viscosity of suspensions containing particles with different shapes.[421,422] A third direction of generalization of Equation 308 is to calculate the next term in the series with respect to the volume fraction, ϕ. Batchelor[623] took into account the long-range hydrodynamic interaction between the particles to derive:

$$\eta = \eta_m [1 + 2.5\phi + 6.2\phi^2 + O(\phi^3)] \tag{309}$$

From a mathematical viewpoint, Equation 309 is an exact result; however, from a physical viewpoint, Equation 309 is not entirely adequate to the real dispersions, as not only the long-range hydrodynamic interactions are operative in colloids. A number of empirical expressions have been proposed in which the coefficient multiplying ϕ^2 is varying between 5 and 15.[624] The development of new powerful numerical methods during the last five years helped for a better understanding of the rheology of emulsions.[625-633] The simple shear and Brownian flow of dispersions of elastic capsules, rough spheres, and liquid droplets were studied in References 626, 630, 632, and 633. The effect of insoluble surfactants and the drop deformation on the hydrodynamic interactions and on the rheology of dilute emulsions are the subject of investigation in References 627, 629, 631. Loewenberg and Hinch[625,628] discussed the basic ideas of the numerical simulations of concentrated emulsion flows. These works are aimed at giving a theoretical interpretation of various experimental results for dilute and concentrated dispersions. When the Peclet number is not small, the convective term in the diffusion equation (Equations 276 and 277) cannot be neglected and the respective problem has no analytical solution. Thus a complex numerical investigation has to be applied.[634,635]

The formulae of Einstein,[615,617] Taylor,[618] and Oldroyd,[619] have been generalized for dilute emulsions of mobile surfaces with account for the Gibbs elasticity and the bulk and surface diffusion and viscosity:[636]

$$\frac{\eta}{\eta_m} = 1 + (1 + \frac{3}{2} < \varepsilon_m >)\phi + \mathrm{O}(\phi^2), \qquad < \varepsilon_m > \equiv \sum R_d^3 \varepsilon_m / \sum R_d^3 \tag{310}$$

where $< \varepsilon_m >$ is the average value of the interfacial mobility parameter, ε_m, for all droplets in the control volume. The mobility parameter of individual drops, ε_m, and the effective surfactant diffusion coefficient, D_{eff}, are:[636]

$$\varepsilon_m \equiv [\frac{\eta_{\mathrm{d}}}{\eta_m} + \frac{2}{5}(\frac{R_d E_{\mathrm{G}}}{2\eta_m D_{\mathrm{eff}}} + \frac{3\eta_{\mathrm{dl}} + 2\eta_{\mathrm{sh}}}{R_d \eta_m})] / [1 + \frac{\eta_{\mathrm{d}}}{\eta_m} + \frac{2}{5}(\frac{R_d E_{\mathrm{G}}}{2\eta_m D_{\mathrm{eff}}} + \frac{3\eta_{\mathrm{dl}} + 2\eta_{\mathrm{sh}}}{R_d \eta_m})] \tag{311}$$

$$D_{\mathrm{eff}} \equiv D_{\mathrm{s}} + \frac{R_d D}{2h_a} + \frac{R_d D_d}{3h_{d,a}} \tag{312}$$

(see Equation 305 and below). If the droplet size distribution in the emulsion, and the interfacial rheological parameters are known, then the average value $<\varepsilon_m>$ can be estimated. For monodisperse emulsions the average value, $<\varepsilon_m>$, and the interfacial mobility parameter, ε_m, are equal. In the special case of completely mobile interfaces, that is $R_d E_{\mathrm{G}}/(\eta_m D_{\mathrm{eff}}) \to 0$ and $(3\eta_{\mathrm{dl}} + 2\eta_{\mathrm{sh}})/(R_d \eta_m) \to 0$, the mobility parameter, ε_m, does not depend on the droplet size, and from Equation 311 and 312 the Taylor[618] formula is obtained. It is important to note that the Taylor formula takes into account only the bulk properties of the phases (characterized by

η_d/η_m); in such a case ε_m is independent of R_d and the Taylor equation is applicable also to polydisperse emulsions. If only the Marangoni effect is neglected ($E_G \to 0$), then Equations 311 and 312 become equivalent to the Oldroyd[619] formula which is originally derived only for monodisperse emulsions.

For higher values of the particle volume fraction, the rheological behavior of the colloidal dispersions becomes rather complex. We will consider qualitatively the observed phenomena, and next we will review available semi-empirical expressions.

For a simple shear (Couette) flow, the relation between the applied stress, τ, and the resulting shear rate, $\dot{\gamma}$, can be expressed in the form:

$$\tau = \eta\dot{\gamma} \tag{313}$$

(For example, when a liquid is sheared between two plates parallel to the *xy*-plane, one has $\dot{\gamma} = \partial v_x/\partial z$.) A typical plot of $\dot{\gamma}$ vs. τ is shown in Figure 52(a). For low and high shear rates, one observes Newtonian behavior (η = const.), whereas in the intermediate region a transition from the lower shear rate viscosity, η_0, to the higher shear rate viscosity, η_∞, takes place. This is also visualized in Figure 52(b), where the viscosity of the colloidal dispersion, η, is plotted vs. the shear rate, $\dot{\gamma}$; note that in the intermediate zone η has a minimum.[415]

Note also that both η_0 and η_∞ depend on the particle volume fraction, ϕ. De Kruif et al.[624] proposed the semi-empirical expansions:

$$\frac{\eta_0}{\eta_m} = 1 + 2.5\phi + (4 \pm 2)\phi^2 + (42 \pm 10)\phi^3 + \ldots \tag{314}$$

$$\frac{\eta_\infty}{\eta_m} = 1 + 2.5\phi + (4 \pm 2)\phi^2 + (25 \pm 7)\phi^3 + \ldots \tag{315}$$

as well as two empirical expressions which can be used in the whole range of values of ϕ:

$$\frac{\eta_0}{\eta_m} = \left(1 - \frac{\phi}{0.63}\right)^{-2}, \qquad \frac{\eta_\infty}{\eta_m} = \left(1 - \frac{\phi}{0.71}\right)^{-2} \tag{316}$$

In regard to the dependence of η on the shear stress, τ, Russel et al.[278] reported that for the intermediate values of τ, corresponding to non-Newtonian behavior (Figures 52(a) and (b)), the experimental data correlate reasonably well with the expression

$$\frac{\eta - \eta_\infty}{\eta - \eta_0} = \frac{1}{1 + (\tau/\tau_c)^n} \tag{317}$$

with $1 \le n \le 2$, where τ_c is the value of τ for which $\eta = (\eta_0 + \eta_\infty)/2$. In its own turn, τ_c depends on the particle volume fraction ϕ, (see Figure 52(c)). One sees that τ_c increases with

the volume fraction, ϕ, in dilute dispersions then passes through a maximum and finally decreases down to zero; note that $\tau_c \to 0$ corresponds to $\eta_0 \to \infty$. The peak at $\phi \approx 0.5$ is the only indication that the hard-sphere disorder-order transition either occurs or is rheologically significant in these systems.[278]

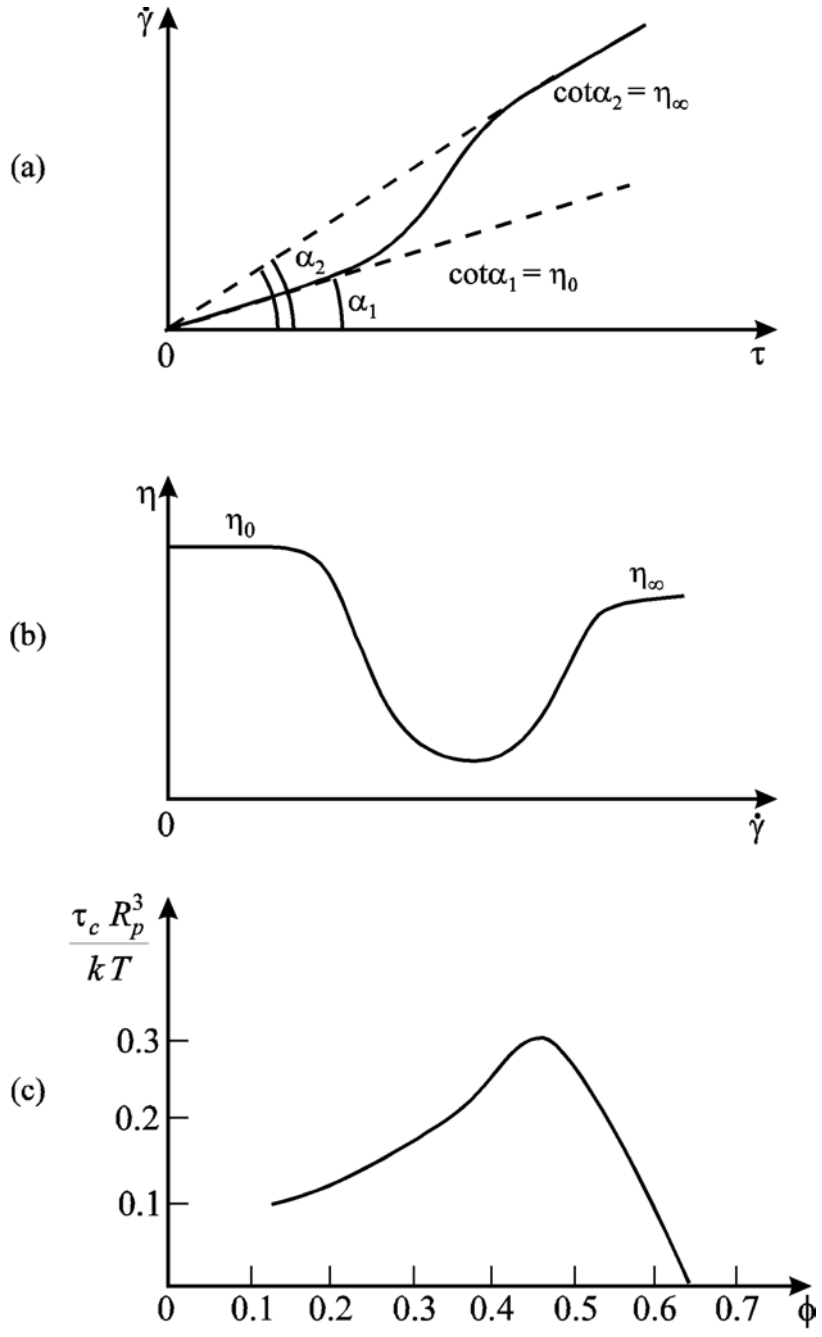

FIGURE 52 Qualitative presentation of basic relations in rheology of suspensions: (a) rate of strain, $\dot{\gamma}$, vs. applied stress, τ, (see Equation 313); (b) average viscosity of a suspension, η, vs. rate of strain, $\dot{\gamma}$; (c) dimensionless parameter τ_c (Equation 317) vs. particle volume fraction ϕ.

The restoring force for a dispersion to return to a random, isotropic situation at rest is either Brownian (thermal fluctuations) or osmotic,[637] the former being most important for submicrometer particles and the latter for larger particles. Changing the flow conditions changes the structure, and this leads to thixotropic effects, which are especially strong in flocculated systems.

Krieger and Dougherty[638] applied the theory of corresponding states to obtain the following expression for the viscosity of hard-sphere dispersions:

$$\frac{\eta}{\eta_m} = \left(1 - \frac{\phi}{\phi_{\max}}\right)^{-[\eta]\phi_{\max}} \tag{318}$$

where $[\eta]$ is the dimensionless intrinsic viscosity, which has a theoretical value of 2.5 for monodisperse rigid spheres, and $\phi_{\max}$ is the maximum packing volume fraction for which the viscosity η diverges. The value of $\phi_{\max}$ depends on the type of packing of the particles[415] (see Table 6). The maximum packing fraction, $\phi_{\max}$, is very sensitive to particle-size distribution and particle shape.[639] Broader particle-size distributions have greater values of $\phi_{\max}$. On the other hand, nonspherical particles lead to poorer space-filling and hence lower $\phi_{\max}$. Table 7 presents the values of $[\eta]$ and $\phi_{\max}$ obtained by fitting the results of a number of experiments on dispersions of asymmetric particles using Equation 318. The trend of $[\eta]$ to increase and of $\phi_{\max}$ to decrease with increasing asymmetry is clearly seen, but the product, $[\eta]\phi_{\max}$, is almost constant; $[\eta]\phi_{\max}$ is about 2 for spheres and about 1.4 for fibers. This fact can be utilized to estimate the viscosity of a wide variety of dispersions.

TABLE 6

Maximum Packing Volume Fraction, ϕ_{max}, for Various Arrangements of Monodisperse Spheres

Arrangement	ϕ_{max}
Simple cubic	0.52
Minimum thermodynamically stable configuration	0.548
Hexagonally packed sheets just touching	0.605
Random close packing	0.637
Body-centred cubic packing	0.68
Face-centred cubic/hexagonal close packed	0.74

TABLE 7

Values of $[\eta]$ and ϕ_{max} for a Number of Dispersions Obtained by Fitting Experimental Data by Means of Equation 318

System	$[\eta]$	ϕ_{max}	$[\eta]\phi_{max}$	Ref.
Spheres (submicron)	2.7	0.71	1.92	de Kruif et al.[624]
Spheres (40 μm)	3.28	0.61	2.00	Giesekus[651]
Ground gypsum	3.25	0.69	2.24	Turian and Yuan[652]
Titanium dioxide	5.0	0.55	2.75	Turian and Yuan[652]
Glass rods (30 × 700 μm)	9.25	0.268	2.48	Clarke[653]
Quartz grains (53 to 76 μm)	5.8	0.371	2.15	Clarke[653]
Glass fibers:				
Axial ratio- 7	3.8	0.374	1.42	Giesekus[651]
Axial ratio- 14	5.03	0.26	1.31	Giesekus[651]
Axial ratio- 21	6.0	0.233	1.40	Giesekus[651]

A number of rheological experiments with foams and emulsions are summarized in the reviews by Prud'home and Khan[640] and Tadros.[641] These experiments demonstrate the influence of films between the droplets (or bubbles) on the shear viscosity of the dispersion as a whole. Unfortunately, there is not a consistent theoretical explanation of this effect accounting for the different hydrodynamic resistance of the films between the deformed fluid particles as compared to the nondeformed spherical particles (see Sections 5.5.2 and 5.5.3). In the case of emulsions and foams, the deformed droplets or bubbles have a polyhedral shape, and maximum packing fraction can be $\phi_{max} \approx 0.9$ and even higher. For this case, a special geometrical rheological theory has been developed.[437,642,643]

Wessel and Ball[644] and Kanai et al.[645] studied in detail the effects of shear rate on the fractal structure of flocculated emulsion drops. They showed that the size of the flocs usually decreases with the increase of the shear stress; often the flocs are split to single particles at high shear rates. As a result, the viscosity decreases rapidly with the increase of the shear rate.

Interesting effects are observed when a dispersion contains both larger and smaller particles, the latter being usually polymer coils, spherical or cylindrical surfactant micelles, or microemulsion droplets. The presence of the smaller particles may induce clustering of the larger particles due to the depletion attraction (see Section 5.4.5.3.3 above); such effects are described in the works on surfactant-flocculated and polymer-flocculated emulsions.[646-649] Other effects can be observed in dispersions representing mixtures of liquid and solid particles. Yuhua et al.[650] have established that if the size of the solid particles is larger than three times the size of the emulsion drops, the emulsion can be treated as a continuous medium (of its own average viscosity), in which the solid particles are dispersed; such a treatment is not possible when the solid particles are smaller.

5.6. KINETICS OF COAGULATION

There are three scenarios for the occurrence of a two-particle collision in a dispersion depending on the type of particle-particle interactions. (1) If the repulsive forces are predominant, the two colliding particles will rebound and the colloidal dispersion will be stable; (2) when at a given separation the attractive and repulsive forces counterbalance each other (the film formed upon particle collision is stable), aggregates or flocs of attached particles can appear; and (3) when the particles are fluid and the attractive interaction across the film is predominant, the film is unstable and ruptures; this leads to coalescence of the drops in emulsions or of the bubbles in foams.

To a great extent, the occurrence of coagulation is determined by the energy, U, of particle-particle interaction. U is related to the disjoining pressure, Π, by means of Equations 162 and 163. Qualitatively, the curves Π vs. h (see Figure 13) and U vs. h are similar. The coagulation is called fast or slow depending on whether the electrostatic barrier (see Figure 13) is less than kT or much higher than kT. In addition, the coagulation is termed "reversible" or "irreversible" depending on whether the depth of the primary minimum (see Figure 13) is comparable with kT or much greater than kT.

Three types of driving forces can lead to coagulation: (1) The body forces, such as gravity and centrifugal force, cause sedimentation of the heavier particles in suspensions or creaming of the lighter droplets in emulsions. (2) For the particles that are smaller than about 1 μm, the Brownian stochastic force dominates the body forces, and the Brownian collision of two particles becomes a prerequisite for their attachment and coagulation; and (3) the temperature gradient in fluid dispersions causes termocapillary migration of the particles driven by the Marangoni effect. The particles moving with different velocities can collide and form aggregates.

5.6.1 IRREVERSIBLE COAGULATION

The kinetic theory of fast irreversible coagulation was developed by Smoluchowski.[654,655] Later the theory was extended to the case of slow and reversible coagulation. In any case of coagulation (flocculation), the general set of kinetic equations reads:

$$\frac{dn_k}{dt} = \frac{1}{2}\sum_{i=1}^{k-1} a_f^{i,k-i} n_i n_{k-i} - n_k \sum_{i=1}^{\infty} a_f^{k,i} n_i + q_k \qquad (k = 1, 2, ...) \tag{319}$$

Here, t is time; n_1 denotes the number of single particles per unit volume; n_k is the number of aggregates of k particles (k = 2, 3, ...) per unit volume; $a_f^{i,j}$ (i,j = 1, 2, 3, ...) are rate constants of flocculation (coagulation; see Figure 53); q_k denotes the flux of aggregates of size k which are products of other processes, different from the flocculation itself (say, the reverse process

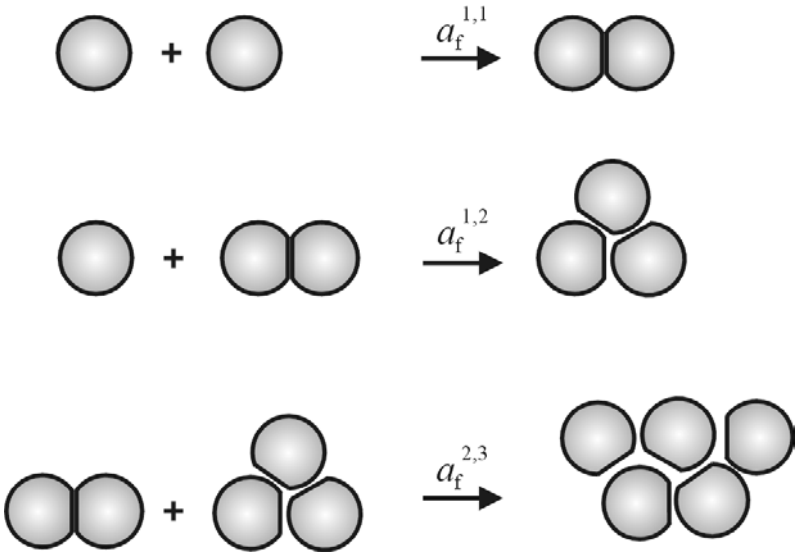

FIGURE 53. Elementary acts of flocculation according to the Smoluchowski scheme; $a_f^{i,j}$ (i,j = 1, 2, 3, ...) are rate constants of flocculation.

of aggregate disassembly or the droplet coalescence in emulsions; see Equations 331 and 335 below). In the special case of irreversible coagulation without coalescence, one has $q_k \equiv 0$. The first term in the right-hand side of Equation 319 is the rate of formation of k aggregates by the merging of two smaller aggregates, whereas the second term expresses the rate of loss of k aggregates due to their incorporation into larger aggregates. The total concentration of aggregates (as kinetically independent units), n, and the total concentration of the constituent particles (including those in aggregated form), n_{tot}, can be expressed as:

$$n = \sum_{k=1}^{\infty} n_k \,, \qquad n_{\text{tot}} = \sum_{k=1}^{\infty} k n_k \tag{320}$$

The rate constants can be expressed in the form:

$$a_f^{i,j} = 4\pi D_{i,j}^{(0)} (R_i + R_j) E_{i,j} \tag{321}$$

where $D_{i,j}^{(0)}$ is the relative diffusion coefficients for two flocks of radii R_i and R_j and aggregation number i and j, respectively; $E_{i,j}$ is the so-called collision efficiency.[470,656] Below we give expressions for $D_{i,j}^{(0)}$ and $E_{i,j}$ appropriate for various physical situations.

The Einstein approach (see Equation 307), combined with the Rybczynski-Hadamar equation (Equation 304) leads to the following expression for the relative diffusivity of two isolated Brownian droplets:

$$D_{i,j}^{(0)} = \frac{kT}{2\pi\eta}\frac{\eta_d + \eta}{3\eta_d + 2\eta}\left(\frac{1}{R_i} + \frac{1}{R_j}\right) \qquad \text{(perikinetic coagulation)} \qquad (322)$$

The limiting case $\eta_d \to 0$ corresponds to two bubbles, whereas in the other limit ($\eta_d \to \infty$) Equation 322 describes two solid particles or two fluid particles of tangentially immobile surfaces.

When the particle relative motion is driven by a body force or by the thermocapillary migration (rather than by self-diffusion), Equation 322 is no longer valid. Instead, in Equation 321 one has to formally substitute the following expression for $D_{i,j}^{(0)}$ (see Rogers and Davis[657]):

$$D_{i,j}^{(0)} = \frac{1}{4}(R_i + R_j)\left|\mathbf{v}_i - \mathbf{v}_j\right| \qquad \text{(orthokinetic coagulation)} \qquad (323)$$

Here $\mathbf{v}_j$ denotes the velocity of a flock of aggregation number j. Physically, Equation 323 accounts for the fact that some particle (usually a larger one) moves faster than the remaining particles and can "capture" them upon collision. This type of coagulation is called *orthokinetic* to distinguish it from the self-diffusion-driven perikinetic coagulation described by Equation 322. In the case of gravity-driven flocculation, one can identify $\mathbf{v}_j$ with the velocity U in Equation 304, where F is to be set equal to the gravitational force exerted on the particle; for a solid particle or a fluid particle of tangentially immobile surface, this yields $v_j = 2g\Delta\rho R_j^2/(9\eta)$ with g being the acceleration due to gravity and $\Delta\rho$ being the density difference between the two phases.

In the case of orthokinetic coagulation of liquid drops driven by the thermocapillary migration, the particle velocity $\mathbf{v}_j$ is given by the expression (see Young et al.[658]):

$$\mathbf{v}_j = \frac{2R_j E_T \lambda}{(3\eta_d + 2\eta)(\lambda_d + 2\lambda)}\nabla(\ln T) \qquad \text{(thermocapillary velocity)} \qquad (324)$$

where the thermal conductivity of the continuous and disperse phases are denoted by λ and λ_d, respectively. The interfacial thermal elasticity, E_T, is defined by Equation 282.

The collision efficiency, $E_{i,j}$, in Equation 321 accounts for the interactions (of both hydrodynamic and intermolecular origin) between two colliding particles. The inverse of $E_{i,j}$ is often called the *stability ratio* or the *Fuchs factor*[659] and can be expressed in the following general form:[14,470]

$$W_{i,j} = \frac{1}{E_{i,j}} = 2\int_0^\infty \frac{\beta(s)}{(s+2)^2}\exp\left[\frac{U_{i,j}(s)}{kT}\right] ds\,, \qquad s \equiv \frac{2h}{R_i + R_j} \qquad (325a)$$

$$\beta \equiv \left(2\pi\eta R_* \frac{3\eta_d + 2\eta}{\eta_d + \eta} \right)^{-1} \frac{F_z}{V_z}$$

where, as usual, h is the closest surface-to-surface distance between the two particles; R_* is defined by Equation 259; $U_{i,j}(s)$ is the energy of (nonhydrodynamic) interactions between the particles (see Section 5.4 above); $\beta(s)$ accounts for the hydrodynamic interactions; and F_z/V_z is the particle friction coefficient. Thus, $\beta \to 1$ for $s \to \infty$, insofar as for large separations the particles obey the Rybczynski-Hadamar equation (Equation 304). In the opposite limit, $s << 1$, i.e., close approach of the two particles, F_z/V_z can be calculated from Equation 260, 283, 284, or 288, depending on the specific case. In particular, for $s << 1$, one has $\beta \propto 1/s$ for two solid particles (or fluid particles of tangentially immobile surfaces), $\beta \propto s^{-1/2}$ for two liquid droplets, and $\beta \propto \ln s$ for two gas bubbles. One sees that for two solid particles ($\beta \propto 1/s$), the integral in Equation 325a may be divergent. To overcome this problem, one usually accepts that for the smallest separations $U_{i,j}$ is dominated by the van der Waals interaction, as given by Equation 174, i.e., $U_{i,j} \to -\infty$, and, consequently, the integrand in Equation 325a tends to zero for $s \to 0$.

Note that the value of $W_{i,j}$ is determined mainly by the values of the integrand in the vicinity of the electrostatic maximum (barrier) of $U_{i,j}$, (see Figure 13), insofar as $U_{i,j}$ enters Equation 325a as an exponent. By using the method of the saddle point, Derjaguin[14] estimated the integral in Equation 325a:

$$W_{i,j} \equiv \frac{1}{E_{i,j}} \approx \left[\frac{8\pi kT}{-U''_{i,j}(s_m)} \right]^{1/2} \frac{\beta(s_m)}{(s_m + 2)^2} \exp\left[\frac{U_{i,j}(s_m)}{kT} \right] \tag{325b}$$

where s_m denotes the value of s corresponding to the maximum. One sees that the larger the barrier, $U_{i,j}(s_m)$, the smaller the collision efficiency, $E_{i,j}$, and the slower the coagulation.

Note also that for imaginary particles, which experience neither long-range surface forces ($U_{i,j} = 0$) nor hydrodynamic interactions ($\beta = 1$), Equation 325a yields a collision efficiency $E_{i,j} = 1$ and Equation 321 reduces to the Smoluchowski[654,655] expression for the rate constant of the fast irreversible coagulation. In this particular case, Equation 319 represents an infinite set of nonlinear differential equation. If all flocculation rate constants are the same and equal to a_f, the problem has a unique exact solution:[654,655]

$$n = \frac{n_0}{1 + a_f n_0 t/2}, \qquad n_k = n_0 \frac{(a_f n_0 t/2)^{k-1}}{(1 + a_f n_0 t/2)^{k+1}} \qquad (k = 1, 2, \ldots) \tag{326}$$

It is supposed that the total average concentration of the constituent particles (in both singlet and aggregated form), n_{tot}, does not change and is equal to the initial number of particles, n_0.

Unlike n_{tot}, the concentration of the aggregates, n, decreases with time, while their size increases. Differentiating Equation 326 one obtains:

$$\frac{dn}{dt} = -\frac{a_f}{2} n^2, \qquad \frac{d\overline{V}}{dt} = \frac{a_f}{2}\phi_0, \qquad \overline{V} \equiv \frac{\phi_0}{n} \tag{327}$$

where $\overline{V}$ is the average volume per aggregate and ϕ_0 is the initial volume fraction of the constituent particles. Combining Equations 321 and 327, one obtains the following result for perikinetic (Brownian) coagulation:

$$\frac{\overline{V}}{V_0} = 1 + \frac{t}{t_{Br}}, \qquad t_{Br} = \frac{R_0^2}{3\phi_0 D_0 E_0} \tag{328}$$

where $V_0 = 4\pi R_0^3/3$ is the volume of a constituent particle, t_{Br} is the characteristic time of the coagulation process in this case, E_0 is an average collision efficiency, and D_0 is an average diffusion coefficient.

In contrast, $\overline{V}$ is not a linear function of time for orthokinetic coagulation. When the flocculation is driven by a body force, i.e., in case of sedimentation or centrifugation, one obtains:[656]

$$\frac{\overline{V}}{V_0} = \left(1 - \frac{t}{3t_{bf}}\right)^{-3}, \qquad t_{bf} = \frac{2R_0}{3\phi_0 \mathrm{v}_{bf} E_0} \tag{329}$$

where t_{bf} is the characteristic time in this case and v_{bf} is an average velocity of aggregate motion. As discussed above, when the body force is gravitational, one has $\mathrm{v}_{bf} = 2g\Delta\rho R_0^2/(9\eta)$.

When the orthokinetic coagulation is driven by the thermocapillary migration, the counterpart of Equation 329 reads:[656]

$$\frac{\overline{V}}{V_0} = \exp\left(\frac{t}{t_{tm}}\right), \qquad t_{tm} = \frac{2R_0}{3\phi_0 \mathrm{v}_{tm} E_0} \tag{330}$$

where v_{tm} is an average velocity of thermocapillary migration and t_{tm} is the respective characteristic time. Note that $D_0 \propto R_0^{-1}$, $\mathrm{v}_{bf} \propto R_0^2$ and $\mathrm{v}_{tm} \propto R_0$, (see Equations 307 and 324). Then, from Equations 328 to 330, it follows that the three different characteristic times exhibit different dependencies on particle radius: $t_{Br} \propto R_0^3$, $t_{bf} \propto R_0^{-1}$, while t_{tm} is independent of R_0. Thus, the Brownian coagulation is faster for the smaller particles, the body force-induced coagulation is more rapid for the larger particles, whereas the thermocapillary driven coagulation is not so sensitive to the particle size.[660]

The Smoluchowski scheme based on Equations 326 and 327 has found numerous applications.[278] An example for biochemical application is the study[661,662] of the kinetics of flocculation of latex particles caused by human gamma globulin in the presence of specific

"key-lock" interactions. The infinite set of Smoluchowski equations (Equation 319) was solved by Bak and Heilmann[663] in the particular case when the aggregates cannot grow larger than a given size; an explicit analytical solution was obtained by these authors.

5.6.2 REVERSIBLE COAGULATION

In the case of reversible coagulation, the flocs can disaggregate because the primary minimum (Figure 13) is not deep enough.[14] For example, an aggregate composed of $i + j$ particles can be split on two aggregates containing i and j particles. We denote the rate constant of this reverse process by $a_r^{i,j}$ (see Figure 54(a)). It is assumed that both the straight process of flocculation (Figure 53) and the reverse process (Figure 54(a)) take place. The kinetics of aggregation in this more general case is described by the Smoluchowski set of equations, Equation 319, where one has to substitute:

$$q_1 = \sum_{i=1}^{\infty} a_r^{1,i} n_{i+1}\,, \qquad q_k = \sum_{i=1}^{\infty} a_r^{k,i} n_{i+k} - \frac{1}{2} n_k \sum_{i=1}^{k-1} a_r^{i,k-i} \qquad (k = 2, 3, \ldots) \tag{331}$$

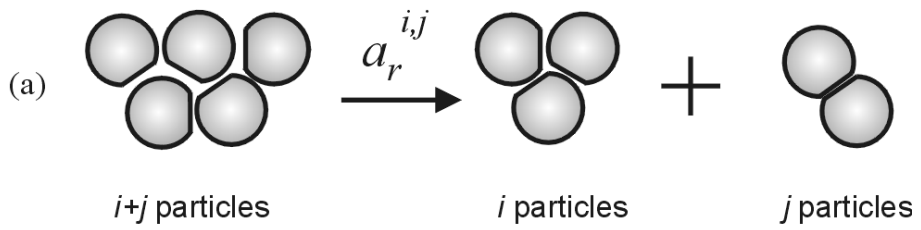

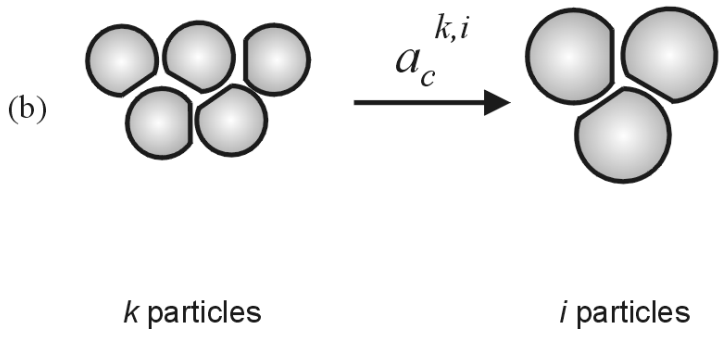

FIGURE 54. Elementary acts of aggregate splitting (a) and droplet coalescence within an aggregate (b); $a_r^{i,j}$ and $a_c^{k,i}$ (i,j,k = 1, 2, 3, ...) are the rate constants of the respective processes.

In Equation 331 q_k equals the rate of formation of k aggregates in the process of disassembly of larger aggregates minus the rate of decay of the k aggregates. As before, the total number of constituent particles, n_{tot}, does not change. However, the total number of the aggregates, n, can either increase or decrease depending on whether the straight or the reverse process prevails. Summing up all equations in 319 and using Equation 331, one derives the following equation for n:

$$\frac{dn}{dt} = \frac{1}{2}\sum_{i=1}^{\infty}\sum_{j=1}^{\infty}\left(a_r^{i,j} n_{i+j} - a_f^{i,j} n_i n_j\right) \tag{332}$$

Martinov and Muller[664] reported a general expression for the rate constants of the reverse process:

$$a_r^{i,j} = \frac{D_{i,j}^{(0)} E_{i,j}}{Z_{i,j}} \frac{1}{(R_i + R_j)^2} \tag{333}$$

where $Z_{i,j}$ is the so-called irreversible factor, which can be presented in the form

$$Z_{i,j} = \frac{1}{8}\int_{U_{i,j}<0} (s+2)^2 \exp\left[-\frac{U_{i,j}(s)}{kT}\right] ds \tag{334}$$

The integration in Equation 334 is carried out over the region around the primary minimum, where $U_{i,j}$ takes negative values (see Figure 13). In other words, $Z_{i,j}$ is determined by the values of $U_{i,j}$ in the region of the primary minimum, whereas $E_{i,j}$ is determined by the values of $U_{i,j}$ in the region of the electrostatic maximum, (see Equations 325b and 334). When the minimum is deeper, $Z_{i,j}$ is larger and the rate constant in Equation 333 is smaller. In addition, as seen from Equations 325b and 333, the increase of the height of the barrier also decreases the rate of the reverse process. The physical interpretation of this fact is that in order to detach from an aggregate a particle has to first go out from the well and then to "jump" over the barrier (Figure 13).

To illustrate the effect of the reverse process on the rate of flocculation, we solved numerically the set of Equations 319, 331, and 332. To simplify the problem, we used the following assumptions: (1) the Smoluchowski assumption that all rate constants of the straight process are equal to a_f; (2) aggregates containing more than M particles cannot decay; (3) all rate constants of the reverse process are equal to a_r; and (4) at the initial moment, only single constituent particles of concentration n_0 are available. In Figure 55, we plot the calculated curves of n_0/n vs. the dimensionless time, $\tau = a_f n_0 t/2$, for a fixed value, $M = 4$, and various values of the ratio of the rate constants of the straight and the reverse process, $b = 2a_r/(n_0 a_f)$. Note that n is defined by Equation 320. One sees that in an initial time interval all curves in Figure 55 touch the Smoluchowski distribution (corresponding to $b = 0$), but after this period one observes a reduction in the rate of flocculation which is larger for the curves with larger

values of b (larger rate constants of the reverse process). These S-shaped curves are typical for the case of reversible coagulation, which is also confirmed by the experiment.[14,665]

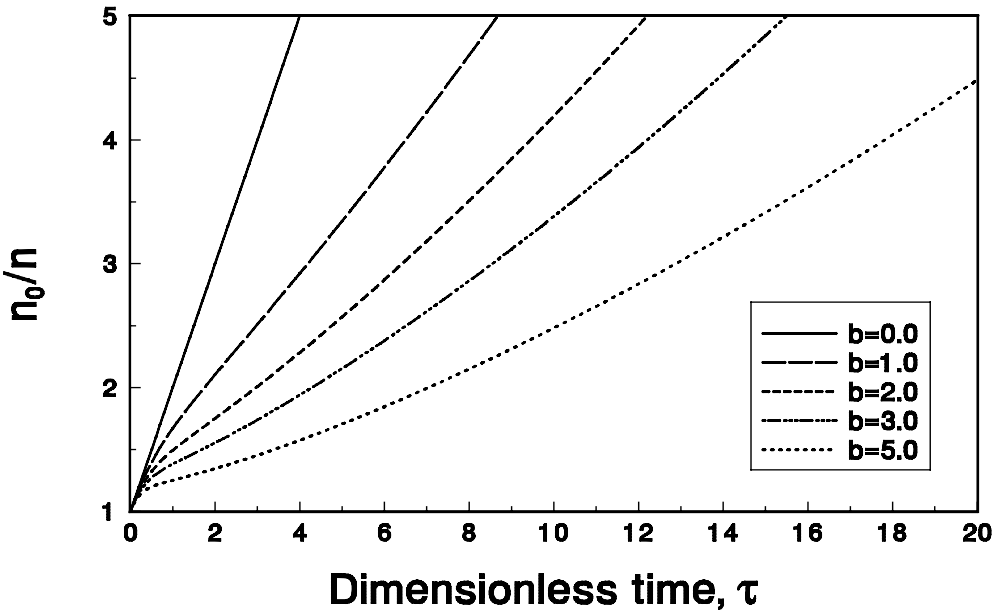

FIGURE 55. Reversible coagulation: theoretical plot of the inverse dimensionless aggregate concentration, n_0/n, vs. the dimensionless time, $\tau = a_f n_0 t/2$, in the case of $M = 4$ and various values of the dimensionless ratio, $b = 2a_r/(n_0 a_f)$, of the rate constants of the reverse and straight process, a_r and a_f .

5.6.3 KINETICS OF SIMULTANEOUS FLOCCULATION AND COALESCENCE IN EMULSIONS

When coalescence is present, in addition to the flocculation, the total number of constituent drops, n_{tot} (see Equation 320), does change, in contrast with the case of pure flocculation considered above.[32] Hartland and Gakis,[666] and Hartland and Vohra[667] were the first to develop a model of coalescence that relates the lifetime of single films to the rate of phase separation in emulsions of fairly large drops (approximately 1 mm) in the absence of surfactant. Their analysis was further extended by Lobo et al.[668] to quantify the process of coalescence within an already creamed or settled emulsion (or foam) containing drops of size less than 100 μm; these authors also took into account the effect of surfactants, which are commonly used as emulsifiers. Danov et al.[669] generalized the Smoluchowski scheme to account for the fact that the droplets within the flocs can coalesce to give larger droplets, as illustrated in Figure 54(b). In this case, in the right-hand side of Equation 319 one has to substitute[669]

$$q_1 = \sum_{i=2}^{\infty} a_c^{i,1} n_i \,, \qquad q_k = \sum_{i=k+1}^{\infty} a_c^{i,k} n_i - n_k \sum_{i=1}^{k-1} a_c^{k,i} \qquad (k = 2, 3, \ldots) \qquad (335)$$

where $a_c^{k,i}$ is the rate constant of transformation (by coalescence) of an aggregate containing k droplets into an aggregate containing i droplets (see Figure 54(b)). The newly formed aggregate is further involved in the flocculation scheme, which thus accounts for the fact that the flocculation and coalescence processes are interdependent. In this scheme, the total coalescence rate, $a_{c,\mathrm{tot}}^{i}$, and the total number of droplets, n_{tot}, obey the following equations:[669]

$$\frac{dn_{\mathrm{tot}}}{dt} = -\sum_{i=2}^{\infty} a_{c,\mathrm{tot}}^{i} n_i \,, \qquad a_{c,\mathrm{tot}}^{i} = \sum_{k=1}^{i-1} (i-k) a_c^{i,k} \qquad (i = 2, 3, \ldots) \qquad (336)$$

To determine the rate constants of coalescence, $a_c^{k,i}$, Danov et al.[439] examined the effects of droplet interactions and Brownian motion on the coalescence rate in dilute emulsions of micrometer- and submicrometer- sized droplets. The processes of film formation, thinning, and rupture were included as consecutive stages in the scheme of coalescence. Expressions for the interaction energy due to the various DLVO and non-DLVO surface forces between two deformed droplets were obtained[266] (see also Section 5.4 above).

Average models for the total number of droplets are also available.[670,671] The average model of van den Tempel[670] assumes linear structure of the aggregates. The coalescence rate is supposed to be proportional to the number of contacts within an aggregate. To simplify the problem, van den Tempel has used several assumptions, one of them being that the concentration of the single droplets, n_1, obeys the Smoluchowski distribution, (Equation 326) for $k = 1$. The average model of Borwankar et al.[671] is similar to that of van den Tempel but is physically more adequate. The assumptions used by the latter authors[671] make their solution more applicable to cases in which the flocculation (rather than the coalescence) is slow and is the rate determining stage. This is confirmed by the curves shown in Figure 56 which are calculated for the same rate of coalescence, but for three different rates of flocculation. For relatively high rates of flocculation (Figure 56(a)), the predictions of the three theories differ. For the intermediate rates of flocculation (Figure 56(b)), the prediction of the model by Borwankar et al.[671] is close to that of the more detailed model by Danov et al.[669] For very low values of the flocculation rate constant, a_f, for which the coalescence is not the rate-determining stage, all three theories[669-671] give numerically close results (Figure 56(c)). (For more details about the coupling of coalescence and flocculation in dilute oil-in-water emulsions see the recent review, Reference 672.)

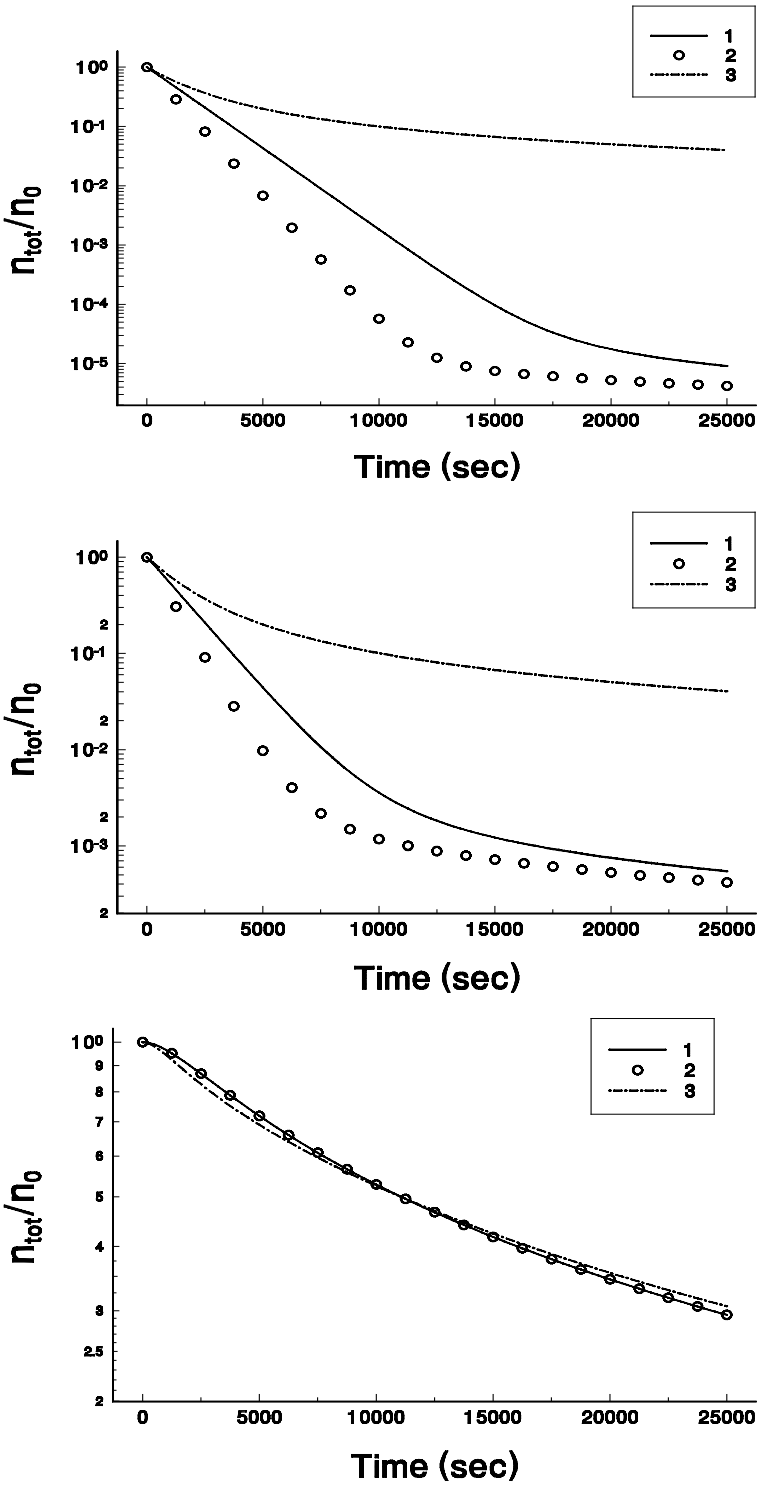

FIGURE 56 Relative change in the total number of drops, n_{tot}, vs. time, t; initial number of primary drops $n_0 = 10^{12}$ cm^{-3}; coalescence rate constant $k_c^{2,1} = 10^{-3}$sec^{-1}. Curve 1: numerical solution of Equation 336; curve 2: output of the model of Borwankar et al.;[671] curve 3: output of the model of van den Tempel;[670] the values of the flocculation rate constant are (a) $a_f = 10^{-11}$ cm^3/s; (b) $a_f = 10^{-13}$ cm^3/s; (c) $a_f = 10^{-16}$ cm^3/s.

REFERENCES

1. Jungermann, E., *Cationic Surfactants,* Marcel Dekker, New York, 1970.
2. Lucassen-Reynders, E.H., *Anionic Surfactants – Physical Chemistry of Surfactant Action*, Marcel Dekker, New York, 1981.
3. Schick, M.J., *Nonionic Surfactants: Physical Chemistry,* Marcel Dekker, New York, 1986.
4. Gibbs, J.W., *The Scientific Papers of J.W. Gibbs*, Vol. 1, Dover, New York, 1961.
5. Ono, S. and Kondo, S., Molecular theory of surface tension in liquids, in *Handbuch der Physik,* Vol. 10, Flügge, S., Ed., Springer, Berlin, 1960.
6. Adamson, A.W. and Gast, A.P. *Physical Chemistry of Surfaces*; Sixth Edition, Wiley, New York, 1997.
7. Freundlich, H., *Colloid and Capillary Chemistry*, Methuen, London, 1926.
8. Langmuir, I., *J. Amer. Chem. Soc.,* 40, 1361, 1918.
9. Volmer, M., *Z. Physikal. Chem.,* 115, 253, 1925.
10. Frumkin, A., *Z. Physikal. Chem.,* 116, 466, 1925.
11. Hill, T.L., *An Introduction to Statistical Thermodynamics*, Addison-Wesley, Reading, MA, 1962.
12. Lucassen-Reynders, E.H., *J. Phys. Chem*., 70, 1777, 1966.
13. Borwankar, R.P. and Wasan, D.T., *Chem. Eng. Sci.,* 43, 1323, 1988.
14. Derjaguin, B.V., *Theory of Stability of Colloids and Thin Liquid Films,* Plenum Press, Consultants Bureau, New York, 1989.
15. Shchukin, E.D., Pertsov, A.V., and Amelina, E.A., *Colloid Chemistry*, Moscow Univ. Press, Moscow, 1982 (Russian); Elsevier, 2001 (English).
16. Zeldowitch, J., *Acta Physicochim. (USSR)*, 1, 961, 1934.
17. Halsey, G. and Taylor, H.S., *J. Chem. Phys.,* 15, 624, 1947.
18. Gurkov, T.G., Kralchevsky, P.A., and Nagayama, K., *Colloid Polym. Sci.,* 274, 227, 1996.
19. Butler, J.A.V., *Proc. Roy. Soc. Ser. A,* 135, 348, 1932.
20. Fainerman, V.B. and Miller, R., *Langmuir*, 12, 6011, 1996.
21. Vaughn, M.W. and Slattery, J. C., *J. Colloid Interface Sci.,* 195, 1, 1997.
22. Makievski, A.V., Fainerman, V.B., Bree, M., Wüstneck, R., Krägel, J., and Miller, R., *J. Phys. Chem. B,* 102, 417, 1998.
23. Landau, L.D. and Lifshitz, E.M., *Statistical Physics,* Part 1, Pergamon, Oxford, 1980.
24. Hachisu, S., *J. Colloid Interface Sci.,* 33, 445, 1970.
25. Kalinin, V.V. and Radke, C.J., *Colloids Surf. A,* 114, 337, 1996.
26. Warszyński, P., Barzyk, W., Lunkenheimer, K., and Fruhner, H., *J. Chys Chem.*, *B,* 102, 10948, 1998.
27. Kralchevsky, P.A., Danov, K.D., Broze, G., and Mehreteab, A., *Langmuir,* 15, 2351, 1999.
28. Prosser, A.J. and Frances, E.I., *Colloids Surf. A,* 178, 1, 2001.

29. Kirkwood, J.G. and Oppenheim, I., *Chemical Thermodynamics*, McGraw-Hill, New York, 1961.

30. Robinson, R.A. and Stokes, R.H., *Electrolyte Solutions,* Butterworths, London, 1959.

31. Gouy, G., *J. Phys. Radium,* 9, 457, 1910.

32. Davies, J. and Rideal, E., *Interfacial Phenomena,* Academic Press, New York, 1963.

33. Grahame, D.C., *Chem. Rev.,* 41, 441, 1947.

34. Israelachvili, J.N., *Intermolecular and Surface Forces*, Academic Press, London, 1992.

35. Kralchevsky, P.A. and Nagayama, K., *Particles at Fluid Interfaces and Membranes*, Elsevier, Amsterdam, 2001.

36. Matijevič, E. and Pethica, B.A., *Trans. Faraday Soc.,* 54, 1382, 1958.

37. van Voorst Vader, F., *Trans. Faraday Soc.*, 56, 1067, 1960.

38. Tajima, K., *Bul. Chem. Soc. Jpn,* 44, 1767, 1971.

39. Stern, O., *Ztschr. Elektrochem.,* 30, 508, 1924.

40. Tajima, K., Muramatsu, M., and Sasaki, T., *Bul. Chem. Soc. Jpn*, 43, 1991, 1970.

41. Tajima, K., *Bul. Chem. Soc. Jpn*, 43, 3063, 1970.

42. Danov, K.D., Kolev, V.L, Kralchevsky, P.A., Broze, G., and Mehreteab, A., manuscript in preparation.

43. Cross, A.W. and Jayson, G.G., *J. Colloid Interface Sci.*, 162, 45, 1994.

44. Johnson, S.B., Drummond, C.J., Scales, P.J., and Nishimura, S., *Langmuir,* 11, 2367, 1995.

45. Alargova, R.G., Danov, K.D., Petkov, J.T., Kralchevsky, P.A., Broze, G., and Mehreteab, A., *Langmuir,* 13, 5544, 1997.

46. Rathman, J.F. and Scamehorn, J.F., *J. Phys. Chem.*, 88, 5807, 1984.

47. Berr, S.S., Coleman, M.J., Marriot, J., and Johnson Jr., J.S., *J. Phys. Chem*., 90, 6492, 1986.

48. Rosen, M.J., *Surfactants and Interfacial Phenomena*, Wiley, New York, 1989.

49. Clint, J., *Surfactant Aggregation*, Chapman & Hall, London, 1992.

50. Alargova, R.G., Danov, K.D., Kralchevsky, P.A., Broze, G., and Mehreteab, A., *Langmuir,* 14, 4036, 1998.

51. Dimov, N.K., Kolev, V.L., Kralchevsky, P.A., Lyutov, L.G., Brose, G., and Mehreteab, A., *J. Colloid Interface Sci*., 256, 23 (2002).

52. Valkovska, D.S., Danov, K.D., and Ivanov, I.B., *Colloids Surf. A,* 175, 179, 2000.

53. Danov, K.D., Kralchevsky, P.A., and Ivanov, I.B., in *Encyclopedic Handbook of Emulsion Technology*, Sjöblom, J., Ed., Marcel Dekker, New York, 2001, chap. 26.

54. Dukhin, S.S., Kretzschmar, G., and Miller, R., *Dynamics of Adsorption at Liquid Interfaces*, Elsevier, Amsterdam, 1995.

55. Eastoe, J. and Dalton, J.S., *Adv. Colloid Interface Sci.,* 85, 103, 2000.

56. Lord Rayleigh, *Proc. Roy. Soc. (Lond.)*, 29, 71, 1879.

57. N. Bohr, *Phil. Trans. Roy. Soc. (Lond.)*, *A*, 209, 281, 1909.

58. Defay, R. and Pétré, G., Dynamic surface tension, in *Surface and Colloid Science,* Vol. 3, Matijevič, E., Ed., Wiley, New York, 1971, p. 27.

59. Miller, R. and Kretzschmar, G., *Adv. Colloid Interface Sci*., 37, 97, 1991.

60. Wantke, K.-D., Lunkenheimer, K., and Hempt, C., *J. Colloid Interface Sci.*, 159, 28, 1993.

61. Chang, C.-H. and Franses, E.I., *J. Colloid Interface Sci.*, 164, 107, 1994.

62. Johnson, D.O. and Stebe, K.J., *J. Colloid Interface Sci.*, 182, 525, 1996.

63. Horozov, T. and Arnaudov, L., *J. Colloid Interface Sci.*, 219, 99, 1999.

64. Horozov, T. and Arnaudov, L., *J. Colloid Interface Sci.*, 222, 146, 2000.

65. van den Tempel, M. and Lucassen-Reynders, E.H., *Adv. Colloid Interface Sci.*, 18, 281, 1983.

66. Langevin, D., *Colloids Surf.*, 43, 121, 1990.

67. Lemaire, C. and Langevin, D., *Colloids Surf.*, 65, 101, 1992.

68. Grigorev, D.O., Krotov, V.V., and Noskov, B.A., *Colloid J.*, 56, 562, 1994.

69. Mysels, K.J., *Colloids Surf.*, 43, 241, 1990.

70. Kralchevsky, P.A., Radkov, Y.S., and Denkov, N.D., *J. Colloid Interface Sci.*, 161, 361, 1993.

71. Fainerman, V.B., Miller, R., and Joos, P., *Colloid Polym. Sci.*, 272, 731, 1994.

72. Fainerman, V.B. and Miller, R., *J. Colloid Interface Sci.*, 176, 118, 1995.

73. Horozov, T.S., Dushkin, C.D., Danov, K.D., Arnaudov, L.N., Velev, O.D., Mehreteab, A., and Broze, G., *Colloids Surf. A*, 113, 117, 1996.

74. Mishchuk, N.A., Dukhin, S.S., Fainerman, V.B., Kovalchuk, V.I., and Miller, R., *Colloids Surf. A*, 192, 157, 2001.

75. van den Bogaert, R. and Joos, P., *J. Phys. Chem.*, 83, 17, 1979.

76. Möbius, D. and Miller R., Eds., *Drops and Bubbles in Interfacial Research*, Elsevier, Amsterdam, 1998.

77. Jho, C. and Burke, R., *J. Colloid Interface Sci.*, 95, 61, 1983.

78. Joos, P. and van Hunsel, J., *Colloid Polym. Sci.* 267, 1026, 1989.

79. Fainerman, V.B. and Miller, R., *Colloids Surf. A*, 97, 255, 1995.

80. Miller, R., Bree, M., and Fainerman, V.B., *Colloids Surf. A,* 142, 237, 1998.

81. Senkel, O., Miller, R., and Fainerman, V.B., *Colloids Surf. A*, 143, 517, 1998.

82. Bain, C.D., Manning-Benson, S., and Darton, R.C., *J. Colloid Interface Sci.,* 229, 247, 2000.

83. Rotenberg, Y., Boruvka, L., and Neumann, A.W., *J. Colloid Interface Sci.,* 37, 169, 1983.

84. Makievski, A.V., Loglio, G., Krägel, J., Miller, R., Fainerman, V.B., and Neumann, A.W., *J. Phys. Chem.,* 103, 9557, 1999.

85. Joos, P., *Dynamic Surface Phenomena,* VSP BV, AH Zeist, The Netherlands, 1999.

86. Ward, A.F.H. and Tordai, L., *J. Chem. Phys.*, 14, 453, 1946.

87. Miller, R., *Colloid Polym. Sci.*, 259, 375, 1981.

88. McCoy, B.J., *Colloid Polym. Sci.*, 261, 535, 1983.

89. Hansen, R.S., *J. Chem Phys.,* 64, 637, 1960.

90. Filippov, L.K., *J. Colloid Interface Sci.*, 164, 471, 1994.

91. Daniel, R. and Berg, J.C., *J. Colloid Intrface Sci.,* 237, 294, 2001.

92. Sutherland, K.L., *Austr. J. Sci. Res.*, A5, 683, 1952.

93. Abramowitz, M. and Stegun, I.A., *Handbook of Mathematical Functions,* Dover, New York, 1965.

94. Korn, G.A. and Korn, T.M., *Mathematical Handbook*, McGraw-Hill, New York, 1968.

95. Danov, K.D., Kolev, V.L., Kralchevsky, P.A., Broze, G., and Mehreteab, A., *Langmuir,* 16, 2942, 2000.

96. Dukhin, S.S., Miller, R., and Kretzschmar, G., *Colloid Polym. Sci.*, 261, 335, 1983.

97. Dukhin, S.S. and Miller, R., *Colloid Polym. Sci.,* 272, 548, 1994.

98. MacLeod, C. and Radke, C.J., *Langmuir,* 10, 3555, 1994.

99. Vlahovska, P.M., Danov, K.D., Mehreteab, A., and Broze, G., *J. Colloid Interface Sci.*, 192, 194, 1997.

100. Danov, K.D., Vlahovska, P.M., Kralchevsky, P.A., Broze, G., and Mehreteab, A., *Colloids Surf. A*, 156, 389, 1999.

101. Diamant, H. and Andelman, D., *J. Phys. Chem.,* 100, 13732, 1996.

102. Diamant, H., Ariel, G., and Andelman, D., *Colloids Surf. A,* 183-185, 259, 2001.

103. Nayfeh, A.H., *Perturbation Methods*, Wiley, New York, 1973.

104. Danov, K.D., Kolev, V.L., Arnaudov, L.N., Kralchevsky, P.A., Broze, G., and Mehreteab, A., manuscript in preparation.

105. Durbut, P., Surface Activity, in *Handbook of Detergents,* Part A, Broze, G., Ed., Marcel Dekker, New York, 1999, chap. 3.

106. Bond, W.N. and Puls, H.O., *Phil. Mag.*, 24, 864, 1937.

107. Doss, K.S.G., *Koll. Z.*, 84, 138, 1938.

108. Blair, C.M., *J. Chem. Phys.*, 16, 113, 1948.

109. Ward, A.F.H., *Surface Chemistry*, London, 1949.

110. Dervichian, D.G., *Koll. Z.*, 146, 96, 1956.

111. Hansen, R.S. and Wallace, T., *J. Phys. Chem.*, 63, 1085, 1959.

112. Baret, J.F., *J. Phys. Chem.*, 72, 2755, 1968.

113. Baret, J.F., *J. Chem. Phys.*, 65, 895, 1968.

114. Baret, J.F., *J. Colloid Interface Sci.*, 30, 1, 1969.

115. Borwankar, R.P. and Wasan, D.T., *Chem. Eng. Sci.*, 38, 1637, 1983.

116. Dong, C., Hsu, C.-T., Chin, C.-Y., and Lin, S.-Y., *Langmuir,* 16, 4573, 2000.

117. Laplace, P.S., *Traité de mécanique céleste*; Suppléments au Livre X, 1805, 1806.

118. Bakker, G., Kapillatytät und oberflächenspannung, in *Handbuch der Experimentalphysik,* Band 6, Akademische Verlagsgesellschaft, Leipzig, 1928.

119. Princen, H.M., The equilibrium shape of interfaces, drops, and bubbles, in *Surface and Colloid Science*, Vol. 2, Matijevic, E., Ed., Wiley, New York, 1969, p. 1.

120. Finn, R., *Equilibrium Capillary Surfaces*, Springer-Verlag, New York, 1986.

121. Weatherburn, C.E., *Differential Geometry in Three Dimensions*, Cambridge, 1930.

122. McConnell, A.J., *Application of Tensor Analysis,* Dover, New York, 1957.

123. Young, T., *Philos. Trans. Roy. Soc. Lond.*, 95, 55, 1805.

124. Jonson, R.E. and Dettre, Wettability and contact angles, in *Surface and Colloid Science,* Vol. 2, Matijevic, E., Ed., Wiley, New York, 1969, p. 85.

125. Starov, V.M., *Adv. Colloid Interface Sci.*, 39, 147, 1992.

126. Neumann, F., *Vorlesungen über die Theorie der Capillarität,* B.G. Teubner, Leipzig, 1894.

127. Ivanov, I.B., Kralchevsky, P.A., and Nikolov, A.D., *J. Colloid Interface Sci.*, 112, 97, 1986.

128. Hartland, S. and Hartley, R.W., *Axisymmetric Fluid-Liquid Interfaces,* Elsevier, Amsterdam, 1976.

129. Kralchevsky, P.A., Eriksson, J.C., and Ljunggren, S., *Adv. Colloid Interface Sci.*, 48, 19, 1994.

130. Tachev, K.D., Angarska, J.K., Danov, K.D., and Kralchevsky, P.A., *Colloids Surf. B*, 19, 61, 2000.

131. Meunier, J. and Lee, L.T., *Langmuir*, 7, 1855, 1991.

132. Dan, N., Pincus, P., and Safran, S.A., *Langmuir*, 9, 2768, 1993.

133. Kralchevsky, P.A., Paunov, V.N. Denkov, N.D., and Nagayama, K., *J. Chem. Soc. Faraday Trans.*, 91, 3415, 1995.

134. Petsev, D.N., Denkov, N.D., and Kralchevsky, P.A., *J. Colloid Interface Sci.*, 176, 201, 1995.

135. De Gennes, P.G. and Taupin, C., *J. Phys. Chem.*, 86, 2294, 1982.

136. Concus, P., *J. Fluid Mech.*, 34, 481, 1968.

137. Kralchevsky, P.A., Ivanov, I.B., and Nikolov, A.D., *J. Colloid Interface Sci.*, 112, 108, 1986.

138. Abramowitz, M. and Stegun, I.A., *Handbook of Mathematical Functions,* Dover, New York, 1965.

139. Jahnke, E., Emde, F., and Lösch, F., *Tables of Higher Functions,* McGraw-Hill, New York, 1960.

140. Lo, L.L., *J. Fluid Mech.*, 132, 65, 1983.

141. Derjaguin, B.V., *Dokl. Akad. Nauk USSR*, 51, 517, 1946.

142. Scheludko, A., *Proc. Koninkl. Nederl. Akad. Wet*., B65, 87, 1962.

143. Scheludko, A., *Adv. Colloid Interface Sci.*, 1, 391, 1967.

144. Dimitrov, A.S., Kralchevsky, P.A., Nikolov, A.D., and Wasan, D.T., *Colloids Surf.*, 47, 299, 1990.

145. J. Plateau, Experimental and theoretical researches on the figures of equilibrium of a liquid mass withdrawn from the action of gravity, in *The Annual Report of the Smithsonian Institution*, Washington D.C., 1863; pp. 207-285.

146. J. Plateau, The figures of equilibrium of a liquid mass, in *The Annual Report of the Smithsonian Institution*, Washington D.C., 1864; pp. 338-369.

147. J. Plateau, *Statique Expérimentale et Théoretique des Liquides Soumis aux Seules Forces Moléculaires*, Gauthier-Villars, Paris, 1873.

148. Zettlemoyer, A.C., *Nucleation,* Marcel Dekker, New York, 1969.

149. Abraham, E.F., *Homogeneous Nucleation Theory,* Academic Press, New York, 1974.

150. Thomson, W. (Lord Kelvin), *Proc. Roy. Soc.*, 9, 225, 1858; *Phil.Mag.*, 17, 61, 1859.

151. Lupis, C.H.P. *Chemical Thermodynamics of Matherials,* North-Holland, New York, 1983.

152. Lifshitz, I.M. and Slyozov, V.V., *Zh. Exp. Teor. Fiz.*, 35, 479, 1958 (in Russian).

153. Wagner, C., *Z. Electrochem.*, 35, 581, 1961.

154. Kalhweit, M., *Faraday Discuss. Chem. Soc.*, 61, 48, 1976.

155. Parbhakar, K., Lewandowski, J., and Dao, L.H., *J. Colloid Interface Sci.*, 174, 142, 1995.

156. Kabalnov, A.S., Pertzov, A.V., and Shchukin, E.D., *Colloids Surf.*, 24, 19, 1987.

157. Kabalnov, A.S. and Shchukin, E.D., *Adv. Colloid Interface Sci.*, 38, 69, 1992.

158. McClements, D.J., Dungan, S.R., German, J.B., and Kinsela, J.E., *Food Hydrocolloids*, 6, 415, 1992.

159. Weiss, J., Coupland, J.N., and McClements, D.J., *J. Phys. Chem*., 100, 1066, 1996.

160. Weiss, J., Canceliere, C., and McClements, D.J., *Langmuir*, 16, 6833, 2000.

161. Kabalnov, A.S., *Langmuir,* 10, 680, 1994.

162. Ivanov, I.B. and Kralchevsky, P.A., Mechanics and thermodynamics of curved thin liquid films, in *Thin Liquid Films,* Ivanov, I.B., Ed., Marcel Dekker, New York, 1988, p. 49.

163. Kralchevsky, P.A. and Ivanov, I.B., *J. Colloid Interface Sci.*, 137, 234, 1990.

164. Kralchevsky, P.A., Danov, K.D., and Ivanov, I.B., Thin liquid film physics, in *Foams: Theory, Measurements and Applications*, Prud'homme, R.K., Ed.; Marcel Dekker, New York, 1995, p. 1.

165. Rusanov, A.I., *Phase Equilibria and Surface Phenomena*, Khimia, Leningrad, 1967 (Russian); *Phasengleichgewichte und Grenzflächenerscheinungen,* Akademie Verlag, Berlin, 1978 (German).

166. Derjaguin, B.V. and Kussakov, M.M., *Acta Physicochem. USSR,* 10, 153, 1939.

167. Exerowa, D. and Scheludko, A., *Bull. Inst. Chim. Phys. Bulg. Acad. Sci.*, 4, 175, 1964.

168. Mysels, K.J., *J. Phys. Chem.*, 68, 3441, 1964.

169. Exerowa, D., *Commun. Dept. Chem. Bulg. Acad. Sci.*, 11, 739, 1978.

170. Kruglyakov, P.M., Equilibrium properties of free films and stability of foams and emulsions, in *Thin Liquid Films,* Ivanov, I.B., Ed., Marcel Dekker, New York, 1988, p. 767.

171. Martynov, G.A. and Derjaguin, B.V., *Kolloidn. Zh.*, 24, 480, 1962.

172. Toshev, B.V. and Ivanov, I.B., *Colloid Polym. Sci.*, 253, 558, 1975.

173. Ivanov, I.B. and Toshev, B.V., *Colloid Polym. Sci.*, 253, 593, 1975.

174. Frumkin, A., *Zh. Phys. Khim. USSR*, 12, 337, 1938.

175. de Feijter, J.A., Thermodynamics of thin liquid films, in *Thin Liquid Films,* Ivanov, I.B., Ed., Marcel Dekker, New York, 1988, p. 1.

176. Kralchevsky, P.A. and Ivanov, I.B., *Chem.Phys. Lett.,* 121**,** 111, 1985.

177. Nikolov, A.D., Kralchevsky, P.A., Ivanov, I.B., and Dimitrov, A.S., *AIChE Symposium Ser. 252,* Vol. 82, 82, 1986.

178. de Feijter, J.A. and Vrij, A., *J.Electroanal. Chem.*, 47, 9, 1972.

179. Kralchevsky, P.A. and Ivanov, I.B., *Chem.Phys. Lett.,* 121**,** 116, 1985.

180. Denkov, N.D., Petsev, D.N., and Danov, K.D., *J. Colloid Interface Sci.*, 176, 189, 1995.

181. Derjaguin, B.V., *Acta Physicochim. USSR,* 12, 181, 1940.

182. Princen, H.M. and Mason, S.G., *J. Colloid Sci.*, 20, 156, 1965.

183. Prins, A., *J. Colloid Interface Sci.*, 29, 177, 1969.

184. Clint, J.H., Clunie, J.S., Goodman, J.F., and Tate, J.R., *Nature* (*Lond.*), 223, 291, 1969.

185. Yamanaka, T., *Bull. Chem. Soc. Jap.*, 48, 1755, 1975.

186. Princen, H.M., *J. Phys. Chem.*, 72, 3342, 1968.

187. Princen, H.M. and Frankel, S., *J. Colloid Interface Sci.*, 35, 186, 1971.

188. Scheludko, A., Radoev, B., and Kolarov, T., *Trans. Faraday Soc.*, 64, 2213, 1968.

189. Haydon, D.A. and Taylor, J.L., *Nature (Lond.)*, 217, 739, 1968.

190. Kolarov, T. and Zorin, Z.M., *Kolloidn. Zh.*, 42, 899, 1980.

191. Kruglyakov, P.M. and Rovon, Yu.G., *Physical Chemistry of Black Hydrocarbon Films,* Nauka, Moskow, 1978 (in Russian).

192. Marinova, K.G., Gurkov, T.D., Dimitrova, T.D., Alargova, R.G., and Smith, D., *Langmuir*, 14, 2011, 1998.

193. Françon, M., *Progress in Microscopy,* Pergamon Press, London, 1961.

194. Beyer, H., *Theorie und Praxis der Interferenzmicroscopie,* Academische Verlagessellschaft, Leipzig, 1974.

195. Zorin, Z.M., *Kolloidn. Zh*., 39, 1158, 1977.

196. Zorin, Z., Platikanov, D., Rangelova, N., and Scheludko, A., in *Surface Forces and Liquid Interfaces*, Derjaguin, B.V., Ed., Nauka, Moscow, 1983, p. 200 (in Russian).

197. Nikolov, A.D., Kralchevsky, P.A., and Ivanov, I.B., *J. Colloid Interface Sci.*, 112, 122, 1986.

198. Lobo, L.A., Nikolov, A.D., Dimitrov, A.S., Kralchevsky, P.A., and Wasan, D.T., *Langmuir*, 6, 995, 1990.

199. Dimitrov, A.S., Nikolov, A.D., Kralchevsky, P.A., and Ivanov, I.B., *J. Colloid Interface Sci.*, 151, 462, 1992.

200. Picard, G., Schneider, J.E., and Fendler, J.H., *J. Phys. Chem.*, 94, 510, 1990.

201. Picard, G., Denicourt, N., and Fendler, J.H., *J. Phys. Chem.*, 95, 3705, 1991.

202. Skinner, F.K., Rotenberg, Y., and Neumann, A.W., *J. Colloid Interface Sci.*, 130, 25, 1989.

203. Dimitrov, A.S., Kralchevsky, P.A., Nikolov, A.D., Noshi, H., and Matsumoto, M., *J. Colloid Interface Sci.*, 145, 279, 1991.

204. Hadjiiski, A., Dimova, R., Denkov, N.D., Ivanov, I.B., and Borwankar, R., *Langmuir*, 12, 6665, 1996.

205. Ivanov, I.B., Hadjiiski, A., Denkov, N.D., Gurkov, T.D., Kralchevsky, P.A., and Koyasu, S., *Biophys. J.*, 75, 545, 1998.

206. Nicolson, M.M., *Proc. Camb. Phil. Soc*., 45, 288, 1949.

207. Chan, D.Y.C., Henry, J.D., and White, L.R., *J. Colloid Interface Sci*., 79, 410, 1981.

208. Paunov, V.N., Kralchevsky, P.A., Denkov, N.D., Ivanov, I.B., and Nagayama, K., *J. Colloid Interface Sci*., 157, 100, 1993.

209. Kralchevsky, P.A., Paunov, V.N., Ivanov, I.B., and Nagayama, K., *J. Colloid Interface Sci*., 151, 79, 1992.

210. Kralchevsky, P.A., Paunov, V.N., Denkov, N.D., Ivanov, I.B., and Nagayama, K., *J. Colloid Interface Sci*., 155, 420, 1993.

211. Kralchevsky, P.A. and Nagayama, K., *Langmuir*, 10, 23, 1994.

212. Kralchevsky, P.A. and Nagayama, K., *Adv. Colloid Interface Sci.*, 85, 145, 2000.

213. Denkov, N.D., Velev, O.D., Kralchevsky, P.A., Ivanov, I.B., Nagayama, K., and Yoshimura, H., *Langmuir,* 8, 3183, 1992.

214. Dimitrov, A.S., Dushkin, C.D., Yoshimura, H., and Nagayama, K., *Langmuir,* 10, 432, 1994.

215. Sasaki, M. and Hane, K., *J. Appl. Phys.,* 80, 5427, 1996.

216. Du, H., Chen, P., Liu, F., Meng, F.-D., Li, T.-J., and Tang, X.-Y., *Materials Chem. Phys.*, 51, 277, 1977.

217. Price, W.C., Williams, R.C., and Wyckoff, R.W.G., *Science*, 102, 277, 1945.

218. Cosslett, V.E. and Markham, R., *Nature*, 161, 250, 1948.

219. Horne, R.W. and Pasquali-Ronchetti, I., *J. Ultrastruct. Res.*, 47, 361, 1974.

220. Harris, J.R., *Micron Microscopica Acta*, 22, 341, 1991.

221. Yoshimura, H., Matsumoto, M., Endo, S., and Nagayama, K., *Ultramicroscopy*, 32, 265, 1990.

222. Yamaki, M., Higo, J., and Nagayama, K., *Langmuir*, 11, 2975, 1995.

223. Nagayama, K., *Colloids Surf. A,* 109, 363, 1996.

224. Burmeister, F., Schäfle, C., Keilhofer, B., Bechinger, C., Boneberg, J., and Leiderer, P., *Adv. Mater*., 10, 495, 1998.

225. Xia, Y., Tien, J., Qin, D., and Whitesides, G.M., *Langmuir,* 12, 4033, 1996.

226. Lindström, H., Rensmo, H., Sodergren, S., Solbrand, A., and Lindquist, S.E., *J. Phys. Chem.,* 100, 3084, 1996.

227. Matsushita, S., Miwa, T., and Fujishima, A., *Langmuir,* 13, 2582, 1997.

228. Murray, C.B., Kagan, C.R., and Bawendi, M.G., *Science,* 270, 1335, 1995.

229. Jap, B.K., Zulauf, M., Scheybani, T., Hefti, A., Baumeister, W., Aebi, U., and Engel, A., *Ultramicroscopy*, 46, 45, 1992.

230. De Rossi, D., Ahluwalia, A., and Mulè, M., *IEEE Eng. Med. Biol.*, 13, 103, 1994.

231. Kralchevsky, P.A. and Denkov, N.D., *Current Opinion Colloid Interface Sci*., 6, 383, 2001.

232. Gil, T., Ipsen, J.H., Mouritsen, O.G., Sabra, M.C., Sperotto, M.M., and Zuckermann, M.J., *Biochim. Biophys. Acta*, 1376, 245, 1998.

233. Mansfield, S.L., Gotch, A.J., and Harms, G.S., *J. Phys. Chem.*, *B*, 103, 2262, 1999.

234. Fisher, L.R. and Malloy A.R., *Annu. Rep. Prog. Chem.,* Sect. C, 95, 373, 1999.

235. Kralchevsky, P.A., Paunov, V.N., and Nagayama, K., *J. Fluid Mech.*, 299, 105, 1995.

236. Camoin, C., Roussel, J.F., Faure, R., and Blanc, R., *Europhys. Lett.*, 3, 449, 1987.

237. Velev, O.D., Denkov, N.D., Paunov, V.N., Kralchevsky P.A., and Nagayama, K., *Langmuir*, 9, 3702, 1993.

238. Dushkin, C.D., Kralchevsky, P.A., Yoshimura, H., and Nagayama, K., *Phys. Rev. Lett.*, 75, 3454, 1995.

239. Lucassen, J., *Colloids Surf.*, 65, 131, 1992.

240. Stamou, D., Duschl, C., and Johannsmann, D., *Phys. Rev.*, *E*, 62, 5263, 2000.

241. Kralchevsky, P.A., Denkov, N.D., and Danov, K.D., *Langmuir,* 17, 2001, 7694.

242. Bowden, N., Terfort, A., Carbeck, J., and Whitesides, G.M., *Science*, 276, 233, 1997.

243. Bowden, N., Choi, I.S., Grzybowski, B.A., and Whitesides, G.M., *J. Am. Chem. Soc.*, 121, 5373, 1999.

244. Velikov, K.P., Durst, F., and Velev, O.D. *Langmuir,* 14, 1148, 1998.

245. Sur, J. and Pak, H.K., *J. Korean Phys. Soc.*, 38, 582, 2001.

246. Danov, K.D., Pouligny, B., Angelova, M.I., and Kralchevsky, P.A., in *Studies in Surface Science and Catalysis,* Vol. 132, Iwasawa Y., Oyama N., and Kunieda H., Eds., Elsevier, Amsterdam, 2001; p. 519.

247. Danov, K.D., Pouligny, B., and Kralchevsky, P.A., *Langmuir,* 17, 2001, 6599.

248. Kralchevsky, P.A., Paunov, V.N., Denkov, N.D., and Nagayama, K., *J. Colloid Interface Sci.*, 167, 47, 1994.

249. Velev, O.D., Denkov, N.D., Paunov, V.N., Kralchevsky, P.A., and Nagayama, K., *J. Colloid Interface Sci.*, 167, 66, 1994.

250. Petkov, J.T., Denkov, N.D., Danov, K.D., Velev, O.D., Aust, R., and Durst, F., *J. Colloid Interface Sci.*, 172, 147, 1995.

251. Danov, K.D., Aust, R., Durst, F., and Lange, U., *J. Colloid Interface Sci.,* 175, 36, 1995.

252. Petkov, J.T., Danov, K.D., Denkov, N.D., Aust, R., and Durst, F., *Langmuir,* 12, 2650, 1996.

253. Petkov, J.T., Gurkov, T.D., and Campbell, B.E., *Langmuir,* 17, 4556, 2001.

254. Derjaguin, B.V., Churaev, N.V., and Muller, V.M., *Surface Forces,* Plenum Press: Consultants Bureau, New York, 1987.

255. Derjaguin, B.V., *Kolloid Zeits.*, 69, 155, 1934.

256. Attard, P. and Parker, J.L., *J. Phys. Chem.*, 96, 5086, 1992.

257. Tabor, D. and Winterton, R.H.S., *Nature*, 219, 1120, 1968.

258. Keesom, W.H., *Proc. Amst*., 15, 850, 1913.

259. Debye, P., *Physik*, 2, 178, 1920.

260. London, F., *Z. Physics*, 63, 245, 1930.

261. Hamaker, H.C., *Physics*, 4, 1058, 1937.

262. Usui, S., Sasaki, H., and Hasegawa, F., *Colloids Surf.*, 18, 53, 1986.

263. Lifshitz, E.M., *Soviet Phys. JETP (Engl. Transl.),* 2, 73, 1956.

264. Dzyaloshinskii, I.E., Lifshitz, E.M., and Pitaevskii, L.P., *Adv. Phys.*, 10, 165, 1961.

265. Nir, S. and Vassilieff, C.S., Van der Waals interactions in thin films, in *Thin Liquid Films,* Ivanov, I.B., Ed., Marcel Dekker, New York, 1988, p. 207.

266. Danov, K.D., Petsev, D.N., Denkov, N.D., and Borwankar, R., *J. Chem. Phys.*, 99, 7179, 1993.

267. Casimir, H.R. and Polder, D., *Phys. Rev.*, 73, 360, 1948.

268. Mahanty, J. and Ninham, B.W., *Dispersion Forces,* Academic Press, New York, 1976.

269. Moelwyn-Hughes, E.A., *Physical Chemistry*, Pergamon Press, London, 1961; chap. 21.

270. Langmuir, I., *J. Chem. Phys.*, 6, 873, 1938.

271. Tenchov, B.G. and Brankov, J.G., *J. Colloid Interface Sci.,* 109, 172, 1986.

272. Vassilieff, C.S., Tenchov, B.G., Grigorov, L.S., and Richmond, P., *J. Colloid Interface Sci.*, 93, 8, 1983.

273. Verwey, E.J.W. and Overbeek, J.Th.G., *The Theory of Stability of Liophobic Colloids,* Elsevier, Amsterdam, 1948.

274. Muller, V.M., *Kolloidn. Zh.*, 38, 704, 1976.

275. McCormack, D., Carnie, S.L., and Chan, D.Y.C., *J. Colloid Interface Sci.*, 169, 177, 1995.

276. Hogg, R., Healy, T.W., and Fuerstenau, D.W., *Trans. Faraday Soc.*, 62, 1638, 1966.

277. Usui, S., *J. Colloid Interface Sci.*, 44, 107, 1973.

278. Russel, W.B., Saville, D.A., and Schowalter, W.R., *Colloidal Dispersions,* University Press, Cambridge, 1989.

279. Debye, P. and Hückel, E., *Z. Phys.*, 24, 185, 1923.

280. McCartney, L.N. and Levine, S., *J. Colloid Interface Sci.*, 30, 345, 1969.

281. Derjaguin, B.V. and Landau, L.D., *Acta Physicochim. USSR,* 14, 633, 1941.

282. Efremov, I.F., Periodic colloidal structures, in *Colloid and Surface Science,* Vol. 8, Matijevic, E., Ed., Wiley, New York, 1976, p. 85.

283. Schulze, H., *J. Prakt. Chem.*, 25, 431, 1882.

284. Hardy, W.B., *Proc. Roy. Soc. (Lond.)*, 66, 110, 1900.

285. Guldbrand, L., Jönsson, B., Wennerström, H., and Linse, P., *J. Chem. Phys.,* 80, 2221, 1984.

286. Kjellander, R. and Marčelja, S., *J. Phys. Chem.,* 90, 1230, 1986.

287. Attard, P., Mitchell, D.J., and Ninham, B.W., *J. Chem. Phys.,* 89, 4358, 1988.

288. Kralchevsky, P.A. and Paunov, V.N., *Colloids Surf.,* 64, 245, 1992.

289. Danov, K.D., Kralchevsky, P.A., and Ivanov, I.B., in *Handbook of Detergents, Part A: Properties*, Broze, G., Ed., Marcel Dekker, New York, 1999, p. 303.

290. Marra, J., *J. Phys. Chem.*, 90, 2145, 1986.

291. Marra, J., *Biophys. J.*, 50, 815, 1986.

292. Kjellander, R., Marčelja, S., Pashley, R.M., and Quirk, J.P., *J. Phys. Chem.*, 92, 6489, 1988.

293. Kjellander, R., Marčelja, S., Pashley, R.M., and Quirk, J.P., *J. Chem. Phys.*, 92, 4399, 1990.

294. Khan, A., Jönsson, B., and Wennerström, H., *J. Phys. Chem.,* 89, 5180, 1985.

295. Kohonen, M.M., Karaman, M.E., and Pashley, R.M., *Langmuir*, 16, 5749, 2000.

296. Paunov, V.N. and Kralchevsky, P.A., *Colloids Surf.,* 64, 265, 1992.

297. Tadros, Th.F., Steric interactions in thin liquid films, in *Thin Liquid Films,* Ivanov, I.B., Ed., Marcel Dekker, New York, 1988, p. 331.

298. Patel, S.S. and Tirel, M., *Ann. Rev. Phys. Chem.*, 40, 597, 1989.

299. Ploehn, H.J. and Russel, W.B., *Adv. Chem. Eng.*, 15, 137, 1990.

300. de Gennes, P.G., *Scaling Concepts in Polymer Physics,* Cornell University Press, Ithaca, NY, 1979, chap. 3.

301. Dolan, A.K. and Edwards, S.F., *Proc. Roy. Soc. (Lond.)*, A337, 509, 1974.

302. Dolan, A.K. and Edwards, S.F., *Proc. Roy. Soc. (Lond.)*, A343, 427, 1975.

303. de Gennes, P.G., *C. R. Acad. Sci. (Paris)*, 300, 839, 1985.

304. de Gennes, P.G., *Adv. Colloid Intrface Sci.,* 27, 189, 1987.

305. Alexander, S.J., *Physique*, 38, 983, 1977.

306. Taunton, H.J., Toprakcioglu, C., Fetters, L.J., and Klein, J., *Macromolecules*, 23, 571, 1990.

307. Klein, J. and Luckham, P., *Nature*, 300, 429, 1982; *Macromolecules*, 17, 1041, 1984.

308. Luckham, P.F. and Klein, J., *J. Chem. Soc. Faraday Trans.*, 86, 1363, 1990.

309. Sonntag, H., Ehmka, B., Miller, R., and Knapschinski, L., *Adv. Colloid Interface Sci.*, 16, 381, 1982.

310. Horn, R.G. and Israelachvili, J.N., *Chem. Phys. Lett.*, 71, 192, 1980.

311. Nikolov, A.D., Wasan, D.T., Kralchevsky, P.A., and Ivanov, I.B., Ordered structures in thinning micellar foam and latex films, in *Ordering and Organisation in Ionic Solutions,* Ise N. and Sogami, I., Eds., World Scientific, Singapore, 1988.

312. Nikolov, A.D. and Wasan, D.T., *J. Colloid Interface Sci.*, 133, 1, 1989.

313. Nikolov, A.D., Kralchevsky, P.A., Ivanov, I.B., and Wasan, D.T., *J. Colloid Interface Sci.,* 133, 13, 1989.

314. Nikolov, A.D., Wasan, D.T., Denkov, N.D., Kralchevsky, P.A., and Ivanov, I.B., *Prog. Colloid Polym. Sci.*, 82, 87, 1990.

315. Wasan, D.T., Nikolov, A.D., Kralchevsky, P.A., and Ivanov, I.B., *Colloids Surf.*, 67, 139, 1992.

316. Asakura, S. and Oosawa, F., *J. Chem. Phys.*, 22, 1255, 1954; *J. Polym. Sci.*, 33, 183, 1958.

317. de Hek, H. and Vrij, A., *J. Colloid Interface Sci.*, 84, 409, 1981.

318. Snook, I.K. and van Megen, W., *J. Chem. Phys.*, 72, 2907, 1980.

319. Kjellander, R. and Marčelja, S., *Chem Phys Lett.*, 120, 393, 1985.

320. Tarazona, P. and Vicente, L., *Mol. Phys.*, 56, 557, 1985.

321. Evans, R., and Parry, A.O., *J. Phys. Condens. Matter*, 2, SA15, 1990.

322. Henderson, J.R., *Mol. Phys.*, 59, 89, 1986.

323. Henderson, D., *J. Colloid Interface Sci.*, 121, 486, 1988.

324. Kralchevsky, P.A. and Denkov, N.D. *Chem. Phys. Lett.*, 240, 385, 1995; *Prog. Colloid Polymer Sci.*, 98, 18, 1995.

325. Carnahan, N.F. and Starling, K.E., *J. Chem. Phys.*, 51, 635, 1969.

326. Kjellander, R. and Sarman, S., *Chem. Phys. Lett.*, 149, 102, 1988.

327. Beresford-Smith, B. and Chan, D.Y.C., *Chem. Phys. Lett*., 92, 474, 1982.

328. Richetti, P. and Kékicheff, P., *Phys. Rev. Lett.*, 68, 1951, 1992.

329. Karlström, G., *Chem. Scripta*, 25, 89, 1985.

330. Bondy, C., *Trans. Faraday Soc.*, 35, 1093, 1939.

331. Patel, P.D. and Russel, W.B., *J. Colloid Interface Sci.*, 131, 192, 1989.

332. Aronson, M.P., *Langmuir*, 5, 494, 1989.

333. van Lent, B., Israels, R., Scheutjens, J.M.H.M., and Fleer, G.J., *J. Colloid Interface Sci.*, 137, 380, 1990.

334. Joanny, J.F., Leibler, L., and de Gennes, P.G., *J. Polym. Sci.*, 17, 1073, 1979.

335. Evans, E. and Needham, D., *Macromolecules*, 21, 1822, 1988.

336. Johnnott, E.S., *Phil. Mag.*, 70, 1339, 1906.

337. Perrin, R.E., *Ann. Phys.*, 10, 160, 1918.

338. Bruil, H.G. and Lyklema, J., *Nature*, 233, 19, 1971.

339. Friberg, S., Linden, St.E., and Saito, H., *Nature*, 251, 494, 1974.

340. Keuskamp, J.W. and Lyklema, J., *ACS Symp. Ser.*, 8, 191, 1975.

341. Kruglyakov, P.M., *Kolloidn. Zh.*, 36, 160, 1974.

342. Kruglyakov, P.M. and Rovin, Yu.G., *Physical Chemistry of Black Hydrocarbon Films,* Nauka, Moscow, 1978 [in Russian].

343. Manev, E., Sazdanova, S.V., and Wasan, D.T., *J. Dispersion Sci. Technol.*, 5, 111, 1984.

344. Basheva, E.S., Nikolov, A.D., Kralchevsky, P.A., Ivanov, I.B., and Wasan, D.T., in *Surfactants in Solution,* Vol. 12, Mittal, K.L., and Shah, D.O., Eds., Plenum Press, New York, 1991, p. 467.

345. Bergeron, V. and Radke, C.J., *Langmuir*, 8, 3020, 1992.

346. Kralchevsky, P.A., Nikolov, A.D., Wasan, D.T., and Ivanov, I.B., *Langmuir*, 6, 1180, 1990.

347. Claesson, P.M., Kjellander, R., Stenius, P., and Christenson, H.K., *J. Chem. Soc. Faraday Trans. I,* 82, 2735, 1986.

348. Parker, J.L., Richetti, P., and Kékicheff, P., *Phys. Rev. Lett.*, 68, 1955, 1992.

349. Basheva, E.S., Danov, K.D., and Kralchevsky, P.A., *Langmuir,* 13, 4342, 1997.

350. Dushkin, C.D., Nagayama, K., Miwa, T., and Kralchevsky, P.A., *Langmuir*, 9, 3695, 1993.

351. Pollard, M.L. and Radke, C.J., *J. Chem. Phys.*, 101, 6979, 1994.

352. Chu, X.L., Nikolov, A.D., and Wasan, D.T., *Langmuir*, 10, 4403, 1994.

353. Chu, X.L., Nikolov, A.D., and Wasan, D.T., *J. Chem. Phys.*, 103, 6653, 1995.

354. Stanley, H.E. and Teixeira, J., *J. Chem. Phys.*, 73, 3404, 1980.

355. Israelachvili, J.N. and Adams, G.E., *J. Chem. Soc. Faraday Trans. 1,* 74, 975, 1978.

356. Israelachvili, J.N. and Pashley, R.M., *Nature*, 300, 341, 1982.

357. Pashley, R.M., *J. Colloid Interface Sci.*, 80, 153, 1981.

358. Pashley, R.M., *J. Colloid Interface Sci.*, 83, 531, 1981.

359. Healy, T.W., Homola, A., James, R.O., and Hunter, R.J., *Faraday Discuss. Chem Soc.*, 65, 156, 1978.

360. Marčelja, S. and Radič, N., *Chem. Phys Lett.*, 42, 129, 1976.

361. Schibi, D. and Ruckenstein, E., *Chem. Phys Lett.*, 95, 435, 1983.

362. Attard, P. and Batchelor, M.T., *Chem. Phys. Lett.*, 149, 206, 1988.

363. Jönsson, B. and Wennerström, H., *J. Chem. Soc. Faraday Trans. 2*, 79, 19, 1983.

364. Leikin, S. and Kornyshev, A.A., *J. Chem. Phys.*, 92**,** 6890, 1990.

365. Israelachvili, J.N. and Wennerström, H., *J. Phys. Chem.*, 96, 520, 1992.

366. Henderson, D. and Lozada-Cassou, M., *J. Colloid Interface Sci.*, 114, 180, 1986; *J. Colloid Interface Sci.*, 162, 508, 1994.

367. Basu, S. and Sharma, M.M., *J. Colloid Interface Sci.*, 165, 355, 1994.

368. Paunov, V.N., Dimova, R.I., Kralchevsky, P.A., Broze, G., and Mehreteab, A., *J. Colloid Interface Sci.,* 182, 239, 1996.

369. Booth, F., *J. Chem. Phys.*, 19, 391, 1951.

370. Bikerman, J.J., *Philos. Mag.*, 33, 384, 1942.

371. Rowlinson, J.S., Development of theories of inhomogeneous fluids, in *Fundamentals of Inhomogeneous Fluids,* Henderson, D., Ed., Marcel Dekker, New York, 1992.

372. Claesson, P., Carmona-Ribeiro, A.M., and Kurihara, K., *J. Phys. Chem.*, 93, 917, 1989.

373. Horn, R.G., Smith, D.T., and Haller, W., *Chem. Phys. Lett.,* 162, 404, 1989.

374. Tchaliovska, S., Herder, P., Pugh, R., Stenius, P., and Eriksson, J.C., *Langmuir*, 6, 1533, 1990.

375. Pashley, R.M., McGuiggan, P.M., Ninham, B.W., and Evans, D.F., *Science*, 229, 1088, 1985.

376. Rabinovich, Y.I. and Derjaguin, B.V., *Colloids Surf.*, 30, 243, 1988.

377. Parker, J.L., Cho, D.L., and Claesson, P.M., *J. Phys. Chem.*, 93, 6121, 1989.

378. Christenson, H.K., Claesson, P.M., Berg, J., and Herder, P.C., *J. Phys. Chem.*, 93, 1472, 1989.

379. Christenson, H.K., Fang, J., Ninham, B.W., and Parker, J.L., *J. Phys. Chem.*, 94, 8004, 1990.

380. Ducker, W.A., Xu, Z., and Israelachvili, J.N., *Langmuir*, 10, 3279, 1994.

381. Eriksson J.C., Ljunggren, S., and Claesson, P.M., *J. Chem. Soc. Faraday Trans. 2,* 85, 163, 1989.

382. Joesten, M.D. and Schaad, L.J., *Hydrogen Bonding,* Marcel Dekker, New York, 1974.

383. Stillinger, F.H. and Ben-Naim, A., *J. Chem. Phys.*, 47, 4431, 1967.

384. Conway, B.E., *Adv. Colloid Interface Sci.*, 8, 91, 1977.

385. Kuzmin, V.L. and Rusanov, A.I., *Kolloidn. Z.*, 39, 455, 1977.

386. Dubrovich, N.A., *Kolloidn. Z.*, 57, 275, 1995.

387. Christenson, H.K. and Claesson, P.M., *Science*, 239, 390, 1988.

388. Parker, J.L., Claesson, P.M., and Attard, P., *J. Phys. Chem.*, 98, 8468, 1994.

389. Carambassis, A., Jonker, L.C., Attard, P., and Rutland, M.W., *Phys. Rev. Lett.*, 80, 5357, 1998.

390. Mahnke, J., Stearnes, J., Hayes, R.A., Fornasiero, D., and Ralston, J., *Phys. Chem. Chem. Phys.*, 1, 2793, 1999.

391. Considine, R.F., Hayes, R.A., and Horn, R.G., *Langmuir*, 15, 1657, 1999.

392. Considine, R.F. and Drummond, C., *Langmuir*, 16, 631, 2000.

393. Attard, P., *Langmuir,* 16, 4455, 2000.

394. Yakubov, G.E., Butt, H.-J., and Vinogradova, O., *J. Phys. Chem. B*, 104, 3407, 2000.

395. Ederth, T., *J. Phys Chem. B*, 104, 9704, 2000.

396. Ishida, N., Sakamoto, M., Miyahara, M., and Higashitani, K., *Langmuir,* 16, 5681, 2000.

397. Ishida, N., Inoue, T., Miyahara, M., and Higashitani, K., *Langmuir,* 16, 6377, 2000.

398. Tanford, C., *The Hydrophobic Effect,* Wiley, New York, 1980.

399. Leckband, D.E., Israelachvili, J.N., Schmitt, F.-J., and Knoll, W., *Science,* 255, 1419, 1992.

400. Helfrich, W., *Z. Naturforsch.*, 33a, 305, 1978.

401. Servuss, R.M. and Helfrich, W., *J. Phys. (France),* 50, 809, 1989.

402. Fernandez-Puente, L., Bivas, I., Mitov, M.D., and Méléard, P., *Europhys. Lett.*, 28, 181, 1994.

403. Safinya, C.R., Roux, D., Smith, G.S., Sinha, S.K., Dimon, P., Clark, N.A., and Bellocq, A.M., *Phys. Rev. Lett.*, 57, 2718, 1986.

404. McIntosh, T.J., Magid, A.D., and Simon, S.A., *Biochemistry*, 28, 7904, 1989.

405. Abillon, O. and Perez, E., *J. Phys. (France),* 51, 2543, 1990.

406. Evans, E.A. and Skalak, R., *Mechanics and Thermodynamics of Biomembranes,* CRC Press, Boca Raton, Florida, 1980.

407. Aniansson, G.A.E., Wall, S.N., Almgren, M., Hoffman, H., Kielmann, I., Ulbricht, W., Zana, R., Lang. J., and Tondre, C., *J. Phys. Chem.*, 80, 905, 1976.

408. Aniansson, G.A.E., *J. Phys. Chem.*, 82, 2805, 1978.

409. Dimitrova, T.D., Leal-Calderon, F., Gurkov, T.D., and Campbell, B., *Langmuir*, 17, 8069, 2001.

410. Bird, R.B., Stewart, W.E., and Lightfoot, E.N., *Transport Phenomena*, Wiley, New York, 1960.

411. Germain, P., *Mécanique des Milieux Continus*, Masson et Cie, Paris, 1962.

412. Batchelor, G.K., *An Introduction of Fluid Mechanics*, Cambridge University Press, London, 1967.

413. Slattery, J.C., *Momentum, Energy, and Mass Transfer in Continua*, R.E. Krieger, Huntington, New York, 1978.

414. Landau, L.D. and Lifshitz, E.M., *Fluid Mechanics*, Pergamon Press, Oxford, 1984.

415. Barnes, H.A., Hutton, J.F., and Walters, K., *An Introduction to Rheology*, Elsevier, Amsterdam, 1989.

416. Walters, K., Overview of macroscopic viscoelastic flow, in *Viscoelasticity and Rheology*, Lodge, A.S., Renardy, M., and Nohel, J.A., Eds., Academic Press, London, 1985, p. 47.

417. Boger, D.V., *Ann. Rev. Fluid Mech.*, 19, 157, 1987.

418. Barnes, H.A., *J. Rheol.*, 33, 329, 1989.

419. Navier, M., *Mém. de l'Acad. d. Sci.*, 6, 389, 1827.

420. Stokes, G.G., *Trans. Cambr. Phil. Soc.*, 8, 287, 1845.

421. Happel, J. and Brenner, H., *Low Reynolds Number Hydrodynamics with Special Applications to Particulate Media*, Prentice-Hall, Englewood Cliffs, New York, 1965.

422. Kim, S. and Karrila, S.J., *Microhydrodynamics: Principles and Selected Applications*, Butterworth-Heinemann, Boston, 1991.

423. Reynolds, O., *Phil. Trans. Roy. Soc. (Lond.)*, A177, 157, 1886.

424. Lamb, H., *Hydrodynamics*, Cambridge University Press, London, 1963.

425. Felderhof, B.U., *J. Chem. Phys.*, 49, 44, 1968.

426. Sche, S. and Fijnaut, H.M., *Surface Sci.*, 76, 186, 1976.

427. Maldarelli, Ch. and Jain, R.K., The hydrodynamic stability of thin films, in *Thin Liquid Films*, Ivanov, I.B., Ed., Marcel Dekker, New York, 1988, p. 497.

428. Valkovska, D.S. and Danov, K.D., *J. Colloid Interface Sci.*, 241, 400, 2001.

429. Taylor, P., *Proc. Roy. Soc. (Lond.)*, A108, 11, 1924.

430. Dimitrov, D.S. and Ivanov, I.B., *J. Colloid Interface Sci.*, 64, 97, 1978.

431. Ivanov, I.B., Dimitrov, D.S., Somasundaran, P., and Jain, R.K., *Chem. Eng. Sci.*, 40, 137, 1985.

432. Ivanov, I.B. and Dimitrov, D.S., Thin film drainage, in *Thin Liquid Films*, Ivanov, I.B., Ed., Marcel Dekker, New York, 1988, p. 379.

433. O'Neill, M.E. and Stewartson, K., *J. Fluid Mech.*, 27, 705, 1967.

434. Goldman, A.J., Cox, R.G., and Brenner, H., *Chem. Eng. Sci.*, 22, 637, 1967.

435. Goldman, A.J., Cox, R.G., and Brenner, H., *Chem. Eng. Sci.*, 22, 653, 1967.

436. Levich, V.G., *Physicochemical Hydrodynamics*, Prentice-Hall, Englewood Cliffs, New Jersey, 1962.

437. Edwards, D.A., Brenner, H., and Wasan, D.T., *Interfacial Transport Processes and Rheology*, Butterworth-Heinemann, Boston, 1991.

438. Charles, G.E. and Mason, S.G., *J. Colloid Sci.*, 15, 236, 1960.

439. Danov, K.D., Denkov, N.D., Petsev, D.N., Ivanov, I.B., and Borwankar, R., *Langmuir*, 9, 1731, 1993.

440. Danov, K.D., Valkovska, D.S., and Ivanov, I.B., *J. Colloid Interface Sci.*, 211, 291, 1999.

441. Hartland, S., Coalescence in dense-packed dispersions, in *Thin Liquid Films*, Ivanov, I.B., Ed., Marcel Dekker, New York, 1988, p. 663.

442. Hetsroni, G., Ed., *Handbook of Multiphase System*, Hemisphere Publishing, New York, 1982, pp. 1-96.

443. Davis, A.M.J., Kezirian, M.T., and Brenner, H., *J. Colloid Interface Sci.*, 165, 129, 1994.

444. Brenner, H., *Chem. Eng. Sci.*, 18, 1, 1963.

445. Brenner, H., *Chem. Eng. Sci.*, 19, 599, 1964; *Chem. Eng. Sci.*, 19, 631, 1964.

446. Brenner, H. and O'Neill, M.E., *Chem. Eng. Sci.*, 27, 1421, 1972.

447. Van de Ven, T.G.M., *Colloidal Hydrodynamics*, Academic Press, London, 1988.

448. Jeffery, G.B., *Proc. Lond. Math. Soc.*, 14, 327, 1915.

449. Stimson, M. and Jeffery, G.B., *Proc. R. Soc. (Lond.)*, A111, 110, 1926.

450. Cooley, M.D.A. and O'Neill, M.E., *Mathematika*, 16, 37, 1969.

451. Cooley, M.D.A. and O'Neill, M.E., *Proc. Cambridge Philos. Soc.*, 66, 407, 1969.

452. Davis, M.H., *Chem. Eng. Sci.*, 24, 1769, 1969.

453. O'Neill, M.E. and Majumdar, S.R., *Z. Angew. Math. Phys.*, 21, 164, 1970; *Z. Angew. Math. Phys.*, 21, 180, 1970.

454. Davis, M.H., *Two Unequal Spheres in a Slow Linear Shear Flow*, Rept. NCAR-TN/STR-64, National Center for Atmospheric Research, Bolder, CO, 1971.

455. Batchelor, G.K., *J. Fluid Mech.*, 74, 1, 1976.

456. Davis, R.H. and Hill, N.A., *J. Fluid Mech.*, 236, 513, 1992.

457. Batchelor, G.K., *J. Fluid Mech.*, 119, 379, 1982.

458. Batchelor, G.K. and Wen, C.-S., *J. Fluid Mech.*, 124, 495, 1982.

459. Jeffrey, D.J. and Onishi, Y., *J. Fluid Mech.*, 139, 261, 1984.

460. Fuentes, Y.O., Kim, S., and Jeffrey, D.J., *Phys. Fluids*, 31, 2445, 1988; *Phys. Fluids*, A1, 61, 1989.

461. Stokes, G.G., *Trans. Cambridge Phil. Soc.*, 1, 104, 1851.

462. Exerowa, D. and Kruglyakov, P. M., *Foam and Foam Films: Theory, Experiment, Application*, Elsevier, New York, 1998.

463. Ivanov, I.B., Radoev, B.P., Traykov, T.T., Dimitrov, D.S., Manev, E.D., and Vassilieff, C.S., *Proceedings of the International Conference on Colloid Surface Science*, Wolfram, E., Ed., Akademia Kiado, Budapest, 1975, p. 583.

464. Denkov, N.D., Petsev, D.N., and Danov, K.D., *Phys. Rev. Let.*, 71, 3226, 1993.

465. Valkovska, D.S., Danov, K.D., and Ivanov, I.B., *Colloid Surf. A*, 156, 547, 1999.

466. Davis, R.H., Schonberg, J.A., and Rallison, J.M., *Phys. Fluids*, A1, 77, 1989.

467. Chi, B.K. and Leal, L.G., *J. Fluid Mech.*, 201, 123, 1989.

468. Ascoli, E.P., Dandy, D.S., and Leal, L.G., *J. Fluid Mech.*, 213, 287, 1990.

469. Yiantsios, S.G. and Davis, R.H., *J. Fluid Mech.*, 217, 547, 1990.

470. Zhang, X. and Davis, R.H., *J. Fluid Mech.*, 230, 479, 1991.

471. Chesters, A.K., *Trans. Inst. Chem. Engrs. A*, 69, 259, 1991.

472. Yiantsios, S.G. and Davis, R.H., *J. Colloid Interface Sci.*, 144, 412, 1991.

473. Yiantsios, S.G. and Higgins, B.G., *J. Colloid Interface Sci.*, 147, 341, 1991.

474. Joye, J.-L., Hirasaki, G.J., and Miller, C.A., *Langmuir*, 8, 3083, 1992.

475. Joye, J.-L., Hirasaki, G.J., and Miller, C.A., *Langmuir*, 10, 3174, 1994.

476. Abid, S. and Chestrers, A.K., *Int. J. Multiphase Flow*, 20, 613, 1994.

477. Li, D., *J. Colloid Interface Sci.*, 163, 108, 1994.

478. Saboni, A., Gourdon, C., and Chesters, A.K., *J. Colloid Interface Sci.*, 175, 27, 1995.

479. Rother, M.A., Zinchenko, A.Z., and Davis, R.H., *J. Fluid Mech.*, 346, 117, 1997.

480. Singh, G., Miller, C.A., and Hirasaki, G.J., *J. Colloid Interface Sci.*, 187, 334, 1997.

481. Cristini, V., Blawzdziewicz, J., and Loewenberg, M., *J. Fluid Mech.*, 366, 259, 1998.

482. Bazhlekov, I.B., Chesters, A.K., and van de Vosse, F.N., *Int. J. Multiphase Flow*, 26, 445, 2000.

483. Bazhlekov, I.B., van de Vosse, F.N., and Chesters, A.K., *Journal of Non-Newtonian Fluid Mechanics*, 93, 181, 2000.

484. Chesters, A.K. and Bazhlekov, I.B., *J. Colloid Interface Sci.*, 230, 229-243, 2000.

485. Boulton-Stone, J.M. and Blake, J.R., *J. Fluid Mech.*, 254, 437, 1993.

486. Frankel, S. and Mysels, K., *J. Phys. Chem.*, 66, 190, 1962.

487. Velev, O.D., Constantinides, G.N., Avraam, D.G., Payatakes, A.C., and Borwankar, R.P., *J. Colloid Interface Sci.*, 175, 68, 1995.

488. Exerowa, D., Nikolov, A., and Zacharieva, M., *J. Colloid Interface Sci.*, 81, 419, 1981.

489. de Vries, A.J., *Rec. Trav. Chim. Pays-Bas.*, 77, 441, 1958.

490. Vrij, A., *Discuss. Faraday Soc.*, 42, 23, 1966.

491. Ivanov, I.B., Radoev, B.P., Manev, E.D., and Sheludko, A.D., *Trans. Faraday Soc.*, 66, 1262, 1970.

492. Gumerman, R.J. and Homsy, G.M., *Chem. Engng. Commun.*, 2, 27, 1975.

493. Malhotra, A.K. and Wasan, D.T., *Chem. Engng. Commun.*, 48 35, 1986.

494. Valkovska, D. S., Danov, K.D., and Ivanov, I.B., *Adv. Colloid Interface Sci.*, 96, 101, 2002.

495. Manev, E.D., Sazdanova, S.V., and Wasan, D.T., *J. Colloid Interface Sci.*, 97, 591, 1984.

496. Ivanov, I.B., *Pure Appl. Chem.*, 52, 1241, 1980.

497. Aveyard, R., Binks, B.P., Fletcher, P.D.I., and Ye, X., *Prog. Colloid Polymer Sci.*, 89, 114, 1992.

498. Velev, O.D., Gurkov, T.D., Chakarova, Sv.K., Dimitrova, B.I., and Ivanov, I.B., *Colloids Surf. A*, 83, 43, 1994.

499. Dickinson, E., Murray, B.S., and Stainsby, G., *J. Chem. Soc. Faraday Trans.*, 84, 871, 1988.

500. Ivanov, I.B., Lectures at INTEVEP, Petroleos de Venezuela, Caracas, June 1995.

501. Ivanov, I.B. and Kralchevsky, P.A., *Colloid Surf. A*, 128, 155, 1997.

502. Basheva, E.S., Gurkov, T.D., Ivanov, I.B., Bantchev, G.B., Campbell, B., and Borwankar, R.P., *Langmuir*, 15, 6764, 1999.

503. Boussinesq, M.J., *Ann. Chim. Phys.*, 29, 349, 1913; *Ann. Chim. Phys.*, 29, 357, 1913.

504. Aris, R., *Vectors, Tensors, and the Basic Equations of Fluid Mechanics*, Prentice Hall, Englewood Cliffs, NJ, 1962.

505. Brenner, H. and Leal, L.G., *J. Colloid Interface Sci.*, 62, 238, 1977.

506. Brenner, H. and Leal, L.G., *J. Colloid Interface Sci.*, 65, 191, 1978.

507. Brenner, H. and Leal, L.G., *AIChE J.*, 24, 246, 1978.

508. Brenner, H. and Leal, L.G., *J. Colloid Interface Sci.*, 88, 136, 1982.

509. Stone, H.A., *Phys. Fluids*, A2, 111, 1990.

510. Valkovska, D.S. and Danov, K.D., *J. Colloid Interface Sci.*, 223, 314, 2000.

511. Stoyanov, S.D. and Denkov, N.D., *Langmuir*, 17, 1150, 2001.

512. Feng, S.-S., *J. Colloid Interface Sci.*, 160, 449, 1993.

513. Stebe, K.J. and Maldarelli, Ch., *Phys. Fluids*, A3, 3, 1991.

514. Stebe, K.J. and Maldarelli, Ch., *J. Colloid Interface Sci.*, 163, 177, 1994.

515. Scriven, L.E., *Chem. Eng. Sci.*, 12, 98, 1960.

516. Scriven, L.E. and Sternling, C.V., *J. Fluid Mech.*, 19, 321, 1964.

517. Slattery, J.C., *Chem. Eng. Sci.*, 19, 379, 1964; *Chem. Eng. Sci.*, 19, 453, 1964.

518. Slattery, J.C., *I&EC Fundam.*, 6, 108, 1967.

519. Slattery, J.C., *Interfacial Transport Phenomena*, Springer-Verlag, New York, 1990.

520. Barton, K.D. and Subramanian, R.S., *J. Colloid Interface Sci.*, 133, 214, 1989.

521. Feuillebois, F., *J. Colloid Interface Sci.*, 131, 267, 1989.

522. Merritt, R.M. and Subramanian, R.S., *J. Colloid Interface Sci.*, 131, 514, 1989.

523. Mannheimer, R.J. and Schechter, R.S., *J. Colloid Interface Sci.*, 12, 98, 1969.

524. Pintar, A.J., Israel, A.B., and Wasan, D.T., *J. Colloid Interface Sci.*, 37, 52, 1971.

525. Gardner, J.W. and Schechter, R.S., *Colloid Interface Sci.*, 4, 98, 1976.

526. Li, D. and Slattery, J.C., *J. Colloid Interface Sci.*, 125, 190, 1988.

527. Tambe, D.E. and Sharma, M.M., *J. Colloid Interface Sci.*, 147, 137, 1991.

528. Tambe, D.E. and Sharma, M.M., *J. Colloid Interface Sci.*, 157, 244, 1993.

529. Tambe, D.E. and Sharma, M.M., *J. Colloid Interface Sci.*, 162, 1, 1994.

530. Horozov, T., Danov, K., Kralchevsky, P., Ivanov, I., and Borwankar, R., A local approach in interfacial rheology: theory and experiment, in First World Congress on Emulsion, Paris, 3-20, 137, 1993.

531. Danov, K. D., Ivanov, I. B., and Kralchevsky, P. A., Interfacial rheology and emulsion stability, in Second World Congress on Emulsion, Paris, 2-2, 152, 1997.

532. de Groot, S.R. and Mazur, P., *Non-equilibrium Thermodynamics*, Interscience, New York, 1962.

533. Moeckel, G.P., *Arch. Rat. Mech. Anal.*, 57, 255, 1975.

534. Rushton, E. and Davies, G.A., *Appl. Sci. Res.*, 28, 37, 1973.

535. Haber, S., Hetsroni, G., and Solan, A., *Int. J. Multiphase Flow*, 1, 57, 1973.

536. Reed, L.D. and Morrison, F.A., *Int. J. Multiphase Flow*, 1, 573, 1974.

537. Hetsroni, G. and Haber, S., *Int. J. Multiphase Flow*, 4, 1, 1978.

538. Morrison, F.A. and Reed, L.D., *Int. J. Multiphase Flow*, 4, 433, 1978.

539. Beshkov, V.N., Radoev, B.P., and Ivanov, I.B., *Int. J. Multiphase Flow*, 4, 563, 1978.

540. Murdoch, P.G. and Leng, D.E., *Chem. Eng. Sci.*, 26, 1881, 1971.

541. Reed, X.B., Riolo, E., and Hartland, S., *Int. J. Multiphase Flow*, 1, 411, 1974; *Int. J. Multiphase Flow*, 1, 437, 1974.

542. Ivanov, I.B. and Traykov, T.T., *Int. J. Multiphase Flow*, 2, 397, 1976.

543. Traykov, T.T. and Ivanov, I.B., *Int. J. Multiphase Flow*, 3, 471, 1977.

544. Lu, C.-Y.D. and Cates, M.E., *Langmuir*, 11, 4225, 1995.

545. Jeelany, S.A.K. and Hartland, S., *J. Colloid Interface Sci.*, 164, 296, 1994.

546. Zapryanov, Z., Malhotra, A.K., Aderangi, N., and Wasan, D.T., *Int. J. Multiphase Flow*, 9, 105, 1983.

547. Malhotra, A.K. and Wasan, D.T., *Chem. Eng. Commun.*, 55, 95, 1987.

548. Malhotra, A.K. and Wasan, D.T., Interfacial rheological properties of adsorbed surfactant films with applications to emulsion and foam stability, in *Thin Liquid Films*, Ivanov, I.B., Ed., Marcel Dekker, New York, 1988, p. 829.

549. Singh, G., Hirasaki, G.J., and Miller, C.A., *J. Colloid Interface Sci.*, 184, 92, 1996.

550. Traykov, T.T., Manev, E.D., and Ivanov, I.B., *Int. J. Multiphase Flow*, 3, 485, 1977.

551. Bancroft, W.D., *J. Phys. Chem.*, 17, 514, 1913.

552. Griffin, J., *Soc. Cosmet. Chem.*, 5, 4, 1954.

553. Davies, J.T., in Proceedings of the 2nd International Congress on Surface Activity, Vol. 1, Butterworths, London, 1957, p. 426.

554. Shinoda, K. and Friberg, S., *Emulsion and Solubilization*, Wiley, New York, 1986.

555. Davis, H.T., Factors determining emulsion type: HLB and beyond, in Proc. First World Congress on Emulsion 19-22 Oct. 1993, Paris, 1993, p. 69.

556. Israelachvili, J., The history, applications and science of emulsion, in Proc. First World Congress on Emulsion 19-22 Oct. 1993, Paris, 1993, p. 53.

557. Kralchevsky, P.A., *J. Colloid Interface Sci.*, 137, 217, 1990.

558. Gompper, G. and Schick, M., *Phys. Rev.*, B41, 9148, 1990.

559. Lerczak, J., Schick, M., and Gompper, G., *Phys. Rev.*, 46, 985, 1992.

560. Andelman, D., Cates, M.E., Roux, D., and Safran, S., *J. Chem. Phys.*, 87, 7229, 1987.

561. Chandra, P. and Safran, S., *Europhys. Lett.*, 17, 691, 1992.

562. Danov, K.D., Velev, O.D., Ivanov, I.B., and Borwankar, R.P., Bancroft rule and hydrodynamic stability of thin films and emulsions, in First World Congress on Emulsion 19-22 Oct. 1993, Paris, 1993, p. 125.

563. Kunieda, H., Evans, D.F., Solans, C., and Yoshida, *Colloids Surf.*, 47, 35, 1990.

564. Koper, G.J.M., Sager, W.F.C., Smeets, J., and Bedeaux, D., *J. Phys. Chem.*, 99**,** 13291, 1995.

565. Ivanov, I.B., Danov, K.D., and Kralchevsky, P.A., *Colloids Surf. A*, 152, 161, 1999.

566. Velev, O.D., Gurkov, T.D., and Borwankar, R.P., *J. Colloid Iterface Sci.*, 159, 497, 1993.

567. Velev, O.D., Gurkov, T.D., Ivanov, I.B., and Borwankar, R.P., *Phys. Rev. Lett.*, 75, 264, 1995.

568. Danov, K., Ivanov, I., Zapryanov, Z., Nakache, E., and Raharimalala, S., Marginal stability of emulsion thin film, in *Proceedings of the Conference of Synergetics, Order and Chaos*, Velarde, M., Ed., World Scientific, Singapore, 1988, p. 178.

569. Valkovska, D.S., Kralchevsky, P.A., Danov, K.D., Broze, G., and Mehreteab, A., *Langmuir*, 16, 8892, 2000.

570. Danov, K.D., Gurkov, T.D., Dimitrova, T.D., and Smith, D., *J. Colloid Interface Sci.*, 188, 313, 1997

571. Ivanov, I.B., Chakarova, S.K., and Dimitrova, B.I., *Colloids Surf.*, 22, 311, 1987.

572. Dimitrova, B.I., Ivanov, I.B., and Nakache, E., *J. Dispersion Sci. Technol.*, 9, 321, 1988.

573. Sternling, C.V. and Scriven, L.E., *AIChE J.*, 5, 514, 1959.

574. Lin, S.P. and Brenner, H.J., *J. Colloid Interface Sci.*, 85, 59, 1982.

575. Holly, F.J., in *Wetting, Spreading and Adhesion* , Padday, J.F., Ed., Accademic Press, New York, 1978, p. 439.

576. Castillo, J.L. and Velarde, M.G., *J. Colloid Interface Sci.*, 108, 264, 1985.

577. Davis, R.H., *Adv. Colloid Interface Sci.*, 43, 17, 1993.

578. Uijttewaal, W.S.J., Nijhof, E.-J., and Heethaar, R.M., *Phys. Fluids*, A5, 819, 1993.

579. Zapryanov, Z. and Tabakova, S., *Dynamics of Bubbles, Drops and Rigid Particles*, Kluwer Academic Publishers, London, 1999.

580. Lorentz, H.A., *Abhandl. Theoret. Phys.*, 1, 23, 1906.

581. Faxen, H., *Arkiv. Mat. Astron. Fys.,* 17, 27, 1923.

582. Wakiya, S., *J. Phys. Soc. Jpn,* 12, 1130, 1957.

583. Dean, W.R. and O'Neill, M.E., *Mathematika*, 10, 13, 1963.

584. O'Neill, M.E., *Mathematika*, 11, 67, 1964.

585. Cooley, M.D.A. and O'Neill, M.E., *J. Inst. Math. Appl.*, 4, 163, 1968.

586. Keh, H.J. and Tseng, C.H., *Int. J. Multiphase Flow*, 1, 185, 1994.

587. Schonberg, J. and Hinch, E.J., *J. Fluid Mech.*, 203, 517, 1989.

588. Ryskin, G. and Leal, L.G., *J. Fluid Mech.*, 148, 1, 1984; *J. Fluid Mech.*, 148, 19, 1984; *J. Fluid Mech.*, 148, 37, 1984.

589. Liron, N. and Barta, E., *J. Fluid Mech.*, 238, 579, 1992.

590. Shapira, M. and Haber, S., *Int. J. Multiphase Flow*, 14, 483, 1988.
591. Shapira, M. and Haber, S., *Int. J. Multiphase Flow*, 16, 305, 1990.
592. Yang, S.-M. and Leal, L.G., *J. Fluid Mech.*, 149, 275, 1984.
593. Yang, S.-M. and Leal, L.G., *Int. J. Multiphase Flow*, 16, 597, 1990.
594. Lebedev, A.A., *Zhur. Russ. Fiz. Khim.*, 48, 1916.
595. Silvey, A., *Phys. Rev.*, 7, 106, 1916.
596. Hadamar, J.S., *Comp. Rend. Acad. Sci. (Paris)*, 152, 1735, 1911.
597. Rybczynski, W., *Bull. Intern. Acad. Sci. (Cracovie)*, A, 1911.
598. He, Z., Dagan, Z., and Maldarelli, Ch., *J. Fluid Mech.*, 222, 1, 1991.
599. Danov, K.D., Aust, R., Durst, F., and Lange, U., *Chem. Eng. Sci.*, 50, 263, 1995.
600. Danov, K.D., Aust, R., Durst, F., and Lange, U., *Chem. Eng. Sci.*, 50, 2943, 1995.
601. Danov, K.D., Aust, R., Durst, F., and Lange, U., *Int. J. Multiphase Flow.*, 21, 1169, 1995.
602. Danov, K.D., Gurkov, T.D., Raszillier, H., and Durst, F., *Chem. Eng. Sci.*, 53, 3413, 1998.
603. Stoos, J.A. and Leal, L.G., *J. Fluid Mech.*, 217, 263, 1990.
604. Danov, K.D., Dimova, R.I., and Pouligny, B., *Phys. Fluids*, 12, 2711, 2000.
605. Dimova, R.I., Danov, K.D., Pouligny, B., and Ivanov, I.B., *J. Colloid Interface Sci.*, 226, 35, 2000.
606. Angelova, M.I. and Pouligny, B., *Pure Appl. Optics*, 2, 261, 1993.
607. Pouligny, B., Martinot-Lagarde, G., and Angelova, M.I., *Progr. Colloid Polym. Sci.*, 98, 280, 1995.
608. Dietrich, C., Angelova, M., and Pouligny, B., *J. Phys. II France*, 7, 1651, 1997.
609. Velikov, K., Dietrich, C., Hadjiski, A., Danov, K., and Pouligny, B., *Europhys. Lett.*, 40(4), 405, 1997.
610. Velikov, K., Danov, K., Angelova, M., Dietrich, C., and Pouligny, B., *Colloids Surf. A*, 149, 245, 1999.
611. Dimova, R., Dietrich, C., Hadjiisky, A., Danov, K., and Pouligny, B., *Eur. Phys. J. B*, 12, 589, 1999.
612. Danov, K.D., Pouligny, B., Angelova, M.I., and Kralchevsky, P.A., in *Studies in Surface Science and Catalysis*, Vol. 132, Elsevier, Amsterdam, 2001.
613. Hunter, R.J., *Foundation of Colloid Science*, Vol. 1, Clarendon Press, Oxford, 1987.
614. Hunter, R.J., *Foundation of Colloid Science*, Vol. 2, Clarendon Press, Oxford, 1989.
615. Einstein, A., *Ann. Phys.*, 19, 289, 1906.
616. Kubo, R., *Rep. Prog. Phys.*, 29, 255, 1966.
617. Einstein, A., *Ann. Phys.*, 34, 591, 1911.
618. Taylor, G.I., *Proc. Roy. Soc. A*, 138, 41, 1932.
619. Oldroyd, J.G., *Proc. Roy. Soc. A*, 232, 567, 1955.
620. Taylor, G.I., *Proc. Roy. Soc. A*, 146, 501, 1934.
621. Fröhlich, H. and Sack, R., *Proc. Roy. Soc. A*, 185, 415, 1946.

622. Oldroyd, J.G., *Proc. Roy. Soc. A*, 218, 122, 1953.

623. Batchelor, G.K., *J. Fluid Mech.*, 83, 97, 1977.

624. De Kruif, C.G., Van Iersel, E.M.F., Vrij, A., and Russel, W.B., *J. Chem. Phys.*, 83, 4717, 1985.

625. Loewenberg, M. and Hinch, E.J., *J. Fluid Mech.*, 321, 395, 1996.

626. Da Cunha, F.R. and Hinch, E.J., *J. Fluid Mech.*, 309, 211, 1996.

627. Li, X. and Pozrikidis, C., *J. Fluid Mech.*, 341, 165, 1997.

628. Loewenberg, M., *J. Fluids Eng.*, 120, 824, 1998.

629. Blawzdziewicz, J., Vajnryb, E., and Loewenberg, M., *J. Fluid Mech.*, 395, 29, 1999.

630. Ramirez, J.A., Zinchenko, A., Loewenberg, M., and Davis, R.H., *Chem. Eng. Sci.*, 54, 149, 1999.

631. Blawzdziewicz, J., Vlahovska, P., and Loewenberg, M., *Physica A*, 276, 50, 2000.

632. Breyannis, G. and Pozrikidis, C., *Theor. Comp. Fluid Dynam.*, 13, 327, 2000.

633. Li, X. and Pozrikidis, C., *Int. J. Multiphase Flow*, 26, 1247, 2000.

634. Rednikov, A.Y., Ryazantsev, Y.S., and Velarde, M.G., *Phys. Fluids*, 6, 451, 1994.

635. Velarde, M.G., *Phil. Trans. Roy. Soc., Math. Phys. Eng. Sci.*, 356, 829, 1998.

636. Danov K.D., *J. Colloid Interface Sci.*, 235, 144, 2001.

637. Barnes, H.A., Rheology of emulsions - a review, in Proc. First World Congress on Emulsion 19-22 Oct. 1993, Paris, 1993, p. 267.

638. Krieger, L.M. and Dougherty, T.J., *Trans. Soc. Rheol.*, 3, 137, 1959.

639. Wakeman, R., *Powder Tech.*, 11, 297, 1975.

640. Prud'home, R.K. and Khan, S.A., Experimental results on foam rheology, in *Foams: Theory, Measurements, and Applications*, Prud'home, R.K. and Khan, S.A., Eds., Marcel Dekker, New York, 1996, p. 217.

641. Tadros, T.F., Fundamental principles of emulsion rheology and their applications, in Proc. First World Congress on Emulsion 19-22 Oct. 1993, Paris, 1993, p. 237.

642. Pal, R., Bhattacharya, S.N., and Rhodes, E., *Can. J. Chem. Eng.*, 64, 3, 1986.

643. Edwards, D.A. and Wasan, D.T., Foam rheology: the theory and role of interfacial rheological properties, in *Foams: Theory, Measurements, and Applications*, Prud'home, R.K. and Khan, S.A., Eds., Marcel Dekker, New York, 1996, p. 189.

644. Wessel, R. and Ball, R.C., *Phys. Rev.*, A46, 3009, 1992.

645. Kanai, H., Navarrete, R.C., Macosko, C.W., and Scriven, L.E., *Rheol. Acta*, 31, 333, 1992.

646. Pal, R., *Chem. Eng. Comm.*, 98, 211, 1990.

647. Pal, R., *Colloids Surf. A*, 71, 173, 1993.

648. Prins, A., Liqiud flow in foams as affected by rheological surface properties: a contribution to a better understanding of the foaming behaviour of liquids, in *Hydrodynamics of Dispersed Media*, Hulin, J.P., Cazabat, A.M., Guyon, E., and Carmona, F., Eds., Elsevier/North-Holland, Amsterdam, 1990, p. 5.

649. Babak, V.G., *Colloids Surf. A*, 85, 279, 1994.

650. Yuhua, Y., Pal, R., and Masliyah, J., *Chem Eng. Sci.*, 46, 985, 1991.

651. Giesekus, H., Disperse systems: dependence of rheological properties on the type of flow with implications for food rheology, in *Physical Properties of Foods*, Jowitt, R. et al., Eds., Applied Science Publishers, 1983, chap. 13.

652. Turian, R. and Yuan, T.-F., *AIChE J.*, 23, 232, 1977.

653. Clarke, B., *Trans. Inst. Chem. Eng.*, 45, 251, 1967.

654. von Smoluchowsky, M., *Phys. Z.*, 17, 557, 1916.

655. von Smoluchowsky, M., *Z. Phys. Chem.*, 92, 129, 1917.

656. Wang, H. and Davis, R.H., *J. Colloid Interface Sci.*, 159, 108, 1993.

657. Rogers, J.R. and Davis, R.H., *Mettal. Trans.*, A21, 59, 1990.

658. Young, N.O., Goldstein, J.S., and Block, M.J., *J. Fluid Mech.*, 6, 350, 1959.

659. Fuchs, N.A., *Z. Phys.*, 89, 736, 1934.

660. Friedlander, S.K., *Smoke, Dust and Haze: Fundamentals of Aerosol Behaviour*, Wiley-Interscience, New York, 1977.

661. Singer, J.M., Vekemans, F.C.A., Lichtenbelt, J.W.Th., Hesselink, F.Th., and Wiersema, P.H., *J. Colloid Interface Sci.*, 45, 608, 1973.

662. Leckband, D.E., Schmitt, F.-J., Israelachvili, J.N., and Knoll, W., *Biochemistry*, 33, 4611, 1994.

663. Bak, T.A. and Heilmann, O., *J. Phys. A: Math. Gen.*, 24, 4889, 1991.

664. Martinov, G.A. and Muller, V.M., in *Research in Surface Forces*, Vol. 4, Plenum Press, Consultants Bureau, New York, 1975, p. 3.

665. Elminyawi, I.M., Gangopadhyay, S., and Sorensen, C.M., *J. Colloid Interface Sci.*, 144, 315, 1991.

666. Hartland, S. and Gakis, N., *Proc. Roy. Soc. (Lond.)*, A369, 137, 1979.

667. Hartland, S. and Vohra, D.K., *J. Colloid Interface Sci.*, 77, 295, 1980.

668. Lobo, L., Ivanov, I.B., and Wasan, D.T., *AIChE J.*, 39, 322, 1993.

669. Danov, K.D., Ivanov, I.B., Gurkov, T.D., and Borwankar, R.P., *J. Colloid Interface Sci.*, 167, 8, 1994.

670. van den Tempel, M., *Recueil*, 72, 433, 1953.

671. Borwankar, R.P., Lobo, L.A., and Wasan, D.T., *Colloid Surf.*, 69, 135, 1992.

672. Dukhin, S., Sæther, Ø., and Sjöblom, J., Coupling of coalescence and flocculation in dilute O/W emulsions, in *Encycloped Handbook of Emulsion Technology*, Sjöblom, J., Ed., Marcel Dekker, New York, 2001, p. 71.